

Universidad de Málaga

Escuela Técnica Superior de Ingeniería de Telecomunicación



TESIS DOCTORAL

Analysis of MAC Strategies for Underwater Acoustic Networks

Autor:

Seema Ansari

Directores:

Javier Poncela González

Pablo Otero Roth

Malaga 2018

AUTORIZACIÓN DE LECTURA

DEDICATION

I would like to dedicate this research work to my loving family, S. K. Ansari my husband, my sons Dr. Adeel Ansari & Faran Ansari, my daughter Sana Ahmad, my late parents and my supervisors, Professor Dr. Javier Poncela and Professor Dr. Pablo Otero.

Mr. Shahjehan S. Karim, President Institute of Business Management for his motivational support.

This research work would not have been possible without the culminative and aggregative support from you all.

ACKNOWLEDGMENTS

I would like to thank my husband and my children who have supported and motivated me at a personal level and in difficult times, were always there to uplift my spirits.

I wish to thank Prof. Dr. Javier Poncela and Prof. Dr. Pablo Otero, for their continuous guidance in the completion of this research work as well as for their valuable support as advisors during the entire PhD program. Their supreme mentorship provided a well-rounded experience, which I will treasure in my career. I was positively motivated in my research and received numerous support, appreciation, reinforcement in this research topic. Their encouragement, supervision, valuable suggestions and intellectual activities, from preliminary to the concluding level enabled me to complete the whole work.

I wish to thank my research colleagues who facilitated me to carry out my research. The Technical staff of the Telecommunication/Computer Science department, University of Malaga, Spain for providing me with the lab facilities during my PhD research. Last but not least, I would like to express my appreciation for the financial and organizational support from the University of Malaga, Spain.

ABSTRACT

This thesis presents research on MAC protocols used in underwater communications to explore the underwater world. MAC protocols assist in the access of the shared medium and the collection of data from oceans, for monitoring climate and pollution, calamity avoidance, assisted navigation, strategic surveillance, and exploration of mineral resources. This research will benefit sectors like military, oil and gas industries, fisheries, underwater instrumentation companies, research agencies, etc. The MAC protocol affects the network lifetime of Wireless Sensors Networks. The energy efficiency of the underwater acoustic networks is badly affected by the typical properties of the propagation of acoustic waves. The long propagation delays and data packet collisions hinder the transmission of the data packets, containing useful information for users to perform collective monitoring tasks.

The aim of this study is to propose new mechanisms for MAC protocols designed for underwater acoustic networks to improve their performance. To do so, a previous and thorough comparative analysis of existing protocols is mandatory. Also, to establish a methodologically appropriate comparison procedure. Since underwater communication depends on acoustic waves, a number of challenges like long latency, limited bandwidth, long propagation delay, large bit error rates, momentary losses in connections, severe multipath and occurrences of fading are considered in the design of underwater MAC protocols. Terrestrial MAC protocols, if deployed directly, will perform inefficiently. In this thesis we present MAC protocols tailored for underwater acoustic networks, by classifying them into broad categories, providing performance measurement techniques and comparative analysis to select the best MAC Algorithm for specific application. Floor Acquisition Multiple Access (FAMA) is a MAC protocol that was proposed for underwater acoustic networks as a means to solve the problems of hidden and exposed terminals. A modified version, Slotted FAMA, aimed to provide savings in energy by using timeslots, thus eliminating the need for excessively long control packets in FAMA. However, it has been observed that, due to the high propagation delay in these networks, the cost of losing one ACK is very high, having a significant impact on the performance. The MultiACK and the EarlyACK mechanisms have been analyzed for the MACA protocol, to improve its efficiency. The MultiACK mechanism increases the probability of receiving at least one ACK packet by replying with a train of ACK packets, while the EarlyACK mechanism prevents the repetition of the entire RTS/CTS contention and data transmission cycle by sending an early ACK.

In this research a mathematical analysis of the two variations, MultiACK and EarlyACK mechanisms, in Slotted FAMA is presented. The research includes the modified analytical expressions as well as numerical results. Simulations were carried out using ns-3. The results have been tested and validated using Excel and MATLAB. The performance evaluation of S-FAMA with two variants showed an improvement factor of 65.05% in the probability of receiving an ACK correctly by using the MultiACK mechanism and 60.58% in preventing the repetition of the entire cycle, with EarlyACK. The impact of this improvement factor on delay, DATA packet size and throughput is also analyzed. The transmission energy wasted and consumed in the MultiACK and the EarlyACK mechanisms are analyzed and compared with that of S-FAMA. Throughput has been evaluated, reaching an improvement in both cases, compared to S-FAMA. These mechanisms will have practical usefulness in case of ACK loss, by saving energy and time in critical periods.

RESUMEN

Esta tesis presenta una investigación sobre los protocolos MAC utilizados en la comunicación subacuática para explorar el mundo submarino. Los protocolos MAC ayudan en el acceso al medio compartido y la recopilación de datos de los océanos, para monitorizar el clima y la contaminación, la prevención de catástrofes, la navegación asistida, la vigilancia estratégica y la exploración de los recursos minerales. Esta investigación beneficiará a sectores como las industrias militares, de petróleo y gas, pesquerías, compañías de instrumentación subacuática, organismos de investigación, etc. El protocolo MAC afecta la vida útil de las redes inalámbricas de sensores. La eficiencia energética de las redes acústicas submarinas se ve gravemente afectada por las propiedades típicas de la propagación de las ondas acústicas. Los largos retrasos de propagación y las colisiones de paquetes de datos dificultan la transmisión de los paquetes de datos, que contienen información útil para que los usuarios realicen tareas de supervisión colectivas.

El objetivo de este estudio es proponer nuevos mecanismos para protocolos MAC diseñados para funcionar en redes acústicas submarinas, con el propósito de mejorar su rendimiento. Para alcanzar ese objetivo es necesario realizar un análisis comparativo de los protocolos existentes. Lo que además sienta un procedimiento metodológicamente correcto para realizar esa comparación. Como la comunicación subacuática depende de ondas acústicas, en el diseño de los protocolos de MAC submarinos surgen varios desafíos como latencia prolongada, ancho de banda limitado, largas demoras en la propagación, grandes tasas de error de bit, pérdidas momentáneas en las conexiones, severo efecto multicamino y desvanecimientos. Los protocolos MAC terrestres, si se implementan directamente, funcionarán de manera ineficiente. En esta tesis presentamos los protocolos MAC diseñados para redes acústicas subacuáticas, clasificándolos en amplias categorías, proporcionando técnicas de medición de rendimiento y análisis comparativo para seleccionar el mejor algoritmo MAC para aplicaciones específicas. Floor Acquisition Multiple Access (FAMA) es un protocolo MAC que se propuso para redes acústicas submarinas como medio para resolver los problemas de terminales ocultos y expuestos. Una versión modificada, Slotted FAMA, tenía como objetivo proporcionar ahorros de energía mediante el uso de ranuras de tiempo, eliminando así la necesidad de paquetes de control excesivamente largos en FAMA. Sin embargo, se ha observado que, debido al alto retraso de propagación en estas redes, el coste de perder un ACK es muy alto y tiene un impacto significativo en el rendimiento. Los mecanismos MultiACK y EarlyACK han sido analizados para el protocolo MACA, para mejorar su eficiencia. El mecanismo MultiACK aumenta la probabilidad de recibir al menos un paquete ACK al responder con un tren de paquetes ACK, mientras que el mecanismo EarlyACK evita la repetición de todo el ciclo de contención y transmisión de datos RTS / CTS enviando un ACK temprano.

En esta investigación se presenta un análisis matemático de las dos variantes, los mecanismos MultiACK y EarlyACK, en Slotted FAMA. La investigación incluye las expresiones analíticas modificadas así como los resultados numéricos. Las simulaciones se llevaron a cabo utilizando ns-3. Los resultados han sido probados y validados utilizando Excel y MATLAB. La evaluación del rendimiento de S-FAMA con dos variantes mostró un factor de mejora del 65,05% en la probabilidad de recibir un ACK correctamente utilizando el mecanismo MultiACK y del 60,58% en la prevención de la repetición del ciclo completo, con EarlyACK. El impacto de este factor de mejora en el retardo, el tamaño del paquete de datos y el

rendimiento también se analiza. La energía de transmisión desperdiciada y consumida en los mecanismos MultiACK y EarlyACK se analizan y comparan con S-FAMA. El rendimiento se ha evaluado, alcanzando una mejora en ambos casos, en comparación con S-FAMA. Estos mecanismos tendrán una utilidad práctica en caso de pérdida de ACK, al ahorrar energía y tiempo en períodos críticos.

TABLE OF CONTENT

ABSTRACT.....	i
RESUMEN	ii
TABLE OF CONTENT	iv
LIST OF FIGURES	vi
LIST OF TABLES	viii
LIST OF ABBREVIATIONS.....	x
LIST OF SYMBOLS	xii
Chapter 1 : INTRODUCTION.....	1
1.1 Background	1
1.2 Medium Access Control Protocols.....	2
1.3 Objectives.....	3
1.4 Thesis Organization.....	4
Chapter 2 : STATE OF THE ART	6
2.1 Environment Characteristics	6
2.2 Underwater Acoustic Sensor Networks and Connectivity	8
2.3 Challenges	11
2.4 MAC Protocols.....	12
2.4.1 Performance Overview of MAC Techniques	21
2.5 Analytical Study	25
2.6 Conclusion.....	28
Chapter 3 : THEORETICAL ANALYSIS	30
3.1 Protocol Overview.....	30
3.1.1 Model	31
3.1.2 Analysis.....	32
3.1.3 Performance	34
3.2 Problem Statement	36
3.3 MultiACK Mechanism.....	37
3.3.1 Analysis.....	38
3.3.2 Scenarios	38
3.3.2.1 Scenario-I	38
3.3.2.2 Scenario-II.....	39
3.4 EarlyACK Mechanism	40
3.4.1 Analysis.....	40
3.5 Analysis of Energy Consumption	42
3.6 Comparative Analysis	43
3.6.1 Improvement for MultiACK.....	43
3.6.2 Improvement for EarlyACK	44
3.7 Conclusion.....	44

Chapter 4 : RESULTS AND DISCUSSIONS	45
4.1 MultiACK.....	45
4.1.1 Scenario-I.....	46
4.1.2 Scenario-II.....	56
4.1.3 Comparative Analysis	60
4.2 EarlyACK.....	61
4.3 Energy Consumption.....	69
4.4 Improvement Analysis	72
4.2.1 MultiACK	72
4.2.2 EarlyACK	73
4.5 Comparative Analysis	73
4.6 Conclusion.....	77
Chapter 5 : CONCLUSION	78
References.....	80
Publications.....	85
Journals.....	85
Conferences	86
APPENDIX A.....	87
Curriculum Vitae.....	87

LIST OF FIGURES

Figure 2.1 Example of Underwater Acoustic Sensor Network with multiple nodes and three surface sinks.	9
Figure 2.2: Two-dimensional Underwater Sensor Networks [16].....	9
Figure 2.3: Three-dimensional Underwater Sensor Networks [16].....	10
Figure 2.4: (a) Cluster-head-based and (b) ad-hoc-based MAC topologies [73].Source: https://www.tandfonline.com/action/showCitFormats?doi=10.4103%2F0256- 4602.123119	22
Figure 2.5. Line Topology [35] Source: https://goo.gl/images/Xg2CFt.....	23
Figure 2.6. Star Topology [35] Source: https://goo.gl/images/Xg2CFt.....	23
Figure 2.7: UAN-CW-MAC Throughput (pkts/sec) for 20 nodes.....	28
Figure 3.1: A successful handshake between terminals A and B in Slotted FAMA [42].....	31
Figure 3.2: State Transition diagram for S-FAMA protocol [78].....	32
Figure 3.3: Network Layout [42]	32
Figure 3.4. Throughput vs Offered Load (packets/sec) of Pure Aloha, Slotted Aloha, CSMA and SFAMA.....	35
Figure 3.5. Average Throughput (bps) vs Number of Nodes for S-FAMA, for: $T_{data}=1$ slot and $T_{data}=3$ slots	35
Figure 3.6. Average Throughput (bps) vs Number of Nodes for S-FAMA for $T_{data}=3$ slots	36
Figure 3.7: Message Sequence Charts for: (a) S-FAMA, (b) MultiACK and (c) EarlyACK..	37
Figure 3.8: MultiACK Scenario-I	38
Figure 3.9: MultiACK Scenario-II.....	40
Figure 4.1: Throughput Improvement vs. Number of nodes, MultiACK Scenario-I, for: (a) $BER 10^{-2}$ (b) $BER 10^{-3}$ (c) $BER 10^{-4}$ (d) $BER 10^{-5}$ (e) $BER 10^{-6}$ (f) $BER 10^{-7}$, for $Q=0$.	48
Figure 4.2: Throughput Improvement vs. Number of nodes, MultiACK Scenario-I, for: (a) $BER 10^{-2}$ (b) $BER 10^{-3}$ (c) $BER 10^{-4}$ (d) $BER 10^{-5}$ (e) $BER 10^{-6}$ (f) $BER 10^{-7}$, for $Q=3$ nodes.	49
Figure 4.3: Throughput Improvement vs. BER, MultiACK Scenario-I, for $BER=10^{-7}$ to 10^{-3}	51
Figure 4.4: Throughput Improvement vs T_{data}	51
Figure 4.5: Performance of MultiACK as a function of Transmission range and $T_{data}=1, 3,$ 15 and 30 slots for (a) $BER 10^{-2}$ (b) $BER 10^{-3}$ (c) $BER 10^{-4}$ (d) $BER 10^{-5}$ (e) $BER 10^{-6}$ (f) $BER 10^{-7}$	52
Figure 4.6: Performance of MultiACK Scenario-I as a function of Transmission range and $T_{data}=1, 3, 15$ and 30 slots for (a) $BER 10^{-2}$ (b) $BER 10^{-3}$ (c) $BER 10^{-4}$ (d) $BER 10^{-5}$ (e) $BER 10^{-6}$ (f) $BER 10^{-7}$ with hidden nodes ($Q=3$).	54
Figure 4.7: Throughput (bps) vs offered Load (packets/second) for S-FAMA, $T_{data}=1$ & 3 slots, MultiACK with $T_{data}=1$ slot and EarlyACK with $T_{data}=1$ slot	55
Figure 4.8: Throughput Improvement vs offered Load with MultiACK-Scenario-I, and EarlyACK	56
Figure 4.9: MultiACK Scenario-II: Throughput Improvement vs. Number of nodes for: (a) $BER 10^{-2}$ (b) $BER 10^{-3}$ (c) $BER 10^{-4}$ (d) $BER 10^{-5}$ (e) $BER 10^{-6}$ (f) $BER 10^{-7}$	58
Figure 4.10: Throughput Improvement vs. BER, MultiACK Scenario-II.	58

Figure 4.11: MultiACK Scenario-II.: Throughput Improvement (%) vs. Transmission range, (a) BER 10^{-2} (b) BER 10^{-3} (c) BER 10^{-4} (d) BER 10^{-5} (e) BER 10^{-6} (f) BER 10^{-7}	59
Figure 4.12: Throughput Improvement vs. Tdata, MultiACK Scenario-II, with 16 nodes.	60
Figure 4.13: Throughput Improvement (%) vs. Number of nodes in EarlyACK for (a) BER 10^{-2} (b) BER 10^{-3} (c) BER 10^{-4} (d) BER 10^{-5} (e) BER 10^{-6} (f) BER 10^{-7}	63
Figure 4.14: Throughput Improvement (%) vs. Number of nodes in EarlyACK for Q=3, (a) BER 10^{-2} (b) BER 10^{-3} (c) BER 10^{-4} (d) BER 10^{-5} (e) BER 10^{-6} (f) BER 10^{-7}	64
Figure 4.15: EarlyACK: Throughput Improvement (%) vs. BER	65
Figure 4.16: EarlyACK: Throughput Improvement vs Transmission Range for: (a) BER 10^{-2} (b) BER 10^{-3} (c) BER 10^{-4} (d) BER 10^{-5} (e) BER 10^{-6} (f) BER 10^{-7}	66
Figure 4.17: EarlyACK: Throughput Improvement vs Transmission Range for: (a) BER 10^{-2} (b) BER 10^{-3} (c) BER 10^{-4} (d) BER 10^{-5} (e) BER 10^{-6} (f) BER 10^{-7}	68
Figure 4.18: Throughput Improvement vs Tdata for EarlyACK, with 16 nodes.....	68
Figure 4.19: Analysis of transmission energy wasted in S-FAMA & MultiACK-SFAMA for BER 10^{-5}	70
Figure 4.20: MultiACK energy transmission improvement at different BERs. (10^{-6} to 10^{-2}). ..	71
Figure 4.21: Comparative analysis of transmission energy wasted in unsuccessful transmission in MultiACK and EarlyACK.....	71
Figure 4.22: Comparison of Throughput vs Offered Load in S-FAMA for Tdata =1 and Tdata=3slots.....	74
Figure 4.23: Comparison of Throughput Improvement vs Offered Load in S-FAMA with MultiACK for Tdata=1 & 3 slots.	75
Figure 4.24: Comparison of Throughput Improvement vs Offered Load in S-FAMA with EarlyACK for Tdata=1 & 3 slots.....	75
Figure 4.25: Comparison of Throughput Improvement vs Offered Load for MultiACK and EarlyACK for Tdata=1 & 3 slots.....	76

LIST OF TABLES

Table 2.1: Bandwidths for different ranges in underwater acoustic channels. [4], [16].....	7
Table 2.2: Parameters used in the quantitative analysis.	22
Table 2.3: Quantitative Analysis of MAC Protocols	23
Table 2.4: Quantitative Analysis of Cluster-Head-Based MAC Protocols.....	25
Table 2.5. MACA Parameters.....	27
Table 2.6: The parameters used to analyze the performance UAN-CW-MAC	28
Table 3.1: Effect of varying BER on Average Throughput (bps) vs Nodes for $T_{data}=3$ slots.	36
Table 3.2: Parameters.....	39
Table 4.1: Parameters used in MutliACK: Scenario-I.....	45
Table 4.2:Behaviour of the S-FAMA protocol at high BER 10^{-2} and larger DATA packet size. with $L_{ACK}=100$ bits, BER=0.01, $Q=0$	47
Table 4.3: Impact of Hidden nodes (Q) on throughput Improvement, for $T_{data}=1$ and 16 nodes.....	49
Table 4.4: Quantitative Analysis on Impact of Hidden nodes (Q) on throughput Improvement, for $T_{data}=1$ and 16 nodes, BER 10^{-3}	50
Table 4.5: MultiACK-Scenario-I, Performance Analysis as a function of BER.	50
Table 4.6: Analysis as a function of data length at BER 10^{-5}	52
Table 4.7: Analysis as a function of Transmission range at BER 10^{-3}	53
Table 4.8: MultiACK-Scenario-I, Performance Analysis with $Q=0$ and $Q=3$ hidden nodes and $T_{data}=1$ slot and 16 nodes.	55
Table 4.9: Parameters used in MutliACK: Scenario-II.....	56
Table 4.10: MultiACK-Scenario-II, Performance Analysis as a function of BER.....	58
Table 4.11: Analysis Throughput Improvement vs. T_{data} , MultiACK Scenario-II.....	60
Table 4.12: MutliACK Scenario-I & II, Performance Analysis	60
Table 4.13: MutliACK Scenario-I & II, Comparative Analysis of throughput improvement at BER 10^{-3}	61
Table 4.14: Comparative Analysis: Throughput Improvement vs Transmission Range for $T_{data}=1$ slot.	61
Table 4.15: Parameters for analysis of EarlyACK.....	61
Table 4.16: EarlyACK, Comparative Analysis as a function of BER, with 16 nodes.....	66
Table 4.17: EarlyACK comparative analysis of throughput improvement (%) for $Q=0$ and $Q=3$ at BER 10^{-3}	68
Table 4.18: EarlyACK Comparative Analysis of Throughput Improvement vs T_{data}	69
Table 4.19: Parameters for Energy Consumption per node	69
Table 4.20: Analysis of Total Transmission Energy Wasted in S-FAMA, MultiACK & EarlyACK at BER 10^{-5}	72
Table 4.21: Analysis of Packet Error Rates and Improvement in Total Energy waste in MultiACK & EarlyACK.....	72
Table 4.22: Energy Consumption Analysis at BER 10^{-5}	72
Table 4.23: Impact of Improvement Factor on Throughput	73
Table 4.24: Impact of Improvement Factor on Delay and Throughput for MultiACK and EarlyACK	73

Table 4.25: MutliACK & EarlyACK Comparative Analysis of Throughput Improvement vs Tdata.....	74
Table 4.26: MutliACK & EarlyACK Comparative Analysis of Throughput Improvement for BER 10^{-5}	74
Table 4.27: Quantitative Analysis of S-FAMA, MultiACK and EarlyACK Protocols at BER 10^{-3} to 10^{-6} for Underwater Acoustic Networks.....	77

LIST OF ABBREVIATIONS

Abbreviations	Description
ACK	Acknowledgement
ACMENet	The Acoustic Communication network for Monitoring of Environment in coastal areas Networks
ALOHA- AN	Aloha with Advance Notification
ALOHA-CS	Aloha With Carrier Sense
BER	Bit Error Rate
CDMA	Code Division Multiple Access
CSMA	Carrier Sense Multiple Access
CSMA/CA	Carrier Sense Multiple Access/Collision Avoidance
CSMA/CD	Carrier Sense Multiple Access/ Collision Detection
CTS	Clear to send
DA	Demand assigned
DACAP	Distance Aware-Collision Avoidance protocol
DCF	Distributed Coordination Function
DIFS	Distributed Inter Frame Space
DN-MAC	Dynamic MAC
DOTS	Delay-aware Opportunistic Transmission Scheduling
DSSS	Direct-Sequence Spread Spectrum
FAMA	Floor acquisition multiple Access
FDCA	Full-Duplex Collision Avoidance
FDMA	Frequency Division Multiple Access
FHSS	Frequency-Hopping Spread Spectrum
FSK	Frequency Shift Keying
LPL	Low Power Listening
MAC	Medium Access Control
MACA	Multiple Access with Collision Avoidance
MACA-DT	MACA-Delay Tolerant
MACA-EA	MACA-Early Acknowledgement
MACAW	Medium Access Collision Avoidance- Wireless.
UMACAW	Underwater MACAW
M-FAMA	Multi-session Floor acquisition multiple Access
PER	Packet Error Rate
RA	Random access
RCAMAC	Reservation Channel Acoustic Media Access Protocol
RC-SFAMA	RTS-Competition- Floor acquisition multiple Access
RRA	Reservation Random Access
RTS	Request to send
RTT	Round Trip Time
S-ALOHA	Slotted ALOHA
SBMAC	Smart Blocking MAC
SDMA	Space Division Multiple Access
S-FAMA	Slotted Floor acquisition multiple Access
S-FAMA-DT	Slotted FAMA-Delay Tolerant
TDMA	Time Division Multiple Access
S-TDMA	Spatial TDMA
TDA-MAC	Transmit Delay Allocation MAC
UAC	Underwater Acoustic Channel
UASN	Underwater Acoustic Sensor Network
UW-A	Underwater Acoustic
UWAN	Underwater Acoustic Network
UW-MAC	Underwater-Medium Access Control
WDMA	Wavelength Division Multiple Access
WSNs	Wireless Sensor Networks

LIST OF SYMBOLS

Symbol	Description
\bar{U}	Average useful data transmission time
\bar{B}	Average busy time
\bar{I}	Average idle time
δ	Transmission time of a DATA Packet
i	Number of ACK packets
T_{ACK}	Duration of the ACK packet
T_{CTS}	Duration of the Control packet
L_{ACK}	Number of bits in the ACK packet
L_{DATA}	Number of bits in the Data packet (variable)
BER	Bit Error Rate
P_e, P_{eM}, P_{eEA}	Probability of error in a DATA packet transmission in S-FAMA, MultiACK and EarlyACK
$P_{succ-DATA}$	Probability of successfully transmitting a Data packet containing L_{DATA} bits.
$P_{succ-ACK}$	Probability of successfully transmitting a Multi-ACK packet containing L_{ACK} bits.
T_{data}	Duration of all the slots needed by a data packet
$\bar{T}_{success}$	Time during which DATA is being successfully sent (busy period).
\bar{T}_{fail}	Time during which collisions occur
\bar{T}_{defer}	Time during which transmissions are deferred
D	Probability of success in a Data packet transmission
A / \bar{A}	Probability of success in an ACK packet transmission/Probability no ACK received.
n	Number of ACK retries

CHAPTER 1 : INTRODUCTION

This chapter covers the problem background, objectives to be accomplished, scope, and the thesis structure. A brief summary of the selected MAC Protocols along with the techniques involved for the underwater acoustic networks are described.

1.1 Background

Oceans today play an important role in environmental monitoring, surveillance and resource gathering. Underwater communication has drawn attention of researchers and scientist to explore the underwater world. Underwater communication networks use Medium Access Control (MAC) protocols to govern the behavior of sensor nodes for a successful communication. The study of MAC protocols for underwater acoustic networks is therefore crucial, as the techniques are still in the evolving stage for underwater applications such as collection of oceanographic data.

Underwater communication uses acoustic waves as the typical physical layer technology. Radio waves propagate at long distances through conductive sea water only at ultra low frequencies (30–300 Hz), which require large antennae and high transmission power. Optical waves do not experience high attenuation, but they are affected by scattering. In addition, optical signals transmission requires high accuracy in pointing the narrow laser beams. Thus, links in underwater networks are based on acoustic wireless communications [1].

Underwater communications can be applied to collect data from oceans, offshore discovery, calamity avoidance, assisted navigation, strategic surveillance. The sectors that can benefit most from this research are military, oil and gas industries, fisheries, research agencies, etc. The scope of this research is in the areas such as underwater environmental monitoring, sea exploration, underwater robot operation, detection and ocean mapping, etc. A wide scope of applications aimed for underwater acoustic sensor networks includes applications in the prevention of disaster occurrence, assistance in navigation and strategic surveillance applications. The technology enabling these applications is the underwater acoustic networking, which comprise different number of sensor nodes and vehicles deployed in the region to perform monitoring tasks [2], [3], and [4]:

- **Networks for Ocean Sampling:** The development of underwater networks and sensing is driven by applications. Networks for ocean sampling have the ability to perform sampling of coastal ocean environment. They have the ability to observe and predict the physical properties, such as depth, temperature, salinity, density and flow of the ocean. Networks of sensors, along with AUVs and robotic vehicles, may be used to collect data of phenomena in the underwater environment and provide it off-shore. Sophisticated robotic vehicle and advanced ocean models together enhance the ability to observe and predict the characteristics of the ocean environment.
- **Monitoring of Environment:** Monitoring the environment is another application of UWASNs. They can monitor pollution such as chemical or biological elements in the ocean. They can detect the quality of water in lakes, rivers and oceans by the presence of chemical slurry of antibiotics in underwater. They can provide information on

weather forecast, predict change of climate, etc. Other applications include monitoring of ocean currents and winds, understanding the effect of human interventions on marine environment, biological monitoring like tracking fishes and other micro-organisms.

- **Prevention of Disaster:** UWASNs can provide warnings of tsunamis to coastal areas. They have the ability to measure seismic activities from remote locations or study the effects of earthquakes.
- **Assisted Navigation.** Sensors can be used to trace hazardous rocks or shoals in shallow waters, anchorage locations, sunken wreckages, etc. They can also provide bathymetric information.
- **Distributed Strategic Surveillance.** Sensor networks can be fixed at locations in underwater. They can provide monitoring in collaboration with AUVs to do surveillance for areas which are vulnerable to targeting and intrusion. A 3D underwater sensor network has been designed for a tactical surveillance system [4]. It can detect and classify submarines, small delivery vehicles and divers based on the sensed data gathered from mechanical, magnetic and acoustic micro-sensors. Compared to conventional radar/sonar systems, underwater sensor networks provide high accuracy and can detect and classify low targets by combining data from various kinds of sensors.
- **Mine Exploration.** The concurrent operation of several AUVs along with acoustic and optical sensors, operating simultaneously can perform quick assessment of environment and detection of mine like targets.
- **Industrial Operations.** Underwater sensor networks can be used to explore oil fields reservoirs and other minerals under seabed. They also assist in laying cables underwater by determining routes.

1.2 Medium Access Control Protocols

MAC protocols are needed to control the access of the shared medium. In Wireless Sensor Networks (WSNs) [1], the MAC protocol shares the wireless broadcast medium among sensor nodes and creates a basic network infrastructure for them to communicate with each other. The MAC protocol also has a great impact on the network lifetime of WSNs as it controls the actions of the radio, which is the most power consuming element of resource-limited sensor nodes. In the underwater environment, existing terrestrial WSN MAC protocols are not suitable. In fact Dario Pompili et al. in [5] explain that channel access control in UW-networks presents added tasks owing to the narrow bandwidth, large delays in propagation, too many bit error rates, losses in nodes connectivity, intense multipath and fading phenomenon and channel asymmetry. The unique properties of the UW acoustic communication path need for new efficient, reliable communication protocols to meet these challenges.

The choice of Contention-based and contention-free protocols for underwater networks is driven by the constraints and requirements such as time synchronization, delay-tolerance, time criticality and reliability in messaging, ad-hoc network establishment, number of expected nodes, nature of traffic (continuous or bursty), sleep-wake schedules in sensors and mobility [6].

The energy efficiency in underwater acoustic networks is badly affected by the long propagation delays and data packet collisions. The large propagation delay (0.67 s/km) reduces the throughput of the system and increases the round trip time (RTT). Energy-efficiency in

underwater networks is vital as nodes are generally battery powered and it is not easy to replace their supply.

Owing to the narrow bandwidth of the underwater acoustic channel, most of the existing MAC protocols are based on techniques such as carrier-sense multiple access (CSMA) or code division multiple access (CDMA). The problems of hidden and exposed terminals lower the performance of CSMA protocols because of the problem of connectivity among some nodes. Besides, the throughput of the CSMA protocol rapidly decreases with the increase in delay [7]. To overcome this, the MACA (Multiple Access Collision Avoidance) protocol was proposed by Karn [8]. MACA includes a three-way handshake involving the exchange of RTS-CTS-DATA to establish connectivity between source-destination pairs before the transmission of data packets, thus avoiding collisions.

Fullmer et al. proposed FAMA (Floor Acquisition Multiple Access), in which the carrier sensing feature was used. It solved the problem of the hidden terminal and identified the conditions required to ensure no collisions happen in the transmission of data packets [9]. FAMA requires long RTS and CTS packets to guarantee collision-free transmission. However, in the underwater acoustic channel, where transmissions are expensive, excessively large control packets might be too energy expensive.

In order to reduce these high energy costs, Slotted FAMA (S-FAMA) uses time slots, in the same way as slotted aloha, to reduce the control packet size. The slot length is equal to the maximum propagation delay plus the transmission time of a CTS packet, which assures that only control packets may collide [10]. One major difference between these two protocols is that 4-way handshaking (RTS/CTS/DATA/ACK) is utilized in S-FAMA while 2-way handshaking (DATA/ACK) is applied in slotted ALOHA. A drawback of S-FAMA is that two nodes successfully exchanging RTS/CTS packets are not guaranteed to send their data without collision in a multi-hop environment. Due to the high propagation delay in these networks, the cost of losing one ACK is very high, having a significant impact on the performance. This is because the entire RTS/CTS and data transmission cycle repeats, when an ACK fails to reach the receiver.

Shahabudeen et al. proposed a MACA based protocol called MACA-EA, which uses the basic model RTS/CTS/DATA-TRAIN/ACK. It uses a single ACK for a batch of DATA packets (DATA-TRAIN). In case of ACK loss it uses two retry processes: multi-ACK and early-ACK in MACA-EA. In case of S-FAMA, the RTS/CTS based contention cycle and DATA transmission processes are repeated in the same way in case of ACK loss as in MACA-EA. The key differences in S-FAMA and MACA-EA are: early-ACK and multi-ACK features are not present in S-FAMA. S-FAMA sends all packets including DATA only at the start of a slot whereas MACA-EA uses time slotting only for the RTS contention phase. It uses short DATA packets, which are sent as a batch acknowledged by a single ACK at the end. In case of S-FAMA there is no restriction on the size of a DATA packet. Longer DATA transmission can be achieved through the use of a single long DATA packet with one ACK.

We identified the problems in S-FAMA where improvements could be made. Influenced by MACA-EA research, we proposed MultiACK and EarlyACK mechanisms and mathematical expressions were derived for them.

1.3 Objectives

The objectives of this research are:

1. To evaluate and compare various existing MAC algorithms and protocols for underwater communication using wireless sensor acoustic networks.
2. To study MAC strategies for specific UW applications, and provide analytical analysis where feasible.
3. Perform simulations by varying the parameters of the performance metrics, so as to analyze the behavior of the proposed MAC protocol at the receiver end, for a specific underwater application (environmental monitoring).

The novelty in this research is the enhancement in the performance of S-FAMA by incorporating the mechanisms of MultiACK and EarlyACK to improve its efficiency. Another contribution is the formulation of MultiACK and the EarlyACK analytical models for S-FAMA that helps to compute the total delay in the MultiACK and the EarlyACK retry-based protocol. The mechanisms improve the throughput with respect to number of nodes, transmission range and PER for the two mechanisms. This is the first attempt of incorporating the two mechanisms of MultiACK and EarlyACK in S-FAMA without violation of the S-FAMA algorithm.

To achieve the above objectives, we selected some existing protocols and studied their key features, such as throughput, delay, bit error rate (BER) and energy efficiency. We used ns-3 [83] and MATLAB [84], as the software tools for the evaluation and testing of these protocols. Performance has been evaluated by varying parameters such as number of nodes, transmission range, BER, length of data, propagation delay and energy consumed.

1.4 Thesis Organization

This thesis is organized in five chapters, as described below:

Chapter 1 is the introductory chapter which illustrates the problem background, scope, and the wide-ranging applications for UWASNs. A brief summary of the selected MAC protocols with the techniques involved for the underwater acoustic networks are described. The objectives of the research are discussed followed by the thesis organization.

Chapter 2 covers the review of the state of the art in underwater MAC protocols. It includes the environment characteristics, factors that influence acoustic communications, network architecture and connectivity analysis and challenges associated with network architectures that need to be resolved to facilitate 3D monitoring. The underwater MAC protocols of interest are described in detail. The quantitative analysis of these MAC protocols is also shown. The performance of some selected protocols is analyzed as a preliminary work with simulation results followed by conclusion.

Chapter 3 focuses on the theoretical analysis of their research. The chapter covers the S-FAMA protocol overview, S-FAMA model and the detailed analysis of the analytical expressions derived for S-FAMA. The problem statement is discussed. The MultiACK and EarlyACK models for S-FAMA are described in this section. The mathematical analysis of original S-FAMA and derivations of the mathematical expressions for the proposed mechanisms are done in this chapter. The chapter also covers details of the analyzed scenarios, their comparative analysis and their impact on the improvement of energy, delay and throughput for the MultiACK and EarlyACK mechanisms. Total transmission energy wasted and consumed is also analyzed.

Chapter 4 compares the throughput achieved in S-FAMA with that of the two new variants. We use the mathematical expressions derived for MultiACK and EarlyACK in chapter 3, and

the original throughput equation for S-FAMA to obtain the results. We present the analysis as a function of nodes, transmission range, BER, length of data and total transmission energy wasted and consumed. The quantitative analysis of all these results are discussed.

Finally, **Chapter 5** summarizes the research contribution.

CHAPTER 2 : STATE OF THE ART

One of the biggest challenges in underwater communication networks is the design of MAC (Media Access Control) protocols suitable for the harsh characteristics of the underwater environment, which should target high throughput, low delay in channel access, and low energy consumption with the guarantee of fairness to competing nodes [11].

MAC protocols for underwater wireless sensor networks (WSNs) cannot be implemented directly from the existing terrestrial WSN MAC protocols [12, 13]. The unique properties of the underwater acoustic communication path need for new efficient, reliable communication protocols to meet these challenges. This is due to the large propagation delay of sound, extremely low point-to-point data rates and high BER. In fact, owing to the narrow bandwidth, connection losses, multipath, fading and channel asymmetry, channel access control in underwater networks requires additional tasks [5].

The remaining of this chapter is outlined as follows. Environment characteristics are discussed in Section 2.1, followed by the factors influencing acoustic communications. Underwater acoustic sensors networks topologies and connectivity analysis are covered in Section 2.2. Section 2.3 addresses current challenges while Section 2.4 covers the underwater MAC protocols and their comparative analysis. Performance and results of some selected protocols are covered in Section 2.5. Conclusion of the chapter is given in section 2.6.

2.1 Environment Characteristics

Compared to radio waves, sound has superior propagation characteristics in water, making it the preferred technology for underwater communications [14]. The speed of acoustic signals is slightly higher than 1500 m/s, which is 5 orders of magnitude smaller than the speed of radio waves. Thus, for distances of interest, packets experience large propagation delays. Also, current underwater modems can only provide bit rates in the order of tens of kbps in optimal scenarios. These factors have profound implications on ranging and time synchronization [15].

As described in [2], factors like path loss, noise, propagation delay etc. largely influence the underwater communication and constraint the acoustic channel bandwidth. In [15], it is shown that sound propagation underwater is severely affected by transmission loss, noise, reverberation, and temporal and spatial inconsistency of the channel. Transmission loss and noise are the principal factors determining the available bandwidth, range, and signal-to-noise ratio. Time-varying multipath influences signal design and processing, which determine the information throughput and the communication system performance. These peculiar characteristics of the underwater acoustic channel require deeper understanding of the channel characteristics when designing protocols for underwater sensor networks.

The classification of underwater acoustic communication links is shown in Table 2.1. These links are classified as very long, long, medium, short, and very short as per the range shown in the table along with the available bandwidths [4]. As per the direction of the soundwaves, acoustic links may also be classified as vertical and horizontal. In case of horizontal links, a horizontal transceiver is connected to the underwater sink to communicate with the sensor

nodes. The vertical link is used to relay data from underwater sinks to the surface sink. The surface sink may be equipped with an acoustic transceiver that can handle multiple parallel communications with the deployed underwater sinks. As mentioned in the oceanic literature, *shallow water* denotes water with depth less than 100 m, while *deep water* is used for deeper oceans.

Table 2.1: Bandwidths for different ranges in underwater acoustic channels. [4], [16]

Span	Range [km]	Bandwidth [kHz]
Very Long	1000	< 1
Long	10--100	2—5
Medium	1—10	≈ 10
Short	0.1—1	20—50
Very short	< 0.1	>100

Sound absorption loss in water increases with frequency. Therefore, in order to achieve a long transmission range, the UWANs usually operate in low frequencies. For example, only a few hundreds of kilohertz for short range, few tens of kilohertz for medium distance, and few hundreds of Hertz for long range [16]. The available bandwidth is extremely limited because it can never exceed the upper limit of the operating frequency. It is therefore difficult to achieve a high data rate, given that the signal quality in UWANs is also low [17].

Factors that degrade the performance of acoustic communication systems are discussed below [15].

- *Propagation delay*: Terrestrial wireless sensor networks work at radio frequencies (RF); while acoustic sensors work at sonar frequencies (speed of sound $1.5 \times 10^3 \text{m/s}$). This amounts to a propagation delay of $0.33 \mu\text{s}$ for terrestrial, while 67ms for underwater nodes spacing 100m. Also, current modems used in underwater communications provide bit rates only in tens or hundreds. This has profound implications on ranging and time synchronization [18], [19]. It can produce situations in which before a node ends transmission of a packet, the receiver node may start the reception of the same packet. In addition to Trans-receive collisions at MAC layer in underwater sensor networks, receive-receive collisions are also possible due to time variant large propagation delays. The large propagation delay may break or significantly degrade the performance of many existing protocols.
- *Noise*: A signal in ocean must be detected in background of ambient noises like seismo-acoustic, shipping, bio-acoustic, wind and rain. A number of frequency bands in the spectrum can be associated with readily identifiable noise sources. Frequencies below 1Hz are associated with noise of hydrostatic origin (tides and waves) or with seismic activity. For a frequency in band 1Hz -20Hz oceanic turbulence is the most likely source of noise in deep waters; frequencies in band 20Hz -500Hz are dominated by noise due to distant shipping traffic and sea surface. Higher frequencies are affected by thermal noise originating in the molecular motion of the sea. Underwater acoustic communication is in the frequency range between 200 Hz and 100 kHz. In this frequency range the dominant noise source is wind acting on the sea surface. Noise levels in the ocean have a critical effect on sonar performance. Knudsen [20] has shown a correlation between ambient noise and wind force or sea state. Ambient noise increases about 5dB as the wind strength doubles. Peak wind noise occurs around 500 Hz, and then decreases

about 6dB per octave. At a frequency of 10,000 Hz the ambient noise spectral density is expected to range between 28 dB/Hz and 50 dB/Hz relative to 1 μ Pascal. This suggests the need for wide range control of transmitter power.

- *Bandwidth* The available bandwidth is severely limited [21]. For ranges of 0.1Km and 1000 Km, bandwidths of nearly 100 KHz and 1 KHz respectively are possible. Thus, we expect fairly low data rates in comparison to terrestrial wireless communications. This warrant requirement for efficient physical layer and tradeoff in system design based on available power and channel bandwidth. Application-level techniques need to be explored to maximize the benefits of even limited communication rates.
- *Attenuation* The UW channel is badly affected and signal is weakened, because of attenuation, absorption, multi-path and fading problems. Absorptive losses at 12.5 KHz are 1dB/Km, while at 70 KHz they are 20dB/Km, thus restricting the use of higher frequencies. Attenuation is dependent on frequency as well as distance.
- *Shadow zones and channel characteristics* Sound speed underwater is varying and dependent on salinity, depth and temperature. High BERs and momentary disconnect occurs in shadow zones because of the harsh features of the UW channel.

2.2 Underwater Acoustic Sensor Networks and Connectivity

An Underwater Acoustic Sensor Network (UASN) consists of underwater sensor nodes which are connected via acoustic links to achieve collaborative tasks [22]. Underwater acoustic sensor network deployments may be used in applications for environmental, scientific, military, and commercial purposes. Several topologies are in use, but the most widely used topology is linear. Indeed, placing nodes on a single line offers more opportunities in terms of large coverage and high-rate services [23].

As terrestrial sensor networks, in UASNs it is essential to deliver communication coverage in such a way that the whole monitoring area is covered by the sensor nodes, where every sensor node must be able to set up paths, possibly multi-hop, in order to reach a surface sink. In three-dimensional underwater networks, sensor nodes float at different depths in order to observe a given phenomenon. They can collect data and also help relay data to the sink [24]. William S. Burdic, in his book [25], talks about underwater acoustic systems analysis. It covers information on acoustic signals and how to calculate sonar systems performance. The book provides information on acoustic transducers, sound transmission in the ocean and effects of ambient noise in the ocean.

Figure 2.1 shows an example of an UASN. It consists of multiple sensor nodes that accomplish collaborative monitoring in a given volume. Three sink nodes are deployed on the water surface, equipped with both radio-frequency and acoustic modems. The sink nodes receive acoustic signals from the sensors and transmit the packets to the control center ashore through radio-frequency signal.

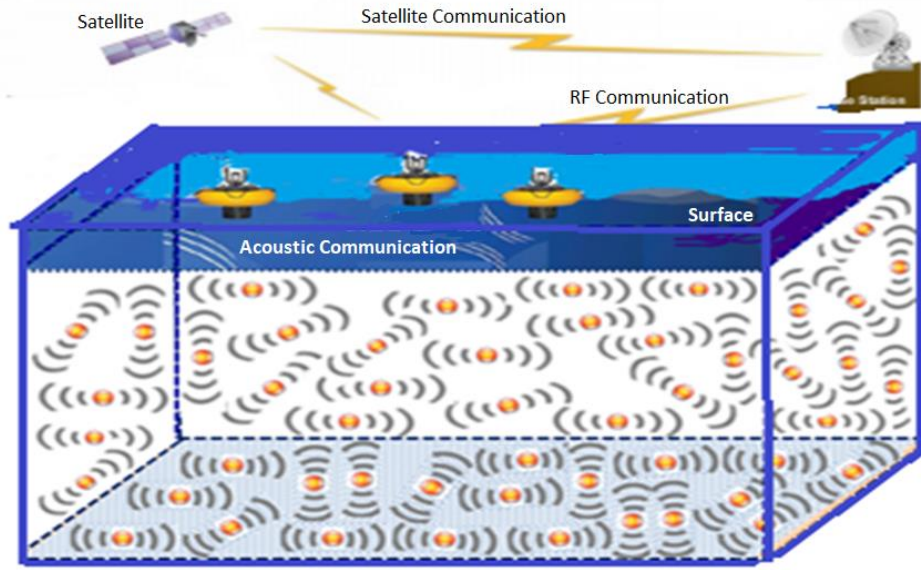


Figure 2.1 Example of Underwater Acoustic Sensor Network with multiple nodes and three surface sinks.

There are several different topologies for Underwater Acoustic Sensor Networks, depending on the application [3]:

- Two-dimensional Underwater Acoustic Sensor Networks for ocean floor monitoring: These are formed by sensor nodes which are fastened to the base of the ocean, Figure 2.2. Environmental monitoring, or monitoring of underwater plates in tectonics are some of the applications of these networks.

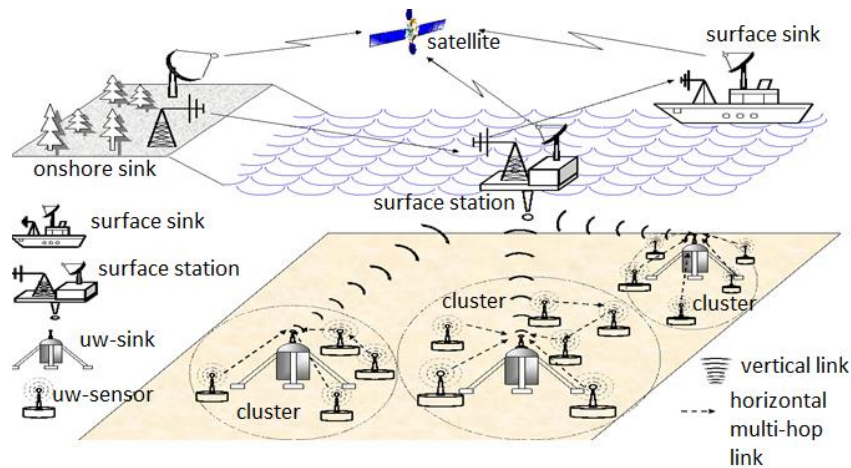


Figure 2.2: Two-dimensional Underwater Sensor Networks [16]

As explained in [3], underwater sensor (uw-sensors) nodes are attached to the floor of the ocean in clusters. These uw-sensors are interconnected via wireless acoustic links to one or more underwater sinks (uw-sinks). These uw-sinks transfer data to the surface station. Uw-sinks are equipped with vertical and a horizontal transceiver: i) to direct commands and configuration data to the sensors; ii) to gather monitored data. The vertical link relays data to the surface station, which is furnished with an acoustic transceiver. The acoustic transceiver is capable of handling multiple simultaneous

communications with the installed uw-sinks. Deep water applications require long coverage transceivers as the depth of the ocean can be as deep as 10 km. It can connect with the *onshore sink* (os-sink) and/or to a *surface sink* (s-sink) via long range RF and/or satellite transmitter.

- Three-dimensional underwater acoustic sensor networks: In these networks, the depth of the sensors may be controlled [2, 3]. 3D UW networks can be applied to identify phenomenon which are difficult to observe by means of sensor nodes at the bottom of the ocean. In these networks the floating sensor nodes at different depths monitor and collect data for a given phenomenon. Sensor nodes could be attached to the surface buoy through adjustable wires, to adjust the depth of each sensor node. Multiple floating buoys could obstruct the ships sailing on the surface and they could be easily detected by the enemies and deactivated. Typical applications are surveillance and monitoring of oceanic phenomenon.

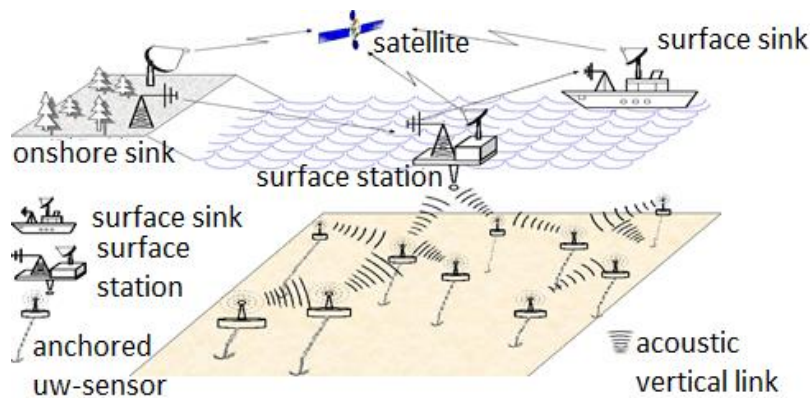


Figure 2.3: Three-dimensional Underwater Sensor Networks [16]

An alternative approach would be to anchor each node to the bottom of the ocean. Depicted in Figure 2.3, each anchor is equipped with a floating buoy and is anchored to the bottom of the ocean. The floating buoy is inflatable by a pump. It pushes the sensor towards the surface of the ocean. The sensor's depth could be regulated by adjusting the wire length that connects it to the anchor and is controlled electronically by an engine residing on the sensor.

For applications such as long term underwater monitoring, the sensor nodes are densely deployed. This is because laying cables underwater for a large area is very costly. Underwater wireless sensor networks solves the problem. Firstly these smart sensors are very economical, so a large number of them can be deployed to cover a large monitoring area with enough density. Second, it can be easily deployed. It does not require special planning or extensive cable connections. Usually the neighboring nodes are only a few tens to hundreds meters apart. The MAC protocol for such underwater sensor networks should be designed to resolve data packet collision efficiently in terms of energy consumption. As the sensor nodes are mostly powered by batteries, it is difficult to change or recharge these batteries in harsh underwater environments [26].

2.3 Challenges

Various challenges evolve and must be resolved so as to allow 3D monitoring. The challenges posed by the underwater channels for underwater sensor networking comprise the following [2], [3]:

- *Range of Sensing:* Sensors must collaboratively control their depth in order to achieve full column coverage, consistent with their sensing ranges. Therefore, it must be doable to acquire sampling of the wanted phenomenon at all depths.
- *Range of Communication:* In 3D underwater networks there is no notion of underwater sink, sensors must have the ability to convey data to the surface station by means of multi-hop paths. Therefore, network devices have to direct their depths in such a way that the network topology is always connected, i.e., at least one path should always be there between every sensor node and the surface station.

In practice [23], some application scenarios involve unicast delivery within a fully connected zone or, equivalently, within a single collision domain. A simple example is the sensor network case where each node has to transfer the data it has collected to specific destination nodes. Other applications may bring nodes to share navigation information, command and control system instructions, or even predefined messages for node safety. This may require the use of broadcast traffic. When the extent of the area to be covered gets larger, it becomes necessary to use multi-hop relaying where a long distance is divided into multiple shorter hops in order to reach the destination node.

The challenges faced in the design of underwater acoustic networks include:

- *Energy:* In underwater acoustic networks, sensor nodes are mostly powered by batteries. The power of the battery is constrained and generally it is not easy to recharge them, since solar energy is not reachable [21]. Further, the high bit error rate and delay in propagation in underwater environment results in energy waste.
- *Failure:* Fouling and corrosion can cause failure in UW sensors [21]. Fouling is caused by incrustation or deposits of undesired materials on the sensors surface and reduces its efficiency, while corrosion is a natural process. It causes gradual destruction of materials due to rusting.

Challenges for MAC Protocols.

The biggest challenge in the design of underwater MAC protocol is the environment in which they operate. Hence the following issues must be addressed in every protocol [27]:

- *Connectivity.* The ability of a node to hear transmission of another node depends upon the transmission power used, on the distance between the two nodes and on the sensitivity of the receiver on the receiving node. Connectivity patterns could be single-hop, dual hop or multihop.
- *Type of Channel.* The medium through which data is transferred from its source to destination. Errors may occur even when single transmission is heard at a node and, the errors between successive transmissions are not independent. Collision is a situation in which, at the receiver, two or more transmissions overlap in time wholly or partially.
- *Synchronization.* When users are not synchronized they can access and transmit their data on the channel at any time. Collisions may occur, and data has to be retransmitted. Slotted systems is an important class of systems in which a global clock exists and marks equally long intervals of time called slots. Transmission of data in such systems occurs

only at the slot boundaries. Synchronization of various degrees is required in slotted protocols.

- *Feedback.* This information can be obtained either by listening to the channel or by acknowledgement messages from the receiving node.
- *Message size.* It is possible that a very long message may not be transmitted in a single transmission. Such messages are split into smaller units called packets. Packet size is measured by the time required to transmit the packet once the channel access has been granted. Packets could be of equal size or randomly varying.
- *Generation of Message.* Packets may be generated by identical users according to a Poisson process. Analyses in the literature show non-Poisson generation processes, where users are not identical. For example, there may be one heavy user and many identical small ones.
- *Number of users.* The user population could be finite or infinite. Conflict-free protocols fail if the user population exceeds a certain limit. Contention based protocols are preferred in such cases.
- *Buffering capability.* Every user is assumed to have a buffer for a single message. It can only generate a new message when the buffer is empty. An alternative could be more buffering, for both finite and infinite, at each user.

2.4 MAC Protocols

As in all shared-medium networks, a medium-access control (MAC) protocol is necessary to regulate and coordinate medium access.

A variety of MAC protocols have been studied for underwater acoustic networks. Mandar Chitre, et al. [6] classifies underwater wireless sensor network (WSN) MAC protocols into: Contention-based (non-orthogonal) and Contention free (scheduled, orthogonal or deterministic) protocols. Examples of Contention based protocols include: Half duplex ALOHA, ALOHA with Acknowledgement (ACK) and retries, ALOHA-CS, CSMA, Medium Access Collision Avoidance (MACA)-based, DACAP etc. Scheduling based MAC protocols assign collision free links to each node in the neighborhood, usually during initialization phase. Links may be assigned as time slots (TDMA), frequency bands (FDMA) or spread spectrum codes (CDMA). Examples of Contention free protocols includes TDMA, FDMA, CDMA, SDMA (Space Division Multiple Access), S-TDMA, UW-MAC etc.

Recent MAC protocols for underwater communication are mostly based on carrier-sense multiple access (CSMA) or code division multiple access (CDMA). In [5], Dario Pompili, et al. showed that CSMA based protocols are susceptible to both hidden and exposed terminal problems. Frequency-division multiple access (FDMA) is not appropriate for the underwater environment owing to the narrow bandwidths and the susceptibility of narrow band systems to fading and multipath. Furthermore, TDMA exhibits a limited channel exploitation efficacy in large-scale networks for the long time guards needed in long-haul UWA links. Moreover, the varying delay produced by multipath renders it very difficult to execute an exact synchronization through a common timing reference.

To overcome the weaknesses of TDMA and FDMA, and to utilize system resources efficiently, Code Division Multiple Access (CDMA) was designed. It resolves the issue of wasting idle resources. The system assigns the complete available frequency spectrum to each user and permits the users the facility to transmit over all time [28].

CDMA [29] is a conflict-free multiple access technique which is favorable for forthcoming underwater networks. Multi-user spread-spectrum approaches comprise frequency hopped spread spectrum (FHSS, using FSK modulation, and lower data rates) and direct-sequence spread spectrum (DSSS, using PSK modulation, and higher data rates); the term CDMA usually refers to multi-user DSSS. Each user is allotted a different spreading code with which to transmit. While this decreases each user's throughput compared with the single-user case, users can convey packets without colliding with transmissions from other users. This would efficiently solve numerous of the MAC hitches related to high propagation delay. Moreover, CDMA has no hard limit on the number of users, and DSSS-based CDMA can perform especially well in multipath environments. CDMA is more tractable in radio channels than in underwater acoustic channels [30]. According to [31] and [11], CDMA is a promising technique for the underwater environment. It is very favorable for frequency-selective fading. It uses Rake filters at the receiver, for compensating the effect of multipath. The receivers can distinguish the signals transmitted at the same time by several devices. CDMA reduces energy consumption and increases throughput of the network by increasing channel reuse and reducing retransmissions of packets

S. Han et al. in 2013 proposed the Multi-session FAMA (M-FAMA) algorithm [32]. The protocol uses long propagation delay in underwater communication to transmit multiple packets simultaneously in the underwater channel, to improve the overall throughput. It uses a Bandwidth Balancing algorithm that guarantees max-min fairness across multiple contending sources. Simulation results show that M-FAMA significantly outperforms existing MAC protocols in representative streaming applications.

In [33] a Full-Duplex Collision Avoidance, FDCA, MAC protocol is proposed. FDCA is an RTS/CTS-based protocol that permits multiple packets concurrently in the underwater channel, thus, improving the throughput. Inspired by FAMA [34], FDCA reduces collisions in the case of channel contention by imposing wait times on the transmissions of control packets. Therefore, the following two conditions are implemented for collision free transmission in FDCA:

- (i) RTS wait time (the time between RTS transmission and reception of CTS at the transmitter) should be greater than the maximum propagation delay (the time for a transmitted packet to reach its maximum transmission range);
- (ii) CTS wait time is equal to the RTS transmission time plus 2 times the maximum propagation delay.

In FDCA, control packets are transmitted using Aloha to achieve channel reservation. If there are no collisions, the node can transmit the DATA packets to the destination node. The low throughput in underwater networks is due to the acoustic waves that cause long propagation delay and the acoustic modems that operate under half-duplex mode. Unfortunately, most MAC protocols are designed for half-duplex modems. The paper models and analyzes the impact of full-duplex modem characteristics on the Aloha protocol. FDCA is a handshaking based protocol that is designed for full-duplex modems to maximize network throughput. Collision avoidance schedule algorithm avoids the collisions at both the receiver and the sender by passively acquired local information (neighboring nodes' propagation delay and expected transmission schedules). Moreover, to cope with the channel's long propagation delay, it launches multiple simultaneous handshaking processes with neighbors to concurrently propagate multiple packets in the underwater channel. FDCA has been compared with state-of-the-art underwater half-duplex protocols such as M-FAMA [32], a variation of FAMA [9] briefly described in section 1.2 and DOTS [35]. The throughput of FDCA is found higher than

M-FAMA and DOTS by 41% and 80% in the single-hop network and by 58% and 87% in the sea swarm network. In FDCA, nodes can initiate multiple handshaking processes with their neighbors achieving temporal and spatial reuse to maximize throughput. Since M-FAMA and DOTS are half-duplex MAC protocols, the throughput of FDCA is higher. This is because full-duplex operation doubles the theoretical bandwidth of the connection [36]. If a link normally runs at 1 Mbps but can work in full-duplex mode, it really has 2 Mbps of bandwidth (1 Mbps in each direction). Also in full-duplex each direction has dedicated bandwidth and collisions cannot occur. This removes the delay and retransmissions that occur in a shared medium.

Xueyuan Su et al. in [37] proposed a Cross-Layer MAC Protocol for Underwater Acoustic Sensor Networks. It communicates with a price-based rate allocation scheme at the network layer. Fully meshed subgraphs in the flow contention graph, called cliques are used. To precisely reveal the clique limitations of the wireless medium, the clique-based price is generalized to act as the congestion signal, which controls the end-to-end rates of multi-hop flows. A maximal clique is a clique that is not a subgraph of any other clique. The MAC protocol then schedules contention-free packet transmissions of single-hop subflows in each maximum clique. Both the MAC protocol and rate allocation algorithm are simple and straight, thus having low computational complexity. Through analysis and simulation, it is shown that the proposed MAC protocol enables multi-hop flows to acquire the max-min fair share of the network bandwidth from the end-to-end perspective. The main contributions of the research are: 1) end-to-end flow rate is considered, 2) in the rate allocation, clique based price is employed to accurately reflect the interference limited characteristic of the wireless medium, 3) both static and dynamic flows could be easily handled, and 4) the implementation of both MAC protocol and rate allocation is totally distributed.

Carrier Sense Multiple Access (CSMA) [37] is a technique in which a transmitting node contends with its neighboring nodes to get the channel. Prior to any transmission, it first senses the carrier. If it finds the carrier free, it begins with its transmission; else it will wait for some random amount of time before retransmission. The random time is usually determined by a back-off algorithm. Carrier sensing in CSMA may not prevent packet collisions, however, the typical situation may allow multiple packets to propagate simultaneously. CSMA consumes less processing resources and is suitable for event driven wireless sensor network applications. It is flexible to network scale and dynamics as it requires no clustering or topology information.

In CSMA, transmission is purely handled by the sender. The problem of hidden and exposed-terminals may occur causing high collisions as neighboring nodes compete for the channel simultaneously. Hidden and exposed-terminals problems arise due to lack of connectivity between certain nodes in adhoc networks. In a hidden terminal situation, a node cannot sense some of the nodes that would interfere with its transmission. In an exposed terminal situation, a node delays its transmission when it overhears a transmission that would not collide with it. CSMA performance degrades in the presence of hidden and exposed terminal problems. CSMA and its variants are generally being used to avoid collisions which are caused by simultaneous transmissions by two or more stations. CSMA is effective in networks that are fully connected and have smaller delay as compared to packet duration. The throughput of the protocol rapidly decreases with the increase in delay [38].

The multiple access with collision avoidance (MACA) protocol [8] utilizes control packets to detect and avoid collisions. The control packets are request-to-send (RTS) and clear-to-send (CTS). If a node has packets to send, it first sends out an RTS to the destination node. On hearing the RTS, the destination node immediately sends a CTS back to the source node indicating it is ready to receive packets. After receiving the CTS, the source node starts to send

the data packets. Any other node hearing the CTS defers its own packets transmission until the current transmission completes. If a node hears an RTS but does not hear any CTS later, it will consider itself an exposed node, and will be free to transmit its packets. Hidden nodes will stop packet transmissions on hearing the CTS. Thus, the problems of hidden and exposed nodes are solved in MACA and the throughput increases consequently. Data collisions are minimized through data deferment; the data transmission length is embedded in the control packet. Collisions in MACA may occur due to different packet delays, e.g. when a terminal has one neighbor very close and the other very far or when the node is hidden.

MACA based protocols are found to be highly suitable in many scenarios of UW where scalability is important and time synchronization is not available [6]. Protocol additions and improvements of MACA have been examined to match them better to the underwater channel. A WAIT command extension was investigated. If the receiver is busy it sends back a WAIT command and sends a CTS later ([39], [40]). Performance of protocols such as MACA can be greatly improved by using packet trains. By dividing the DATA segment into packets, RTS/CTS collisions only affects a small number of packets and do not result in complete retransmission of the DATA ([41], [42], [43]).

Bharghavan et al. in [44] modified MACA by applying ARQ (Automatic Repeat Request) techniques for erroneous packets retransmission, which led to MACAW (MACA-Wireless). The overhead (RTS and CTS) itself consumes the limited channel capacity, but the reduction of retransmissions can more than compensate, resulting in increased throughput. However, when applied in UWANs, where there are large propagation delays, the handshaking of control packets results in substantial dead-time, consuming much of the available channel capacity. Moreover, collisions may be more likely to occur due to the short packet duration relative to the large link delay. The above mentioned outcomes in MACA and MACAW result in a low channel utilization [17].

In [35] it is shown that the long propagation delay in an underwater wireless network generates a unique chance for temporal reuse that allows for multiple concurrent packets propagating within the same contention domain. Temporal reuse allows simultaneous, non-colliding transmissions to different destinations if they are adequately removed from one another, solving the exposed terminal problem. A great deal of attention has been focused on using temporal and/or spatial reuse of acoustic channels to improve the throughput.

Wen Lin et al. in [45] proposed a new MACA-based MAC protocol with delay tolerant (MACA-DT). In handshake techniques, when a node has transmitted an RTS packet, it waits for the CTS packet replied by the destination. However, since the propagation delay in UWASNs is very high, the typical handshaking-based approach is less efficient. MACA-DT protocol utilizes these large gaps, which are normally wasted by conventional MACA protocols. It uses adaptive silent time and simultaneous handshake technique. MACA-DT protocol can improve the channel utilization and alleviate the long end-to-end delay. Silent times are used in MACA to avoid packet collision. In traditional fixed silent time, due to long propagation delay the throughput is seriously restricted. MACA-DT uses the adaptive silent time to reduce the silent time of each 'no intended' receiver. In adaptive silent time the silent time of each 'no intended' node is not fixed. It is determined by the propagation delay between the nodes. The adaptive silent time can be classified as the silent time of 'no intended' receivers that hear an xRTS packet and the silent time of 'no intended' receivers that hear an xCTS packet.

MACA-DT operates in two phases: initialization phase and transmission phase. In the first phase it estimates the propagation delay between nodes and all of their neighbors. In the second

phase, it uses three way handshakes similar to the MACA protocol. A node that wants to transmit a data packet will first use a handshake to its intended neighbor by transmitting an RTS packet. When an intended receiver hears the RTS packet, it will respond with a CTS packet immediately, provided that it is currently not involved in a handshake with another node, and is also not required to remain silent. MACA-DT protocol can process multiple handshakes while nodes wait for the CTS packet from receive nodes.

Zhong et al. (2009) [46] proposed the UMACAW (Underwater MACAW) protocol to enhance throughput and decrease delay in UWANs. It tells how to make use of the rest of the time during the RTS-CTS-DATA-ACK exchange period. As the busy duration (the time of transmitting a message) of a node is considerably shorter compared to the exchange period, it results in severe wastage of channel resources. In UMACAW, a node first listens to the channel and closely observes the overheard packets, then it extracts information of both senders and intended receivers and the busy intervals of neighbors. When a node has a packet to send, it transmits immediately provided it does not interfere with the ongoing transmissions. It takes advantage of the long propagation delay in underwater channel. In UMACAW a node can send and receive messages with several neighbors in the RTS-CTS-DATA-ACK exchange period. No collision will take place if busy time slots coming from other nodes have no overlap. This also reduces the hidden and exposed terminal problems. But, clock synchronization is essential in this proposal as added busy duration messages are being used. This can be overcome by inserting guard times in busy slots.

FAMA (Floor Acquisition Multiple Access) [47] is a reservation based MAC protocol which prescribes the exchange of RTS/CTS messages. In its original version, FAMA allows total control of the channel for one station at a time. RTS/CTS control dialogue and carrier sensing eliminate collisions for data packets and substantially increase channel throughput. After data is successfully transmitted, it waits for a confirmation of correct reception (ACK). In case no CTS is received in response to an RTS, the transmitter backs off and reschedules a later attempt. The protocol also includes error control over the data packet by means of stop-and-wait ARQ with infinite retransmissions. FAMA also assumes that, in order to save energy, nodes are deaf during backoff intervals and that nodes transmit RTSs without listening to the channel.

FAMA has Carrier Sensing capability, which was disabled in MACA. Collision Avoidance is guaranteed if following conditions hold:

- a) RTS length should be greater than the maximum propagation delay, and
- b) CTS length should be greater than the RTS length plus twice the maximum propagation delay plus the hardware transmit-to receive transition time.

These conditions are the basis of the FAMA protocol. FAMA ensures no collision in the channel but the length of control packets is excessive on underwater acoustic channels, and this leads to an unacceptable waste of energy. Hence, FAMA is not an efficient protocol for UANs.

Slotted FAMA adds timeslots to FAMA to reduce the impact of propagation delays, Control packets are received by the destination node and all the terminals in the neighborhood of the source node within the slot time. S-FAMA uses the carrier sensing (CS) and the handshaking features before data transmission. In the course of the initial dialogue, control packets are exchanged to avert multiple transmissions simultaneously. Time slotting eliminates the requirement for unduly long control packets, and thus saves energy; it lowers the probability of collisions by aligning packet transmissions into slots.

S-FAMA uses packet trains to increase the efficiency of the protocol. Once the connection is established, a station will send all the packets in the queue to the same location. The oldest packet is sent first, thus lowering end-to-end delay. In each packet sent, a flag will tell the receiving node if the transmitter is sending more packets in the same train. The main issue in Slotted FAMA is that there is no constraint on the maximum DATA packet transmission time. This is the time that stations overhearing a CTS packet have to wait in order to avoid collisions with a concurrent transmission. DATA packets within a train have to be acknowledged one at a time. J. P. Morris in [48] recommends to change the ARQ protocol acknowledging all the packets at the end of the train. Then, the transmitting node would only resend the erroneous packets. This would increase the efficiency of the protocol.

Zhang, S., et al. in [49], proposed Slotted Floor Acquisition Multiple Access-Delay Tolerant (SFAMA-DT) MAC protocol based on S-FAMA, with data train. SFAMA-DT adapts the original S-FAMA for use in high traffic networks. It introduces RTS/CTS sorting scheme to set multiple handshakes simultaneously and then form a train of data packets of multiple transmission pairs during each round of simultaneous handshakes. Its main contribution is that it overcomes the multiple RTS attempts problem in S-FAMA and increases the network throughput by transmitting a train of data packets.

Slotted-FAMA is not preferred for dense networks since the multiple RTS attempts problem in dense networks is serious and substantially limits the network throughput. To overcome this problem, Liang-fang QIAN et al. in [50] proposed a slotted-FAMA based MAC protocol for underwater acoustic networks, referred to as RC-SFAMA, introducing an RTS competition mechanism to keep the network from excessive frequency of backoff because of the multiple RTS attempts. Thus, useful data transmission can be completed effectively whilst the scenario of a couple of RTS attempts takes place. Simulation results display that RC-SFAMA increases the network throughput performance compared to Slotted-FAMA, and minimizes the energy consumption.

In [51], performance of three MAC protocols, namely, random access based UW-Aloha, handshaking based SASHA, and scheduling based pipelined transmission MAC (PTMAC), have been compared in the real sea environment of Atlantic Ocean with nine nodes connected in a multi-hop string network. The three protocols were tested at both packet and node behavior levels. Their end to end throughput, delay, and packet delivery ratio were analyzed. From their real sea environment experiments they revealed the high packet loss rate and significant channel asymmetry, temporal and spatial transmission range uncertainty and delayed data transmissions effects on performance of MAC.

Nils Morozs et al. investigated the application of underwater acoustic sensor networks for large scale monitoring of the ocean. They proposed two Medium Access Control protocols, namely Transmit Delay Allocation MAC (TDA-MAC) and Accelerated TDA-MAC. They are capable of providing Time Division Multiple Access (TDMA) to sensor nodes without the need for centralized clock synchronization. A thorough simulation study of a network deployed on the sea bed showed that the proposed protocols are capable of closely matching the throughput and packet delay performance of ideal synchronized TDMA. The TDA-MAC protocols also significantly outperform T-Lohi, a classical contention-based MAC protocol for underwater acoustic networks, in terms of network throughput and, in many cases, end-to-end packet delay. Furthermore, the assumption of no clock synchronization among different devices in the network is a major advantage of TDA-MAC over other TDMA-based MAC protocols in the literature. Therefore, it is a feasible networking solution for real-world underwater sensor network deployments [52].

In [53] a protocol named DN-MAC for the dynamic UASN is proposed to overcome the problem of low channel efficiency in case of classical TDMA in underwater acoustic sensor networks. A new guard time setting method is presented in this paper. It uses some prior information, such as the maximum propagation delay in the network and the maximum relative speed of the sensor nodes with respect to the center node and the mechanism of the packet transmission for the sensor nodes. By using the maximum propagation distance and the maximum relative velocity with respect to the center node, the recommended guard time can be set in the initialization period and the data transmission period to avoid collisions. Analysis and simulations show that the proposed method can reduce the time interval of the data packets received at the center node, which can improve the channel efficiency and the performance of the dynamic UASN effectively.

Distance Aware-Collision Avoidance protocol (DACAP) [54] is based on MACA. Nodes do not need to be synchronized, can move, are half-duplex, and use the same transmission power. DACAP focuses on minimizing the duration of time slots that differ from each other, and minimizes the duration of a hand-shake by taking advantage of the receiver's tolerance to interference when the two nodes are closer than the maximal transmission range. This protocol achieves a throughput several times higher than that of the Slotted FAMA, while offering similar savings in energy.

UWAN-MAC in [55] is an Energy-Efficient MAC Protocol that can be used for delay-tolerant applications such as underwater environmental monitoring. Energy is the main performance metric rather than bandwidth utilization. Authors show that under a realistic underwater sensor network scenario, this MAC protocol wastes only 4% of the transmit energy and only 1.5% of the energy due to collisions, when the average number of neighbors is four, and the duty cycle is 0.004 %.

In [56] L. T. Tracy and S. Roy, proposed Reservation Channel Acoustic Media Access Protocol (RCAMAC), which uses channel reservation scheme and is based on the RTS/CTS handshaking method. RCAMAC is quite suitable for UWASNs as it uses a channel reservation scheme. It segments the available bandwidth into control channel and main channel, so that, if there is data to send, it reserves channel time by first transmitting RTS packets in a control channel. It can help to minimize the probability of data packet collisions.

ALOHA does not check the channel state before packet transmissions. Collisions occur when two packets arrive at one node concurrently. This leads to packet loss and significantly reduces the throughput. Therefore, ALOHA does not work well in busy traffic networks. The maximum throughput of ALOHA is only 18.4% i.e., 81.6% of frames end up in collisions and are therefore lost. The peak throughput is achieved when the offered load is $G=0.5$ packets per packet transmission time or 50 percent of normalized offered load to the channel [17].

L. G. Roberts in [57] gave the idea of slotting the time to increase the capacity. The duration of the time slot was equal to the packet transmission time. The packets were transmitted at the beginning of the time slot. Slotted ALOHA has approximately the same performance as pure ALOHA, but with more complicated implementation requirements [58].

In [59], Aloha with half duplex (Aloha-hd) improves throughput and energy waste when the node receives packets destined for itself, else it behaves like pure Aloha. Maximum throughput is around 25%, which is better than the throughput of 18.4%. In Aloha with carrier sense, the busy period information and the propagation delay is estimated from the information received from the overheads of packets. The nodes then compute the time for transmission to prevent collisions. ALOHA with collision avoidance (Aloha-CA) outperforms ALOHA with Carrier

Sense (ALOHA-CS) for different packet sizes. It has better stability than ALOHA-CS at high loads as its throughput does not fall as steeply when the load increases. Aloha with advance notification (Aloha-AN) is an enhanced form of Aloha-CS; it conveys a notification (NTF) packet prior to sending the data packet. Other nodes are then aware of the arrival of the data packet.

Yen-Da Chen et al. in [60], proposed a two-level power control (TLPC) MAC protocol for collision avoidance in underwater acoustic networks. Although IEEE 802.11 DCF is the most famous MAC protocol, it does not work well in underwater environments. TLPC prevents Control/DATA Collision (CDC) and Underwater Large Interference Range Collision (ULIRC) problems. Taking interference into consideration, TLPC adapts the transmission power to resist interference and avoid collisions in order to enhance network throughput. TLPC can not only prevent CDC and ULIRC problems but can also reduce the energy consumption of stations.

Chaima Zidi et al. in [61], proposed a multichannel MAC protocol, MC-UWMAC, a low power MAC protocol operating on multichannel using a single slotted control channel and multiple data channels. To guarantee a collision free communication, MC-UWMAC uses a virtual grid based slot assignment linked with a quorum based data channel allocation. Specifically, control channel slots are dedicated for handshaking. Data transmission takes place in a unique data channel especially reserved for each communicating pair. Simulation results show that MC-UWMAC can greatly improve the network performance especially in terms of energy consumption, packet delivery ratio and end-to-end delay.

UW-MAC, is a CDMA based, power controlled MAC protocol. It is suitable for deep water communications which typically are invulnerable to multipath. UW-MAC targets at attaining three goals, namely, to ensure high network throughput, low channel access delay, and low energy consumption [62], [5]. Throughput Adaptive adjustable and energy-efficient CDMA-based MAC protocol (TAEE-CDMA) focus on the energy efficiency and suppress the MAI problem. Lagrange multiplier method is used to make the node run with minimum energy consumption. The protocol performance is good in decreasing energy consumption and prolonging the network lifetime. It is energy-efficient, real-time and has high reliability [62].

Delay-aware Opportunistic Transmission Scheduling (DOTS) protocol, proposed by Y. Noh et al., exploits passively obtained local information (i.e., neighboring nodes' propagation delay map and their expected transmission schedules) to escalate the chances of simultaneous transmissions while dropping the probability of collisions. DOTS imparts fair medium access even with node mobility and measures throughput and energy consumption per node as a function of the offered load on the sensor network. However, it lacks the support for multiple sessions from the sender, and the channel reuse in DOTS is limited to the receiver side. DOTS consumes more energy than S-FAMA & DACAP, because it delivers by far more frames than these two protocols [35, 63].

MDOTS, enables multiple transmission sessions in DOTS. Here, the term session refers to opening, closing, and managing a communications dialogue between end-user application processes (i.e., a sequence of RTS-CTS-DATA-ACK packet exchanges between a sender and its intended receiver) [35].

TDMA-based MAC protocols have also been designed for efficient data transmission. Each of them has its own advantages and disadvantages. Overall, they minimize data collision, help to decrease energy consumption, and increase transmission efficiency. Their major disadvantage is that it is difficult to use them for real-time data communication. In Time Division Multiple

Access (TDMA) schemes [31], a node can only access its allocated time slot and does not need any contention with its neighbors. TDMA minimizes collisions but the average queuing delay is much higher, as a node has to wait for its allocated time slot before accessing the channel.

The Acoustic Communication network for Monitoring of Environment in coastal area Networks (ACMENet) protocol in [64] employs a time division multiple access (TDMA)-based master-slave network protocol for small networks. Due to the limited battery power of its slave nodes, it is important to minimize their energy consumption of the slave nodes. Slave nodes have a simple design, but the master node is complex. If the master node migrates into large-scale networks, it can face increased collision problems during communication

Super-TDMA MAC protocol, exploits the use of large propagation delays to maximize the network throughput. It is a form of Time Division Multiple Access (TDMA) protocol in which multiple transmissions are allowed in the same time slot and hence concurrently propagate in the medium. Super-TDMA needs frequent switching of transmission and reception modes in the modem. If the underwater acoustic modems are equipped with hardware and software capabilities to achieve better switching times allowing lesser guard periods, the concept of Super-TDMA can prove to be very useful for consideration in future MAC protocols exploiting large propagation delays for UWA networks [65].

Preamble-MAC (P-MAC), [66], is another cluster-head-based MAC protocol. It is a hybrid protocol and employs contention free protocol and slotted MACA. The sink node functions as the cluster head, whereas the sensor nodes send periodically collected data to the sink node. This protocol was developed for implementing an underwater environment data collection system for improving the network throughput by using a dynamic algorithm. It works adaptively and dynamically.

In [67] an Adaptive Propagation-delay-tolerant Collision Avoidance Protocol (APCAP) was proposed. Besides the requirement of RTS and CTS frames, the protocol allows the transmitting node to perform other actions in the period waiting for the CTS. This improves efficiency and throughput when there is a large propagation delay. The mechanism guarantees nodes that can potentially interfere with a forthcoming transmission are properly informed.

Another TDMA-based protocol called the Smart Blocking MAC (SBMAC) protocol [68] has been proposed. It works efficiently on network topologies consisting of master and slave nodes. The main contribution by the authors of the SBMAC protocol is the Smart Calculation Block, which is implemented in the master nodes and determines the policies followed by all the slave nodes. The policies include decisions associated with the transmission period, the data transmission policy (i.e. normal or blocked data), the Acknowledgement (ACK) policy (i.e. No-ACK, Selective-Multiple-ACK, Reduced-Whole-ACK, Multiple-Block-ACK, or Reduced-Block-ACK), etc., The master node broadcasts a beacon message containing the transmission mode, ACK mode, TDMA interval information, gain, and guard time. The main mechanism of this protocol minimizes the transmission amount by calculating control frames for different kinds of transmission methods.

Miguel-Angel Luque-Nieto, et al. in [69] use Spatial-TDMA(S-TDMA) for fixed networks. In this paper, a scheduling procedure to obtain the optimal fair frame is presented, under ideal conditions of synchronization and transmission errors. The main objective is to find the theoretical maximum throughput by overlapping the transmissions of the nodes while keeping a balanced received data rate from each sensor, regardless of its location in the network. The procedure searches for all cliques of the compatibility matrix of the network graph and solves a Multiple-Vector Bin Packing (MVBPP) problem. This work addresses the optimization

problem and provides analytical and numerical results for both the minimum frame length and the maximum achievable throughput.

In [70], Xiaoning Feng et al. proposed a ‘Distributed Receiver-oriented Adaptive Multichannel MAC’ (DRAMAC) protocol. DRAMAC is based on single transceiver in long-delay UWSNs, to reduce the hardware cost. DRAMAC dynamically selects the channel negotiation strategy according to the packet length and the receivers’ network load condition. Using the neighbors’ cooperation information it can detect collisions. DRAMAC achieves a lower delay by using as few communication times as possible during the channel negotiation phase. DRAMAC can significantly improve the network throughput.

Chao Li et al. in [71] proposed a novel distributed delay tolerant MAC protocol (DTMAC) inspired by the coupon collector’s problem. If a node needs to send a packet, the packet will be repeatedly transmitted m times, with a transmission probability to be p . Under the traditional protocol interference model, we first set up a probability model for throughput of DTMAC, and then give the throughput-optimal value for m and p with the successful transmission probability as tuning parameter. As no acknowledgement or channel reservation is used, the throughput of DTMAC is not influenced by propagation delay. In addition, the space unfairness problem no longer exists since DTMAC is not concerned with transmission distance. The simulation results show that the throughput of DTMAC greatly outperforms that of MAC protocols with RTS/CTS scheme in most underwater scenarios.

Clustering is an effective and practical way to enhance the performance of UWSNs. In this paper, Ming Xu et al. proposed a secure MAC protocol for cluster-based UWSNs, called SC-MAC, which aims to ensure the security of data transmission. In SC-MAC, the clusters are formed and updated dynamically. MAC layer information is leveraged by considering the link quality as well as the residual energy of the modem’s battery. After the successful mutual authentication, all sensor nodes from different clusters can protect the data transmission in the continuous communication [72].

2.4.1 Performance Overview of MAC Techniques

An analysis of the performance of state of the art adhoc-based/Cluster-head-based MAC protocols has been compiled in this section.

The Cluster-head-based MAC protocols such as ACMENet, TDMA, P-MAC and SBMAC and Adhoc-based MAC protocols, which includes ALOHA, S-FAMA, RCAMAC, DACAP, UWAN-MAC, were analyzed and compared for throughput performance, bandwidth, probability of error, energy consumption, offered load and fairness in [73]. The throughput performance of cluster-head-based MAC protocols showed that P-MAC has high level of throughput (0.285), whereas SB-MAC is 0.275, TDMA is 0.24, and ACMENet is 0.23.

The throughput analysis of Adhoc-based MAC protocols shows that pure Aloha has the lowest throughput (0.45) compared to the throughputs of other protocols. This is due to the frequent collisions and retransmissions that take place as the number of nodes increases. Throughput of S-FAMA was found to be the highest (0.63), RCAMAC (0.6) is slightly less than S-FAMA. DACAP has throughput less (0.53) than S-FAMA and RCAMAC while UWAN-MAC’s throughput is 0.46 [73]. Performance analysis of some Adhoc based and Cluster head based MAC protocols is presented in Tables 2.2 and 2.3.

It was analyzed that ACMENet has almost 0.35 packet collision probability and low collision avoidance (0.65), while TDMA shows a collision probability of 0.32; P-MAC has high level (0.725) of collision avoidance, and SBMAC has a packet collision probability of 0.287.

The packet collision probability of pure Aloha was higher (0.7) than that of other Adhoc-based MAC protocols, hence ALOHA has lowest (0.3) collision avoidance; S-FAMA has the lowest (0.14) collision probability, hence high (0.86) collision avoidance; DACAP has medium (0.44) collision probability hence collision avoidance of (0.56); RCAMAC has low collision probability of 0.25, hence high collision avoidance of 0.75. UWAN-MAC has medium (0.39) collision probability and medium (0.61) collision avoidance [73].

The received energy consumed by a receiver for the failed deliveries due to collisions was analyzed. The fraction of received energy wasted is at most equal to the fraction of transmission energy wasted. It was noted that for the special case in which all the packets have the same duration, this fraction of received energy wasted due to collisions reduces to the collision rate [65]. The transmission energy wasted due to collision in pure Aloha was higher than that of other ad-hoc-based MAC protocols [73].

Throughput as a function of offered load for DOTS and three CSMA protocols namely S-FAMA, DACAP, CS-ALOHA with ACK protocols' performance was evaluated. The results showed that DOTS outperforms S-FAMA and CS ALOHA by two times and DACAP by 70% [35].

The quantitative analysis of ad-hoc-based (ALOHA, S-FAMA, RCAMAC, DACAP, UWAN-MAC), and Cluster-head-based (ACMENet, TDMA, P-MAC and SBMAC) was carried out using Cluster-head-based and ad-hoc-based MAC topologies as shown in Figure 2.4 (a) & (b).

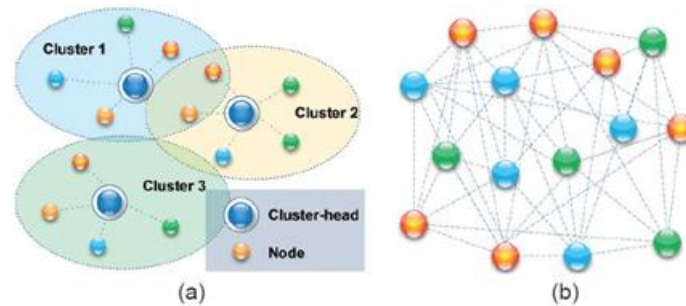


Figure 2.4: (a) Cluster-head-based and (b) ad-hoc-based MAC topologies [73].Source: <https://www.tandfonline.com/action/showCitFormats?doi=10.4103%2F0256-4602.123119>

The parameters used to analyze performance of ALOHA, S-FAMA, RCAMAC, DACAP, UWAN-MAC are shown in Table 2.2 [73].

Table 2.2: Parameters used in the quantitative analysis.

Parameters	Values
Network Area	500 m × 500 m
Data rate	1 kbps
Data transmission duration	200ms
Control packet transmit duration	< 80ms

Acoustic speed	1500m/s
Number of nodes	1-100
Transmit power	< 100W

The topologies used in [35] by Youngtae Noh et al. to analyze and compare DOTS and three CSMA protocols, S-FAMA, DACAP, CS-ALOHA with the performance of ACK protocols are shown in Figure 2.5 and Figure 2.6.



Figure 2.5. Line Topology [35] Source: <https://goo.gl/images/Xg2CFt>

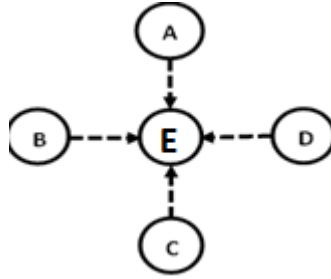


Figure 2.6. Star Topology [35] Source: <https://goo.gl/images/Xg2CFt>

Line (4-nodes) topology and star (four nodes and one sink) topology, in a 3D region of 5km x 5km x 5km were used. Simulation duration was kept at one hour per run. Data frames of size 512 bytes were transmitted and the transmission range was 750m. As indicated previously, their results showed that DOTS outperforms S-FAMA and CS ALOHA by two times and DACAP by 70% [35].

The summary of the quantitative analysis of Medium Access Control techniques is shown in Table 2.3 and Table 2.4. It indicates the name, topology, internodal distance, collision probability, energy consumption throughput, propagation delay, and fairness parameters for MAC protocols. For cells where data is not available (NA) is used.

Table 2.3: Quantitative Analysis of MAC Protocols

Protocol	Topology	Inter-Node Distance	Collision Avoidance	Energy Consumption	Throughput	Delay	Real time	Performance metrics
Pure ALOHA	Adhoc-based 2-D (300m x 300m)	1341 m	0.3	12000W	0.45	NA	Yes	Throughput
ALOHA-HD	Adhoc-based 2-D (3km x 3km)	1341 m	NA	NA	0.25	NA	Yes	NA

CS-ALOHA	3-D (5km x 5km x 5km) Line & Star	Line: 750m to 1.5km Star: 750m to 1.5 km	NA	High 12000W	0.425 (line) 0.002 (Star)	2.07s (Line) & 3.86s (Star)	Yes	Throughput
ALOHA-CA	Adhoc-based 2-D (3km x 3km)	1341 m	NA	NA	0.45	NA	Yes	Throughput
ALOHA-AN	Adhoc-based 2-D (3km x 3km)	1341 m	0.6	NA	0.59	NA	Yes	Throughput
S-FAMA	3-D (5km x 5km x 5km) Line & Star	Line: 750m to 1.5km Star: 750m to 1.5 km	0.86	2900W in Line & 5000mWhr in Star	0.63 0.04	Min 5.05s. (Line) Ave. 20.93 (Star)	No	Throughput & delay
DACAP	3-D (5km x 5km x 5km) Line & Star	Line: 750m to 1.5km Star: 750m to 1.5 km	0.56	3800W in Line & 6000mWhr In Star topology	0.53 0.046	Min 4.06s (Line) Ave 16.23s (Star)	No	Energy
DOTS	3-D (5km x 5km x 5km) Line & Star	Line: 750m to 1.5km Star: 750m to 1.5 km	NA	9000mWhr (Higher than SFAMA & DACAP in Star topology)	0.08	Min. 4.16s (Line) Ave 8.86s (Star)	No	Throughput & fairness
RCAMAC	Adhoc-based 2-D (500m x 500m)	NA	0.75	3000W	0.6	NA	Yes	Channel Utilization
UWAN-MAC	Adhoc-based 2-D (500m x 500m)	100m	0.61	4400W	0.46	0.2s	Yes	Energy
MACA-EA	Sea Trial	Max. 400-500m Min. 200m	NA	NA	0.25	0.4s	NA	Throughput
MACA-WAIT	Sea Trial	Max. 400-500m Min. 200m	NA	NA	NA	0.5s	NA	Throughput & Energy
MACAW	NA	NA	NA	NA	NA	NA	NA	Throughput

Table 2.4: Quantitative Analysis of Cluster-Head-Based MAC Protocols

Protocol	Topology	Inter-Node Distance	Collision Avoidance	Energy Consumption	Throughput	Delay	Real time data communication	Performance metrics
ACMEN et	Cluster-head-based (500mx 500m)	NA	0.65	5500W	0.240	NA	No	Throughput & Collision avoidance
TDMA based MAC in UWN	Cluster-head-based (500mx 500m)	NA	0.68	4800W	0.245	NA	No	Delay & Throughput
P-MAC	Cluster-head-based (500mx500 m)	NA	0.725	4250W	0.277	NA	No	Throughput ; delay; energy consumption
SBMAC	Cluster-head-based (500mx500 m)	NA	0.713	4000W	0.275	NA	No	Throughput
UW-MAC CDMA-based protocol	3-D shallow water (500x 500 x 50) m ³	NA	NA	15μJ/bit	0.8	1.5s	No	Energy
TAAE-CDMA	(300x300x 20)m ³	NA	NA	0.5J/pkt at 1.2pkt/sec arrival rate	NA	5.1s at 1.2pkt/sec arrival rate	Yes	Energy

2.5 Analytical Study

The throughput is an important parameter for measuring the performance for reliable data transfer. Some papers term it as “Saturation Throughput,” that is the network throughput when at all times it has data to transport [74]. This measure also determines the utilization of the channel or efficiency. The normalized throughput is defined as the number of successfully transmitted packets per unit of time normalized by the system capacity [75].

In this section the performance of existing MAC protocols, namely: ALOHA, CSMA, MACA, MACA-EA, S-FAMA is shown. Poisson arrivals have been considered for the offered traffic [69], [75] & [42].

The throughput (S) of Pure ALOHA is given by (2.1), and its maximum is 18.4%, which occurs at an offered load of 50% the maximum capacity [27].

$$S = Ge^{-2G} \quad (2.1)$$

Where S is the throughput, G is the normalized offered load, If T is the packet length, the vulnerable time is $2 \cdot T$ and $G = g \cdot T$ is the normalized offered load, being g the offered load. The maximum throughput is $1/(2e)$ frames per frame-time.

The throughput of Slotted ALOHA [53] is 36.8%, as collisions of packets are reduced. But if there is a delay in propagation, its performance degrades to pure ALOHA. The throughput is given by (2.2) [70]:

$$S = Ge^{-G} \quad (2.2)$$

The throughput of the CSMA (S_{CSMA}) is expressed by (2.3):

$$S_{CSMA} = \frac{Ge^{-Ga}}{G(1 + 2a) + e^{-Ga}} \quad (2.3)$$

The parameters shown in (2.3) present normalized quantities with respect to the packet transmission time. The offered traffic is assumed Poisson, with average value 'G' measured in packets per packet transmission time. It consists of both the arrival of new packets and rescheduled packets resulting from collisions and deferred transmission. The ratio of propagation delay to packet transmission time is denoted by $a \geq 1$. Where 'a' is the normalized propagation delay ('normalized' means expressing the propagation delay in unit of the length of data packet). Packet transmission time 'T' is chosen as 1 [76].

The throughput for MACA is given by (2.4) [76]:

$$S = \frac{\bar{U}}{\bar{B} + \bar{I}} \quad (2.4)$$

where S is the throughput per node, \bar{U} is the average useful data transmission time, \bar{B} is the average busy time and \bar{I} is the average idle time. Table 2.5 shows the MACA parameters. The throughput of MACA for the upper bound and lower bound are expressed by (2.5) and (2.6) respectively [21]:

The upper bound throughput $S_{a>x}^U$:

$$S_{a>x}^U = \frac{e^{-Gx}(1 - e^{-G(a-x)})e^{-Gx} + e^{-G(a+x)}}{(\bar{B}_{1min} + \bar{B}_2 + \bar{B}_3 + \bar{B}_{4min} + \bar{B}_5) + \frac{1}{G}} \quad (2.5)$$

The lower bound throughput $S_{a>x}^L$:

$$S_{a>x}^L = \frac{e^{-G(a+x)}}{(\bar{B}_{1max} + \bar{B}_2 + \bar{B}_3 + \bar{B}_{4max} + \bar{B}_5) + \frac{1}{G}} \quad (2.6)$$

Table 2.5. MACA Parameters.

Parameter	Value
\bar{B}_i	Busy period of case 'i'
\bar{B}_1	Case when second RTS is transmitted in the time period $[0, x]$
\bar{B}_2	RTS including the second RTS are transmitted only in the time period $(x, a]$
\bar{B}_3	RTSs including the second RTS are transmitted only in the time period $(a, a+x]$
\bar{B}_4	Case when RTS and second RTS is transmitted in the time period $(x, a]$ and a number of RTS are transmitted in the time period $(a, a+x]$
\bar{B}_5	no RTS is transmitted in the time period $[0, a+x]$

Matsuno et al. have shown that the lower bounds become higher nearly upto the upper bounds for both $x=0.05$ and $x=0.005$, where x represents the RTS recognition time, which is the time required for network node controller (NNC) to recognize an RTS packet. G is the offered traffic and 'a' is the normalized packet delay. For high traffic, when x is small ($x=0.005$), the throughput of MACA is high, whereas it decreases for large RTS recognition times (when $x = 0.05$). The reason is that the chances of data packet transmission failure become higher as the RTS recognition times grows.

Observations suggest that CSMA throughput is higher than that of MACA in the traffic below nearly 3, but the situation gets reversed for the traffic above 3. The authors show that MACA is not always more effective than CSMA for large RTS recognition time [76].

In MACA-EA, L_D is the data packet length and ' $1/L_D$ ' is the system capacity. B packets are sent as a batch in time s_b and only k_D packets succeed on an average, due to decoding and detection losses. Thus, the normalized throughput T per node for MACA-EA is expressed as shown in (2.7) [75].

$$T = \frac{\frac{k_D B}{s_b}}{\left(\frac{1}{L_D}\right)} \quad (2.7)$$

where k_D represents the overall data packet success probability and s_b is the mean batch service time. The mean batch service time is defined as the average delay from the time a batch is intended for transmission (RTS Contention starts) until it is successfully transmitted. B is the batch size. From (2.7) it can be seen that the larger the batch size, the better the throughput. The MACA-EA protocol can achieve good throughput for saturated load [75].

Contention Window is a type of network protocol that permits nodes to contend for network access. That is, two or more nodes may try to send messages across the network simultaneously. All nodes choose a random back off interval between zero and CW and wait for the chosen number of slot times before trying to access the channel. Initially, CW is set to CWMin (minimum contention window size). When there is a collision, the contention window size is doubled, until a maximum value: CWMax. This technique of randomization and scaling the contention window size is used to reduce collisions.

A preliminary analysis of UAN Contention Window (UAN-CW-MAC) was performed using network simulator ns-3. Throughput curves were obtained for UAN-CW-MAC with 20 nodes and one surface sink (see Figure 2.7). The parameters shown in Table 2.6 were used in the analysis.

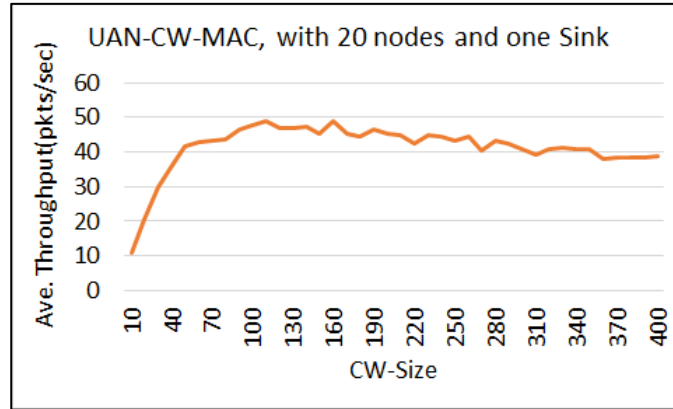


Figure 2.7: UAN-CW-MAC Throughput (pkts/sec) for 20 nodes.

Table 2.6: The parameters used to analyze the performance UAN-CW-MAC

Parameters	Values
Data rate	80Hz
Depth	70 m
Boundary	1000 m
Packet Size	32 Bytes
CWmin (Min. CW)	10
CWmax (Max. CW)	400
CW-Step	10
Position of sink:	250:250:70
Mean range from gateway:	166.966
Min. range	72.406

The nodes were deployed randomly (according to RNG seed) in a finite square region with the X and Y coordinates of the nodes distributed uniformly. The CW parameter is varied throughout the simulation in order to show the variation in throughput with respect to changes in CW. As the CW-size increases, the average throughput increases up to a maximum at CW=160, where the average throughput for three runs is 48.896 Packets per second (pkts/sec). The throughput is found to slightly decrease for higher values. As the CW increases more nodes try to compete to acquire the channel, resulting in collisions.

The equations for S-FAMA are discussed in chapter 3.

2.6 Conclusion

In chapter 2, we have described the state of the art on underwater MAC protocols. The chapter covers the environment characteristics and factors that influence acoustic communications. State of the art MAC protocols are described. Performance of some selected ad-hoc based and cluster-head based MAC protocols for underwater acoustic networks have been presented, with quantitative analysis of various parameters like throughput, delay and energy consumption etc.

Throughput equations for some selected protocols have been discussed. Simulation results obtained from ns-3 have also been covered.

CHAPTER 3 : THEORETICAL ANALYSIS

In this chapter we present the performance analysis of S-FAMA based on its analytical expressions, identify problems and propose solutions to improve the performance of the protocol. We derive the mathematical expressions for the proposed solutions. MultiACK and EarlyACK mechanisms [75] have been studied for S-FAMA and their throughput improvement, without violating the conditions defined for S-FAMA, has been analyzed. The comparison between algorithms has been carried out using parameters such as achieved throughput, delay, error rate, transmission efficiency, etc. With this analysis it was possible to recommend appropriate mechanisms or propose some improvements.

In FAMA, to guarantee collision avoidance, RTS length should be greater than the maximum propagation delay and CTS length should be greater than RTS length plus twice the maximum propagation delay plus the hardware transmit-to-receive transition time. Although FAMA increases the life-time of the RTS and CTS packets to prevent collisions with DATA packets, the efficiency of FAMA protocol is impacted heavily by propagation delays, due to the multi-way handshakes [29]. FAMA in its original form is not suitable for underwater networks but with enhancements such as slotting, it can be used in underwater effectively.

S-FAMA, a variant of FAMA, was introduced to overcome the problems of MACA and FAMA. It was designed to save energy by introducing time-slotting. In underwater communications, energy saving is vital as sensors are powered by batteries which cannot be recharged easily. In S-FAMA, in case of an ACK loss, the cost of retransmitting the entire RTS/CTS and DATA transmission cycle is very high. The motivation behind this research was to prevent the possibility of losing an ACK, which would save the energy wasted in the repetition of the whole cycle and improve the performance of S-FAMA. This could be achieved by minimizing the probability of losing an ACK and improving the efficiency of S-FAMA.

Unlike typical slotted MAC protocols, S-FAMA can take advantage of the control messages overheard by making the slot length much longer than the control message length, rather than designing the control message with large duration [77].

We identified problems in S-FAMA (i) with regards to ACK, (ii) with regards to retransmissions to handle failed DATA packets. The idea of adding the two features to the S-FAMA was influenced by [75].

3.1 Protocol Overview

S-FAMA is based on random access. It regulates transmissions by 4-way handshaking, and imposes restrictions on the packet sending times. Each packet (RTS, CTS, DATA or ACK) has to be transmitted at the beginning of one slot, shown in Figure 3.1. It exchanges control packets during the initial dialogue, between the source node and the destination node to prevent several transmissions at the same time [42].

The slot length is determined to ensure absence of data packet collisions. This is achieved with a slot length of $T_{CTS} + \tilde{D}$, where T_{CTS} is the transmission time of a control packet (RTS/CTS)

and \tilde{D} is the propagation delay. For a given network topology the transmission range can be chosen so as to maximize the network performance in terms of throughput and delay. An ARQ protocol is used to acknowledge data reception.

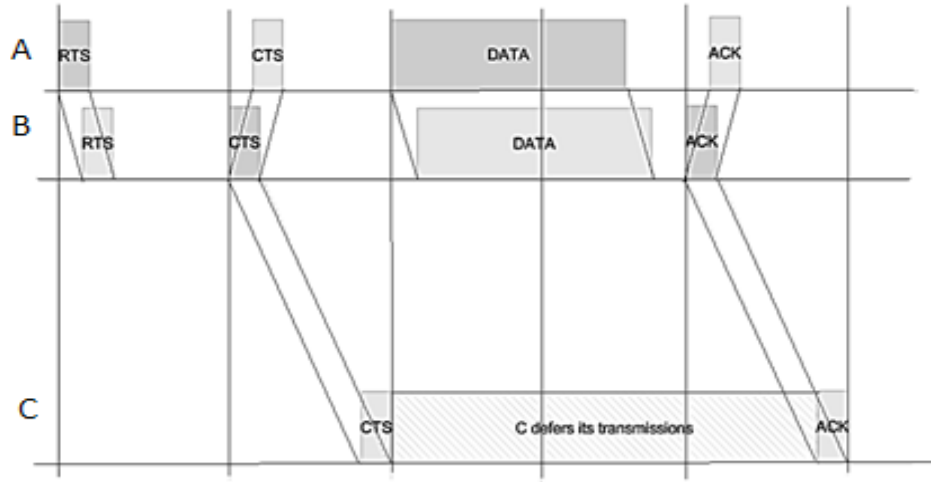


Figure 3.1: A successful handshake between terminals A and B in Slotted FAMA [42]

3.1.1 Model

The behavior of S-FAMA is depicted through the state transition diagram shown in Figure 3.2 [78], with some changes made to keep only the S-FAMA part in the state transition diagram. The description begins in the idle state.

- When a node has a packet to send, while in the idle state, it waits for the next timeslot and transmits RTS at the beginning of the slot. Then, it moves to the TX-RTS state.
- When it receives the CTS from the destination node it enters the TX-Data state and transmits the packet.
- The node remains in the TX Data state, until an ACK is received and then it goes to the idle state.
- If a CTS does not arrive, it backs off (Backoff 1) and reschedules another attempt.
- When the node receives an RTS addressed to itself, in the idle state, it replies with a CTS at the beginning of the next time slot (TX-CTS state) and moves to RX-Data. It remains there until it receives a correct data packet. The node then transmits an ACK (TX-ACK state) and returns to the idle state.
- When the node receives an RTS addressed to another node (xRTS), it waits for the packet to be sent (Wait-Data state). Wait-Data is the time a terminal, after receiving an xRTS, must wait: two slots (long enough for the receiver to send a CTS and the sender to start transmitting data). In case it hears no packet transmission, it means the initiated handshake by the neighbor has been a failure and the node returns to the idle state. In case it hears a packet transmission, it remains in the Wait-Data state until the transmission is successful.
- After receiving a CTS packet intended for another station (xCTS packet), while it is in the idle state, it will go to Wait-ACK and waits for the ACK to be sent. Wait-ACK is

the time from receiving the xCTS to the xACK. After receiving the xCTS packet, the terminal waits long enough to allow the other station to transmit the entire data packet and receive the corresponding ACK packet. If an ACK fails to arrive, indicating packet error, it remains in that state until data is correctly transmitted. When an ACK is detected, it returns to idle state.

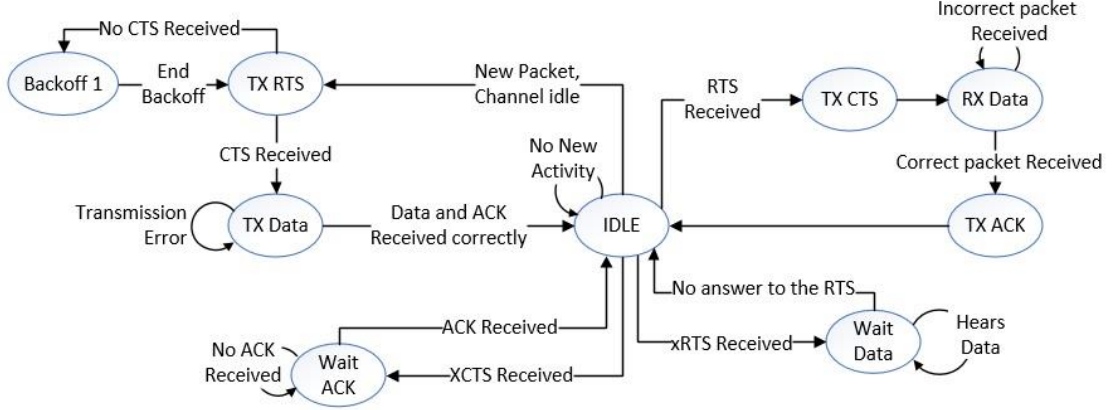


Figure 3.2: State Transition diagram for S-FAMA protocol [78].

3.1.2 Analysis

The network considered for the throughput analysis is shown in Figure 3.3. It is the same as in [42] & [78] for proper comparison of the results. The initiator node is marked with an 'X'. If we assume that every node has N neighbors ($N=6$), each of the N nodes has, itself, Q neighbors, which are hidden from node X . In the figure, nodes a , b , and c are neighbors of node 1 and are hidden from X ($Q = 3$). Each node has a packet ready to send every $1/\lambda$ seconds. The arrivals are modeled as a Poisson distribution with average λ packets per second. Each of the Q nodes sends RTSs to every neighbor of X that the hidden node is neighbor of at a rate λ/N . Table 3.1 shows the description of all symbols used in the analysis. For later analysis, we will use the same variables as in S-FAMA, with subscript 'M' for MultiACK and 'EA' for EarlyACK.

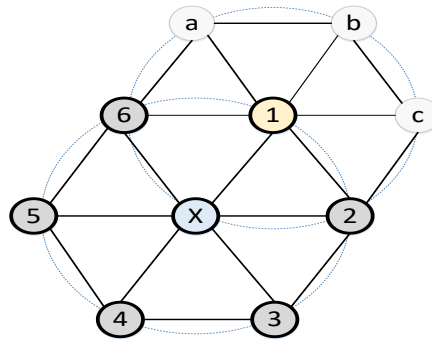


Figure 3.3: Network Layout [42]

The throughput per node (S) is calculated using (3.1), where \bar{U} the average time when useful data is being sent, \bar{B} represents the average time when the channel is being used (Busy period) and \bar{I} is the average time between two busy periods (Idle time):

$$S = \frac{\bar{U}}{\bar{B} + \bar{I}} \quad (3.1)$$

We denote by P_s the probability of success (no collision). It is the probability that no neighbors transmit within the time slot used by a given node X . These transmissions can be the neighbors RTS's or CTS's whose corresponding RTS's has not been heard. The probability of no collision is derived in (3.3). We assume that an RTS sent by a node hidden from X has not collided and that a CTS will be sent. T_{slot} is the sum of the transmission time of a control packet (RTS, CTS) and the maximum propagation delay.

$$P_s = \prod_{i=1}^N e^{-\lambda \times T_{\text{slot}}} \times \prod_{i=1}^N \left(\prod_{j=1}^Q e^{-\frac{\lambda}{N} \times T_{\text{slot}}} \right) \quad (3.2)$$

$$P_s = e^{-(N+Q) \times \lambda \times T_{\text{slot}}} \quad (3.3)$$

As defined in [9], the utilization of the channel is the data portion of the successful transmission period. The average useful data transmission time for node X (Figure 3.3) is given by (3.4), where δ represents the transmission time of a DATA packet.

$$\bar{U} = \frac{\delta}{N + 1} P_s \quad (3.4)$$

Given the Bit Error Rate (BER), P_e is the probability of error in a data packet containing L_{DATA} bits and L_{ACK} is the number of bits in the ACK packet. We define the probability of error in a data packet as (3.5):

$$P_e = 1 - (1 - \text{BER})^{L_{\text{DATA}}} \times (1 - \text{BER})^{L_{\text{ACK}}} \quad (3.5)$$

T_{data} is defined as the duration of all the slots needed by a DATA packet, expressed as an integer. T_{Tot} is the total duration of a successful transmission and is given by (3.6), where $2T_{\text{slot}}$ is the duration of the RTS and CTS slots and T is the time between the start of the transmission of a DATA packet and the time of successful reception of the ACK packet; it is given by $T = (T_{\text{data}} + T_{\text{slot}})/(1 - P_e)$.

$$T_{\text{Tot}} = 2T_{\text{slot}} + T = 2T_{\text{slot}} + \frac{T_{\text{data}} + T_{\text{slot}}}{1 - P_e} \quad (3.6)$$

The average busy time \bar{B} , is defined as (3.7):

$$\bar{B} = \bar{T}_{\text{success}} + \bar{T}_{\text{fail}} + \bar{T}_{\text{defer}} \quad (3.7)$$

\bar{T}_{success} is the time during which data is being successfully sent (3.8):

$$T_{\text{success}} = P_s \times T_{\text{Tot}} \quad (3.8)$$

\bar{T}_{fail} is a period of collisions on the channel (3.9):

$$\bar{T}_{\text{fail}} = \frac{2T_{\text{slot}} \times (1 - P_s)}{N + 1} \quad (3.9)$$

\bar{T}_{defer} is the time during which node X defers its transmission, because the channel has been acquired by another node.

Deferral periods happen when a CTS is heard replying another node's RTS (hidden nodes). This probability is given by [42] (3.10):

$$\text{Probability CTS is over heard} = \frac{QP_s}{(N + 1)} \quad (3.10)$$

The deferral time when a CTS is overheard is shown in (3.11):

$$\text{The deferral time when CTS is overheard} = \frac{(T_{\text{data}} + T_{\text{slot}})}{(1 - P_e)} \quad (3.11)$$

If a terminal senses interference in the channel, a collision is assumed. The probability of collision in the channel is given by (3.12). In this situation, the deferral time is $T_{\text{data}} + T_{\text{slot}}$. Hence, average deferral time is given in (3.13).

$$\text{Probability of collision} = \frac{N(1 - P_s)}{(N + 1)} \quad (3.12)$$

$$\bar{T}_{\text{defer}} = (T_{\text{data}} + T_{\text{slot}}) \left(\frac{QP_s}{(N + 1)(1 - P_e)} + \frac{N}{N + 1} (1 - P_s) \right) \quad (3.13)$$

The average idle time on the channel is given by (3.14):

$$\bar{I} = \frac{1}{\lambda(N + 1)} \quad (3.14)$$

Substituting the values of \bar{U} , \bar{B} and \bar{I} in equation (3.1), the throughput for S-FAMA is given by (3.15), where δ denotes the transmission time of DATA packet [42].

$$S = \frac{\delta P_s}{(N + 1)P_s T_{\text{Tot}} + 2T_{\text{slot}}(1 - P_s) + (T_{\text{data}} + T_{\text{slot}}) \left(\frac{QP_s}{(1 - P_e)} + N(1 - P_s) \right) + \frac{1}{\lambda}} \quad (3.15)$$

Equation (3.15) measures the ‘Throughput per node’ (S) defined as the fraction of time during which a certain node is transmitting correct data. This equation is valid for a static single-hop network.

3.1.3 Performance

The results of the throughput of some MAC protocols discussed in chapter 2 are shown in Figure 3.4. The performance of MAC protocols, namely ALOHA, CSMA, and S-FAMA is shown. Poisson arrivals have been considered for the offered traffic [69], [75] & [42]. Figure 3.4 depicts the throughput vs offered load for CSMA for a propagation delay ‘a’: $a = 1$, $a = 0.1$ and $a = 0.01$.

The performance of CSMA is found effective in fully connected networks with small propagation delay ($a \leq 0.1$) compared to the duration of the packet ($T=1$). The efficiency of the protocol rapidly decreases with the increase in delay ($a=1$). We assumed the network with no hidden terminals. CSMA throughput is seen to be maximum at $G=3$, for $a=0.1$, where G is the number of Packets per packet transmission time.

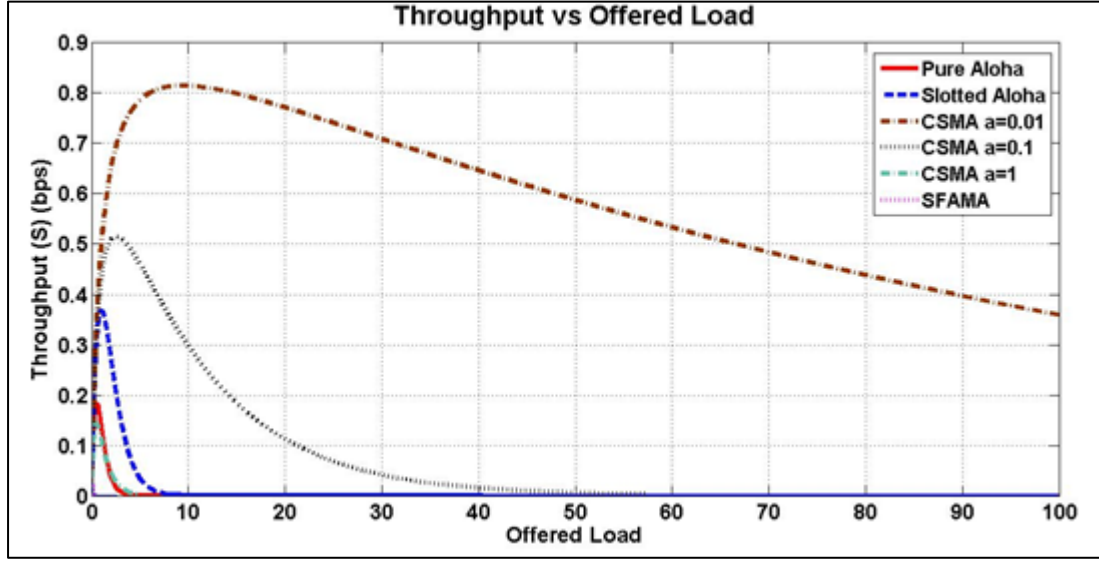


Figure 3.4. Throughput vs Offered Load (packets/sec) of Pure Aloha, Slotted Aloha, CSMA and SFAMA

The results of variations in S-FAMA with varying offered load are also shown. The throughput versus offered load performance for S-FAMA with $T_{data} = 1\text{slot}$ is depicted. The curve shows that S-FAMA has maximum throughput 0.025 at λ equals 0.037 packets/second.

The performance analysis of SFAMA with respect to varying number of nodes is evaluated and shown in Figure 3.5. The average throughput versus number of nodes curves are drawn for different DATA packet sizes at the same BER.

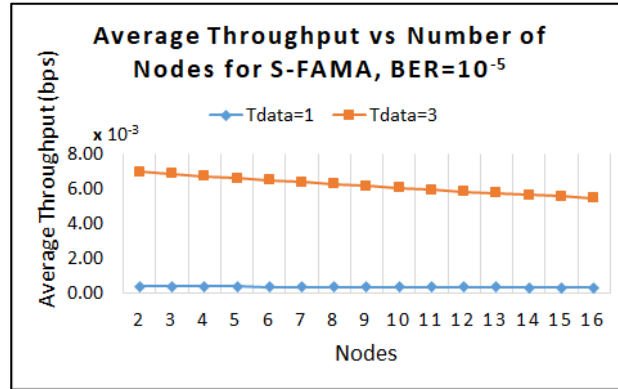


Figure 3.5. Average Throughput (bps) vs Number of Nodes for S-FAMA, for: $T_{data}=1$ slot and $T_{data}=3$ slots

We have considered values of $T_{data}=1\text{slot}$ (DATA packet size 100bits) and $T_{data}=3\text{slots}$ (DATA packet size 1700 bits) for a BER of 10^{-5} . It can be seen that the throughput decreases as the number of nodes increases, as it increases the competition amongst nodes to acquire the channel, resulting in more collisions. Also, from the quantitative analysis it can be seen that the throughput varies inversely with the number of nodes. However, the effect of changing the DATA packet size in Figure 3.5 can also be seen. The average throughput for $T_{data}=3$ slots is much higher than that of $T_{data}=1$ slot. The larger the DATA packet size the larger the throughput.

Figure 3.6 shows the average throughput versus number of nodes for S-FAMA with BER: 10^{-3} , 10^{-4} , 10^{-5} . It can be seen that the throughput decreases as the number of nodes increases. The

average throughput with BER 10^{-3} is lower compared to the throughput at BER 10^{-4} and 10^{-5} . The throughput with two nodes is found to be 5.95×10^{-3} bps, 6.94×10^{-3} bps and 6.99×10^{-3} bps for BERs 10^{-3} , 10^{-4} , 10^{-5} respectively. The throughput with 16 nodes reduces to 3.09×10^{-3} , 5.34×10^{-3} , and 5.48×10^{-3} bps respectively. As explained earlier, this is due to the fact that increasing the number of nodes means more number of hops through the network and more competition to access the channel. This makes it difficult for the nodes to acquire the channel. The effect of varying the BER on the throughput can be seen in Table 3.1 and Figure 3.6. The higher the BER, the lower the throughput with respect to the number of nodes.

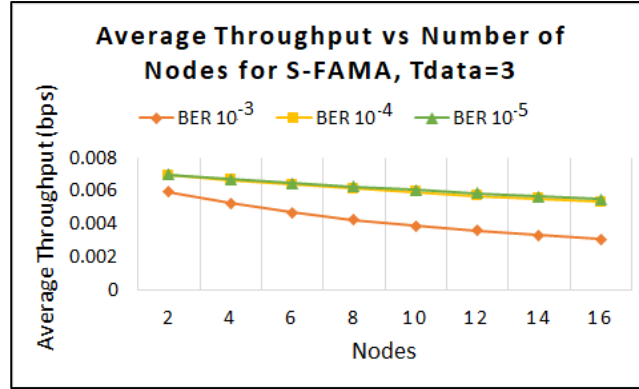


Figure 3.6. Average Throughput (bps) vs Number of Nodes for S-FAMA for $T_{data}=3$ slots

Table 3.1: Effect of varying BER on Average Throughput (bps) vs Nodes for $T_{data} = 3$ slots

Nodes	BER 10^{-3}	BER 10^{-4}	BER 10^{-5}
2	5.95×10^{-3}	6.94×10^{-3}	6.99×10^{-3}
16	3.09×10^{-3}	5.34×10^{-3}	5.48×10^{-3}

3.2 Problem Statement

The successful transmission in S-FAMA comprises the following steps: Before sending DATA, the transmitter sends an RTS at the beginning of the new slot to the receiver. The receiver sends a CTS, at the start of the next slot. The transmitter then sends DATA packets at the start of new slot and waits for acknowledgement (ACK). If an ACK fails to reach the transmitter, the RTS/CTS based contention cycle and DATA transmission processes repeat [75]. The cost of repeating the whole cycle is very high and energy consuming. Figure 3.7(a) shows the RTS/CTS based contention cycle and DATA transmission processes in S-FAMA.

To overcome the problem of high energy consumption due to ACK failure we propose two solutions, namely MultiACK and EarlyACK mechanisms. These mechanism are depicted in Figure 3.7(b) and Figure 3.7(c). The proposed solutions are described below.

1. With regards to the number of acknowledgements:

We propose to add the MultiACK feature to S-FAMA. Instead of sending one ACK packet, the receiver node will send 'i' ACK packets. This increases the probability of receiving at least one ACK packet by sending a batch of ACK packets (ACK-TRAIN). This not only saves energy but improves throughput, delay, reliability. Let's define $T_{MultiACK}$ as the duration of all the slots needed by the MultiACK packet. We propose the following two scenarios:

- I. Scenario-I: Use a number of ACKs such that $i \times T_{ACK} = T_{CTS}$ and $T_{MultiACK} = T_{slot}$, where $i \times T_{ACK}$ is the duration of the train of acknowledgements.

In this scenario, the duration of ACK-Train is the same as that of the control packet, hence it requires just one time slot.

- II. Scenario-II: Use a number of ACKs such that $2T_{slot} > i \times T_{ACK} \geq T_{slot} + T_{CTS}$, $T_{MultiACK} = 2T_{slot}$.

In this scenario the duration of the train of acknowledgement includes one time slot plus the control packet duration on the second slot, hence it requires two time slots.

2. With regards to retransmissions in case of ACK failure:

To handle retransmission of DATA packets in case of ACK failure, the EarlyACK mechanism is proposed (Figure 3.7(c)). The EarlyACK is helpful when the DATA arrives successfully but the ACK is lost. It prevents the repetition of the entire contention and data transmission cycle. It sends an early acknowledgement in response to the repeated RTS for a lost ACK, thus saving energy and preventing the retransmission of the DATA cycle.

The Message Sequence Chart for S-FAMA, S-FAMA with MultiACK and S-FAMA with EarlyACK are shown in Figure 3.7(a), (b) and (c).

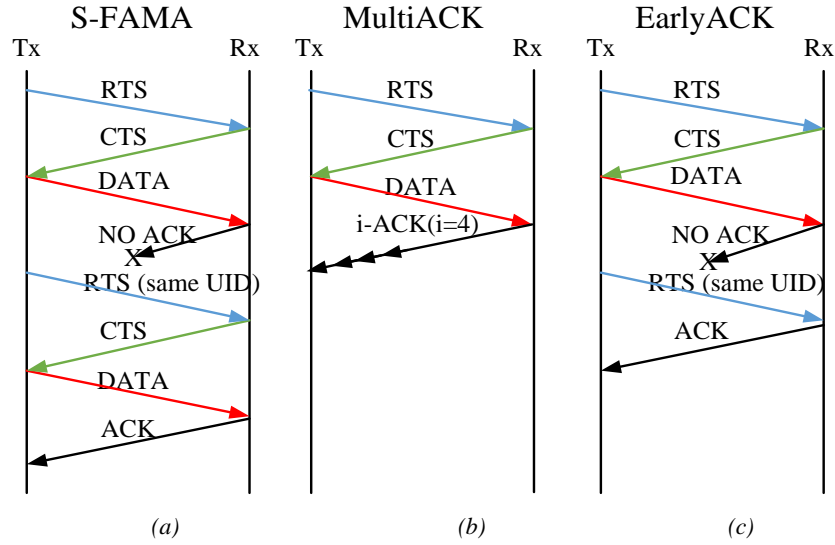


Figure 3.7: Message Sequence Charts for: (a) S-FAMA, (b) MultiACK and (c) EarlyACK.

3.3 MultiACK Mechanism

In MultiACK [75], instead of sending one ACK for each received DATA packet, a train of ‘i’ acknowledgement packets is sent. By sending ‘i’ ACK packets, the probability of receiving at least one ACK is increased. We denote $T_{MultiACK}$ the duration of all slots needed by the MultiACK packet.

Two scenarios have been considered here. In the first scenario, the size of the ACK-Train is the same as that of the control packet L_{CTS} . This is done by shortening the size of ACK packet. $T_{MultiACK}$ is one time slot. In the second scenario, the size of the ACK-Train covers the duration of one time slot plus the duration of the control packet “ T_{CTS} ”. In this scenario, $T_{MultiACK}$ is two time slots.

3.3.1 Analysis

In this section we derive the mathematical expressions for the throughput of MultiACK and present its performance analysis.

The probability of error in a DATA packet in MultiACK is denoted by P_{eM} (3.16). $P_{succ-ACK}$ is the probability of successfully transmitting at least one of the ACKs in the ACK- train (3.17).

$$P_{eM} = 1 - [(P_{succ-DATA}) \times (P_{succ-ACK})] \quad (3.16)$$

$$P_{succ-ACK} = 1 - \prod_{i=1}^i [1 - (1 - BER)^{L_{ACK}}] \quad (3.17)$$

$$P_{eM} = 1 - [((1 - BER)^{L_{DATA}}) \times (1 - \prod_{i=1}^i [1 - (1 - BER)^{L_{ACK}}])] \quad (3.18)$$

3.3.2 Scenarios

3.3.2.1 Scenario-I

In the first scenario, we have considered a duration of the train of ACKs equal to the duration of the control packet (T_{CTS}). Thus, in this case, the transmission of the batch of ACKs requires only one slot (Figure 3.8). We will use subscript ‘M-1’ to denote the variables for this scenario.

The number of ACKs is:

$$i \times T_{ACK} = T_{CTS} = (\text{No. of bits in the control packet}) / \text{Bitrate} \quad (3.19)$$

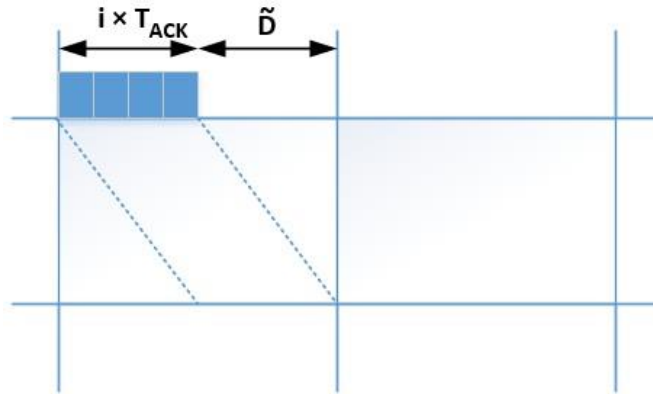


Figure 3.8: MultiACK Scenario-I

The parameter P_{eM} (3.18) varies with “i” and thus affects other variables, T_{M-1} (3.20), $T_{Tot-M-1}$ (3.21), $T_{succ-M-1}$ (3.22) and $T_{defer-M-1}$ (3.23). Consequently, the throughput, S_{M-1} , would be affected (3.24). Table 3.2 contains the description of each term used in the equations.

$$T_{M-1} = \frac{T_{data} + T_{slot}}{1 - P_{eM}} \quad (3.20)$$

Thus,

$$T_{\text{Tot-M-1}} = 2T_{\text{slot}} + \frac{T_{\text{data}} + T_{\text{slot}}}{1 - P_{eM}} \quad (3.21)$$

Where,

$$\bar{T}_{\text{success-M-1}} = P_s \times T_{\text{Tot-M-1}} \quad (3.22)$$

The average deferral time equation changes into

$$\bar{T}_{\text{defer-M-1}} = (T_{\text{data}} + T_{\text{slot}}) \left(\frac{QP_s}{(N+1)(1-P_{eM})} + \frac{N(1-P_s)}{N+1} \right) \quad (3.23)$$

Substituting the values for \bar{U} , \bar{B} and \bar{I} in equation (3.1), the throughput for MultiACK scenario-1 is shown in (3.24):

$$S_{M-1} = \frac{\delta P_s}{(N+1)P_s T_{\text{Tot-M-1}} + 2T_{\text{slot}}(1-P_s) + (T_{\text{data}} + T_{\text{slot}}) \left(\frac{QP_s}{(1-P_{eM})} + N(1-P_s) \right) + \frac{1}{\lambda}} \quad (3.24)$$

Table 3.2: Parameters

Symbols	Description
T_{slot}	Duration of one time slot
T_{CTS}	Duration of a Control packet
T_{ACK}	Duration of an ACK packet
N	Number of neighboring nodes
Q	Number of hidden nodes
R	Bitrate
\tilde{D}	Propagation Delay
L_{DATA}	Number of bits in the DATA packet
L_{ACK}	Number of bits in the ACK packet
T_{data}	Duration of all slots needed by the DATA packet
i	Number of ACKs
$L_{\text{ACK-MA}}$	Number of bits in the single packet of MultiACK

3.3.2.2 Scenario-II

In Scenario II, we take the length of the train of acknowledgements as greater than one time slot but less than two time slots, as shown in Figure 3.9 and expression (3.25). We will use subscript ‘M-2’ to denote the variables for this scenario.

$$2T_{\text{slot}} > i \times T_{\text{ACK}} \geq T_{\text{slot}} + T_{\text{CTS}} \quad (3.25)$$

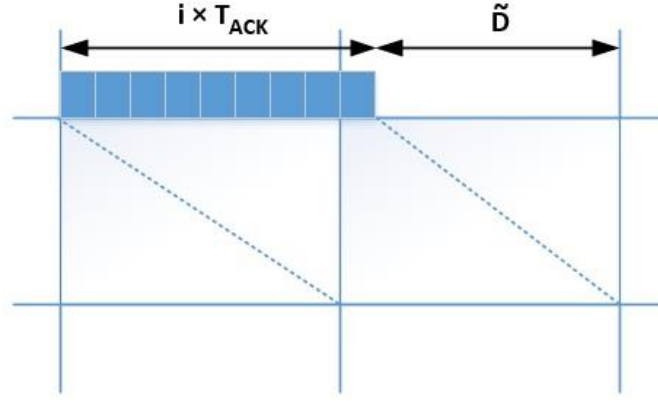


Figure 3.9: MultiACK Scenario-II

In this case we have used the same value of T_{ACK} as in Scenario-I, for the purpose of comparison. The probability P_{eM} now decreases as it varies with ' i ' and, thus, affects variables T_{M-2} (3.26), $T_{Tot-M-2}$ (3.27), $T_{success-M-2}$ (3.28) and $T_{defer-M-2}$ (3.29). Consequently the throughput, S_{M-2} , for this second scenario is given by (3.30).

$$T_{M-2} = \frac{T_{data} + 2T_{slot}}{1 - P_{eM}} \quad (3.26)$$

$$T_{Tot-M-2} = 2T_{slot} + \frac{T_{data} + 2T_{slot}}{1 - P_{eM}} \quad (3.27)$$

$$\bar{T}_{success-M-2} = P_s \times T_{Tot-M-2} \quad (3.28)$$

$$\bar{T}_{defer-M-2} = (T_{data} + 2T_{slot}) \left(\frac{QP_s}{(N+1)(1 - P_{eM})} + \frac{N(1 - P_s)}{N+1} \right) \quad (3.29)$$

$$S_{M-2} = \frac{\delta P_s}{(N+1)P_s T_{Tot-M-2} + 2T_{slot}(1 - P_s) + (T_{data} + 2T_{slot}) \left(\left(\frac{QP_s}{(1 - P_{eM})} \right) + N(1 - P_s) \right) + \frac{1}{\lambda}} \quad (3.30)$$

3.4 EarlyACK Mechanism

The EarlyACK mechanism has been proposed to prevent the repetition of the entire contention and DATA retransmission cycle in S-FAMA, see Figure 3.4 (c). In S-FAMA, when an ACK fails to reach the transmitter, the transmitter sends the RTS with the same unique identification number (UID). In response, the receiver sends an ACK instead of a CTS for the repeated RTS, thus avoiding the retransmission of the data.

3.4.1 Analysis

The probability of successful transmission is given by (3.31), where 'D' is the probability that a DATA packet containing L_{DATA} bits is received successfully (3.34) and 'A' is the probability

that an ACK packet is received successfully (3.35), being L_{ACK} the number of bits in the ACK packet. An ACK-retry occurs when an ACK fails to reach the transmitter; the receiver sends an ACK to the sender in response to the repeated RTS, until an ACK is successfully received. Parameter 'n' denotes the number of ACK-retries for a successful transmission. In EarlyACK, a DATA packet with a specific UID is transmitted only once before receiving a reply from the destination node. If the ACK is lost, instead of sending again the specific DATA packet, an EarlyACK will be sent in response to the repeat RTS. If the ACK is not lost then a new batch of DATA will be formed with a new UID and RTS will be sent for that.

During the EarlyACK phase, only one ACK packet is sent of the same size as the CTS packet. The ACK is assumed to convey all information on lost packets and retransmissions of only lost packets takes place.

$$P_{Succ} = D \times A + (D \times \bar{A} \times [(1 - A^2)^n] \times A^2) \quad (3.31)$$

Let's name P_{eEA} the probability of error in EarlyACK S-FAMA. The new probability of error in a DATA packet is:

$$P_{eEA} = 1 - P_{Succ} \quad (3.32)$$

$$P_{eEA} = \{1 - (D \times A + D \times \bar{A} \times [(1 - A^2)^n] \times A^2)\} \quad (3.33)$$

Where,

$$D = (1 - BER)^{L_{DATA}} \quad (3.34)$$

$$A = (1 - BER)^{L_{ACK}} \quad (3.35)$$

$$\bar{A} = (1 - A) = [1 - (1 - BER)^{L_{ACK}}] \quad (3.36)$$

Hence,

$$P_{eEA} = 1 - \{(1 - BER)^{L_{DATA}} \times (1 - BER)^{L_{ACK}} + (1 - BER)^{L_{DATA}} \times [1 - (1 - BER)^{L_{ACK}}] \times (1 - [(1 - BER)^{L_{ACK}}]^2)^n \times [(1 - BER)^{L_{ACK}}]^2\} \quad (3.37)$$

The new probability of error in a DATA packet affects T_{EA} , the duration between the start of a DATA packet and the successful reception of the ACK packet. As in MultiACK, it will also affect T_{Tot-EA} (3.38), $\bar{T}_{success-EA}$ (3.39), $\bar{T}_{defer-EA}$ (3.40) and, finally, the throughput (3.41):

$$T_{Tot-EA} = 2T_{slot} + \frac{T_{data} + T_{slot}}{1 - P_{eEA}} \quad (3.38)$$

$$\bar{T}_{success-EA} = P_s \times T_{Tot-EA} \quad (3.39)$$

$$\bar{T}_{defer-EA} = (T_{data} + T_{slot}) \left(\frac{QP_s}{(N+1)(1 - P_{eEA})} + \frac{N(1 - P_s)}{N+1} \right) \quad (3.40)$$

The throughput per node (S_{EA}) is now given by:

$$S_{EA} = \frac{\delta P_s}{(N+1)P_s T_{Tot-EA} + 2T_{slot}(1-P_s) + (T_{data} + T_{slot}) \left(\frac{QP_s}{(1-P_{eEA})} + N(1-P_s) \right) + \frac{1}{\lambda}} \quad (3.41)$$

The normalized transmission time of a DATA packet (δ), is calculated as shown in (3.42).

$$\delta = \frac{L_{\text{DATA}}}{\text{Rate} \times T_{\text{slot}}} \quad (3.42)$$

3.5 Analysis of Energy Consumption

In underwater acoustic networks, sensor nodes are mostly powered by batteries that cannot be recharged easily. Further, the underwater environment and harsh characteristics of sea water causes high bit error rate and delay in propagation, resulting in energy waste. It is therefore important to analyze the energy consumption in order to design an energy efficient MAC protocol. In [79], Iyad Tumar presents an analysis of energy consumption in both shallow and deep water. The analysis shows that direct transmission shows bad results in the deep water. The packet relaying technique results in energy savings in the deep water scenario. Clustering schemes save more energy and they show a better performance in shallow water. Sensor nodes should deliver the collected data to the nearest cluster head. This cluster head sends all the information to another cluster head until it reaches the underwater sink relaying case, the data produced by a source sensor is forwarded through multi-hop paths by intermediate sensors until it reaches the surface sink. This technique results in energy savings. What is more, for a fixed distance between sensors, if the number of sensor nodes is increased, the total energy consumed is increased because more nodes are farther away from the surface sink and the power necessary to transmit is proportional to the square of the distance.

The energy consumed during transmission for one hop can be calculated as shown in (3.43), [80, 81]:

$$E_{\text{total}} = N \times P \times T_{\text{tx}} \times K \quad (3.43)$$

where N is the number of hops. P is the transmission power related to the acoustic modems and hydrophones, T_{tx} is the DATA transmission time, and K is the number of packets.

In S-FAMA, the probability of error, P_e , in a data packet containing L_{DATA} bits, assuming independent errors, is shown in (3.5). Thus, the total transmission energy wasted ($E_{\text{w-SF}}$) in unsuccessful transmissions is shown in (3.44).

$$E_{\text{w-SF}} = N \times P \times T_{\text{tx}} \times K \times P_e \quad (3.44)$$

The total transmission energy wasted in the unsuccessful transmission in MultiACK ($E_{\text{w-MA}}$) is calculated by (3.45):

$$E_{\text{w-MA}} = N \times P \times T_{\text{tx}} \times K \times P_{eM} \quad (3.45)$$

We can compare it with that of S-FAMA by dividing (3.45) by (3.44), shown in (3.46).

$$\frac{E_{\text{w-MA}}}{E_{\text{w-SF}}} = \frac{P_{eM}}{P_e} \quad (3.46)$$

The total transmission energy wasted in the unsuccessful transmission in EarlyACK ($E_{\text{w-EA}}$) is given by (3.47):

$$E_{\text{w-EA}} = N \times P \times T_{\text{tx}} \times K \times P_{eEA} \quad (3.47)$$

The transmission energy wasted in EarlyACK is compared with that of S-FAMA using (3.48). For the analysis we divide (3.47) by (3.44). If the ratio is less than 1, it means that the transmission energy wasted in S-FAMA is higher than that of EarlyACK.

$$\frac{E_{w-EA}}{E_{w-SF}} = \frac{P_{eEA}}{P_e} \quad (3.48)$$

The total energy used during successful transmission in S-FAMA (E_{T1}) and MultiACK (E_{T2}) and EarlyACK (E_{T3}) is calculated by expressions (3.49), (3.50) and (3.51) respectively.

$$E_{T1} = N \times T_{tx} \times K \times P \times (1 - P_e) \quad (3.49)$$

$$E_{T2} = N \times T_{tx} \times K \times P \times (1 - P_{eM}) \quad (3.50)$$

$$E_{T3} = N \times T_{tx} \times K \times P \times (1 - P_{eEA}) \quad (3.51)$$

Improvement in total energy used during successful transmission for MutliACK and EarlyACK is obtained by dividing (3.50) by (3.49) and (3.51) by (3.49), shown in (3.52) and (3.53), respectively:

$$\frac{E_{T2}}{E_{T1}} = \frac{1 - P_{eM}}{1 - P_e} \quad (3.52)$$

$$\frac{E_{T3}}{E_{T1}} = \frac{1 - P_{eEA}}{1 - P_e} \quad (3.53)$$

The energy efficiency is calculated using (3.54) for MultiACK and (3.55) for EarlyACK.

$$\eta_{MA} = \left(\frac{E_{T2} - E_{T1}}{E_{T1}} \right) \times 100 \quad (3.54)$$

$$\eta_{EA} = \left(\frac{E_{T3} - E_{T1}}{E_{T1}} \right) \times 100 \quad (3.55)$$

3.6 Comparative Analysis

To compare the throughputs of S-FAMA (S), MultiACK-SFAMA (S_M) and EarlyACK-SFAMA (S_{EA}), we can define an improvement factor for MultiACK (IF_{MA}) and EarlyACK (IF_{EA}) when an ACK fails to reach the sender.

The MultiACK improvement factor is the quotient obtained by dividing the probability of successfully receiving an ACK in MultiACK-SFAMA by the probability of successfully receiving an ACK in S-FAMA. Similarly, EarlyACK improvement factor is the quotient obtained by dividing the probability of successfully receiving an ACK in EarlyACK-SFAMA by the probability of successfully receiving an ACK in S-FAMA. When this factor is greater than one, it shows an improvement.

3.6.1 Improvement for MultiACK

The Improvement Factor for MultiACK (IF_{MA}) is calculated by taking the ratio of “the probability that an ACK is correctly received in MultiACK-SFAMA” and “the probability an ACK is correctly received for S-FAMA”. The expression is shown in (3.57).

$$IF_{MA} = \frac{\text{Probability an ACK is correctly received in MultiACK – SFAMA}}{\text{Probability an ACK is correctly received in SFAMA}} \quad (3.56)$$

$$IF_{MA} = \frac{1 - (1 - (1 - BER)^{L_{ACK}}))^i}{(1 - BER)^{L_{ACK}}} \quad (3.57)$$

3.6.2 Improvement for EarlyACK

The Improvement Factor for EarlyACK (IF_{EA}) is calculated by taking the ratio of “the probability an ACK is correctly received in EarlyACK-SFAMA” and “the probability an ACK is correctly received in S-FAMA”, as shown in (3.59). Thus the improvement in the probability of successfully receiving an ACK in EarlyACK is:

$$IF_{EA} = \frac{\text{Probability an ACK is correctly received in EarlyACK – SFAMA}}{\text{Probability an ACK is correctly received in SFAMA}} \quad (3.58)$$

$$IF_{EA} = \frac{1 - (D \times \bar{A} \times [(1 - A^2)^n] \times A^2)}{(1 - BER)^{L_{ACK}}} \quad (3.59)$$

3.7 Conclusion

In chapter 3 we have identified the problems in S-FAMA and the proposed solutions have been discussed. The MultiACK and EarlyACK mechanisms are explained and analyzed. Mathematical expressions for quantitative analysis are derived for both variants. Comparative analysis of the proposed variations is discussed to calculate the improvement in throughput. Energy consumption analysis with mathematical expressions is covered. Equations for the ‘Improvement Factor’ for both MultiACK and EarlyACK are also derived. The performance evaluation and validation of the results obtained are discussed in Ch.4.

CHAPTER 4 : RESULTS AND DISCUSSIONS

In this chapter the effects of MultiACK and EarlyACK are presented in numerical terms. The performance of the two new variants for different number of nodes, transmission ranges, BERs and offered load are evaluated. The throughput improvement for both scenarios of MultiACK and the EarlyACK are compared. The quantitative analysis of the results of the two variants is presented for performance analysis.

4.1 MultiACK

In the MultiACK mechanism, where a train of ACK packets is sent instead of a single ACK for the received DATA, two scenarios were considered. In the first scenario the duration of the train of ACK packets was considered the same as that of the control packet, T_{CTS} . The length of the ACK packet was shortened so that MultiACK packets could be accommodated in the same duration as T_{CTS} . In the first scenario $T_{MultiACK}$ is equal to one T_{slot} . In the second scenario, $T_{MultiACK}$ needs two T_{slots} . The detailed analysis of the two MultiACK scenarios is discussed below.

The analysis has considered 2-16 nodes and a data packet length of 1 to 30 slots. Results have been obtained in MATLAB using the expressions derived in the previous chapter.

Table 4.1: Parameters used in MutliACK: Scenario-I

Parameter	Values
T_{slot}	$\tilde{D} + T_{CTS}$
T_{CTS}	$(L_{CTS}/R) 0.1s$
L_{CTS} (RTS/CTS packet size)	100 bits
T_{ACK}	$(L_{ACK}/R) 0.025s$
L_{ACK}	25 bits
i	4
N	2-16
Q (hidden nodes)	0
R (Bitrate)	1000bps
Propagation speed	1500 m/s
\tilde{D} (Propagation Delay)	(Distance/Speed)
DATA packet size	100, 1700, 11300, 23300 bits
T_{data}	1, 3, 15 & 30 slots(s)
Distance (Range)	1000m (w.r.t. nodes) 100m to 3000m (w.r.t transmission range)

We have used the expressions (3.15) and (3.24) to plot the graphs for Scenario-I of MultiACK, using the parameters shown in Table 4.1. The throughput improvement was calculated by

taking the ratio of (S_{M-1}/S) shown in (4.4). Same values of T_{ACK} have been used in both scenarios for comparative analysis.

4.1.1 Scenario-I

Using a control packet size (L_{CTS}) of 100 bits and a bitrate of 1000bps, the duration of the control packet (T_{CTS}) is 0.1seconds. To accommodate the ACK-train, we have shortened the length of one ACK-packet to 0.025 seconds. The number of ACKs then is 4.

The propagation delay (\tilde{D}) is calculated using formula (4.1):

$$\tilde{D} = \frac{\text{Distance between furthest pair of nodes(m)}}{\text{Propagation speed (1500m/s)}} \quad (4.1)$$

The performance has been first evaluated as a function of the number of nodes (2-16 nodes). To evaluate the performance as a function of the transmission range, we have used distances from 100m to 3000m. For example, for 1000m distance between the furthest pair of nodes, the propagation delay is 0.7 seconds. Thus, T_{slot} , which is the sum of T_{CTS} and \tilde{D} is 0.8seconds. The formula for calculating T_{slot} is shown in (4.2).

$$T_{slot} = (L_{CTS}/R) + \tilde{D} \quad (4.2)$$

For $T_{data} = k$ slots, L_{DATA} was calculated using formula (4.3):

$$L_{DATA} = [(k-1) T_{slot} + T_{CTS}] \times R \quad (4.3)$$

The duration of all the slots needed by a DATA packet was calculated by $T_{data} = (L_{DATA}/R) + \tilde{D}$. The throughput improvement was obtained using (4.4):

$$\frac{S_{M-1}}{S} = \frac{(N+1)P_s T_{Tot} + 2T_{slot}(1-P_s) + (T_{data} + T_{slot}) \left(\left(\frac{QP_s}{(1-P_e)} \right) + N(1-P_s) \right) + \frac{1}{\lambda}}{(N+1)P_s T_{Tot-M} + 2T_{slot}(1-P_s) + (T_{data} + T_{slot}) \left(\left(\frac{QP_s}{(1-P_{eM})} \right) + N(1-P_s) \right) + \frac{1}{\lambda}} \quad (4.4)$$

4.1.1.1 Analysis as a function of the number of Nodes

Results are illustrated in Figures 4.1(a) to (f) with no hidden nodes. Simulations were carried out with $Q=0$, 2-16 nodes and $BER=10^{-2}$ to 10^{-7} . Results were plotted for different values of T_{data} equal to 1, 3, 15 and 30 slots, which correspond to values of L_{DATA} of 100, 1700, 11300 and 23,300 bits. It can be seen from the results that the percentage improvement for $BER(10^{-2})$, for $T_{data}=1$ and 3 is very high as compared to those of low BER.

At $BER 10^{-2}$, the minimum and maximum throughput improvement, for $T_{data}=1$ are 6.82% and 29.96% which occurs at 2 and 16 nodes, respectively. The highest throughput improvement is 172.5%, and it occurs at $T_{data}=3$, for all 2 to 16 nodes. For higher T_{data} , 15 and 30 slots, it is observed that as T_{data} increases, T_{Tot} increases, which varies inversely with '1-Pe'. Pe varies directly with BER and L_{DATA} . For example, for $T_{data}=1$, $L_{DATA}=100$ bits, Pe is 0.866 and (1-Pe) is 0.134. T_{Tot} is 12.98sec and $T_{Tot-M-1}$ is 5.73sec. The S-FAMA throughput 'S' is 2.44×10^{-4} and the MultiACK throughput S_{M-1} is 3.17×10^{-4} , which gives the throughput improvement of 29.96% with 16 nodes. When $T_{data}=3$ slots, L_{DATA} is 1700 bits, Pe is high 99.99×10^{-2} , which makes '1-Pe' very low (1.39×10^{-8}), which reduces the throughput. The throughput 'S' is

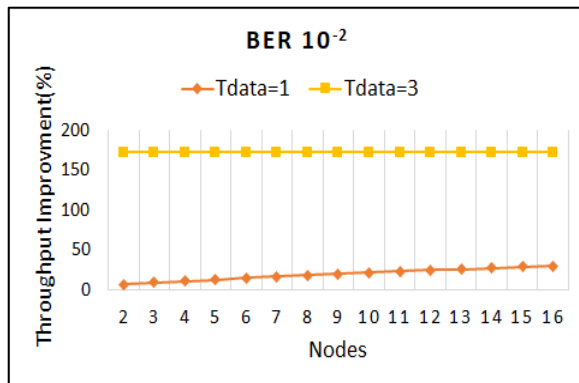
5.79×10^{-10} while S_{M-1} is 1.58×10^{-9} . This gives throughput improvement of 172.53%. Further increase in the T_{data} to 15, where L_{DATA} is 11300bits, P_e increases to '1' and '1- P_e ' goes down to 0. This makes T infinite resulting in T_{Tot} to infinity (Div/0). Since S and S_{M-1} varies inversely with T_{Tot} and $T_{Tot-M-1}$, the throughput does not exist with $T_{data}=15$ and 30 slots. The behavior of S-FAMA for BER 10^{-2} is shown in Table 4.2. The same behavior applies to MultiACK for BER 10^{-2} .

The impact of varying T_{data} can also be seen. The larger the size of the DATA packet, the larger the throughput improvement. As T_{data} increases, it increases the time between start of the DATA packet and the time of successful reception of the ACK packet. When BER is high, the successful transmissions are few, which increases this time. T and T_{M-1} vary inversely with $(1-P_e)$ and $(1-P_{eM})$ respectively. The ratio P_{eM}/P_e is less than 1, indicating P_e in S-FAMA is higher than P_{eM} in MultiACK. Thus the throughput of MultiACK is slightly higher than that of S-FAMA.

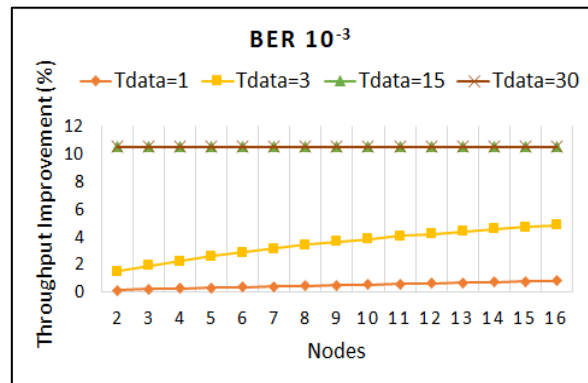
Table 4.2: Behaviour of the S-FAMA protocol at high BER 10^{-2} and larger DATA packet size. with $L_{ACK}=100$ bits, $BER=0.01$, $Q=0$

T_{data}	L_{DATA}	$(1-BER)^{L_{DATA}}$	$1-P_e$	T_{Tot}	$T_{Tot-M-1}$	Throughput 'S'	' S_{M-1} '	Throughput Improvement %
1	100	0.366	0.134	12.98	5.73	2.44×10^{-4}	3.17×10^{-4}	29.98%
3	1700	3.80×10^{-8}	1.39×10^{-8}	2.25×10^8	8.26×10^7	5.79×10^{-10}	1.58×10^{-9}	172.53%,
15	11300	4.76×10^{-50}	0	∞	∞	---	---	---
30	23300	2.00×10^{-102}	0	∞	∞	---	---	---

As BER is reduced to 10^{-3} , the throughput improvement can be seen for higher values of T_{data} . Figure 4.1(b) illustrates the results. At this BER, the minimum and maximum throughput improvement for $T_{data}=1$ are 0.172% and 0.82%, for number of nodes 2 and 16, respectively. At $T_{data}=3$ slots, the minimum and maximum throughput improvement at $N=2$ and 16 are 1.52% and 4.85%, respectively. For $T_{data}=15$ slots, the minimum and maximum throughput improvement (%), is 10.5215% and 10.5224%. while for T_{data} equals 30 slots it is 10.52% for both minimum and maximum. The analysis shows that as T_{data} increases, PER increases, $1-P_e$ decreases, T_{Tot} increases, and throughput improvement increases. Results for lower BER shown in Figure 4.1(c) to (f) confirm that the lower the BER the lower the improvement.



(a)



(b)

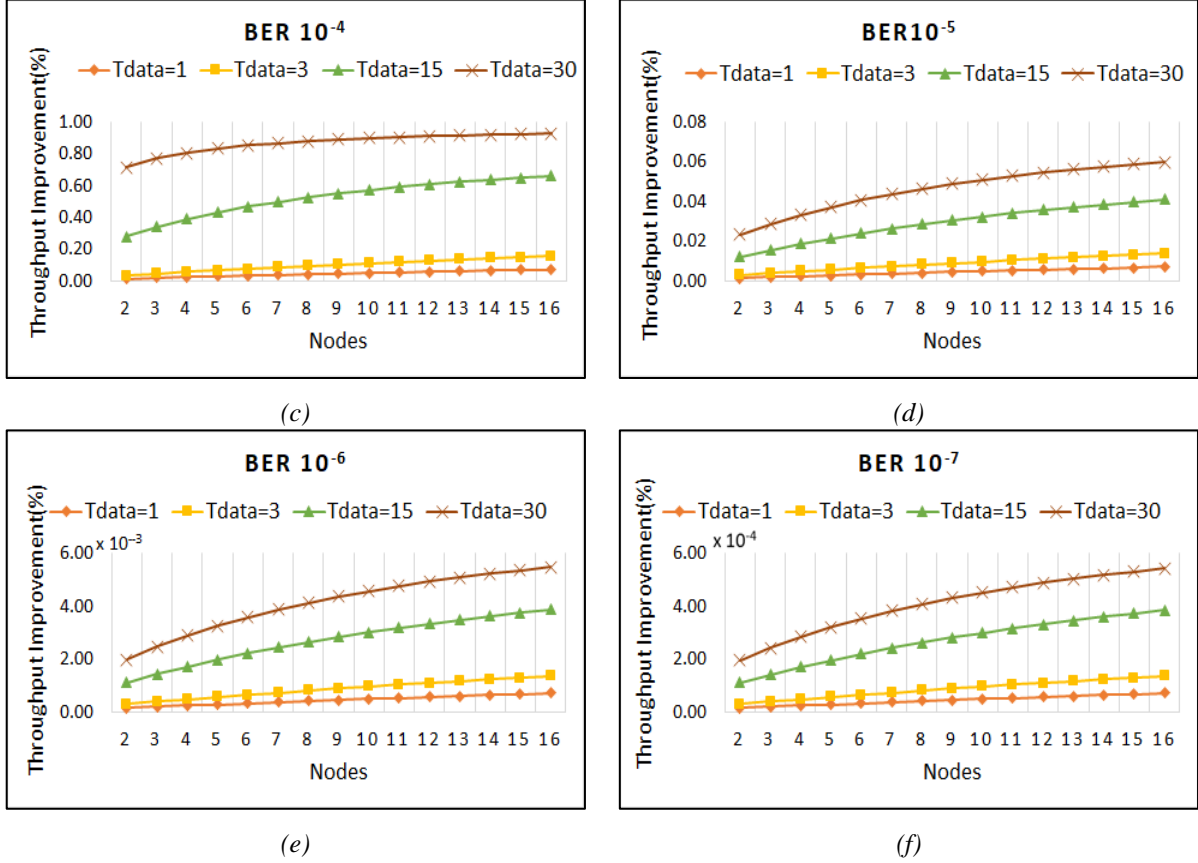


Figure 4.1: Throughput Improvement vs. Number of nodes, MultiACK Scenario-I, for: (a) BER 10^{-2} (b) BER 10^{-3} (c) BER 10^{-4} (d) BER 10^{-5} (e) BER 10^{-6} (f) BER 10^{-7} , for $Q=0$.

Results shown in Figure 4.1(a) to (f) confirm that the MultiACK Scenario I mechanism is appropriate for bad channels, where the BER is high. For low BER, the throughput improvement is marginal, but the MultiACK mechanism can save, in specific moments, energy and time. For example, for a BER of 0.005, ACK size 25 bits and 4 ACK packets, the proposed MultiACK mechanism improves the probability of successfully receiving an ACK by 65.05%.

4.1.1.1 Impact of hidden nodes

The impact of hidden nodes is analyzed. Hidden nodes (Q) in S-FAMA affect several parameters such as the probability of no collision P_s , which further affects parameters like T_{fail} , $T_{success}$ and T_{defer} . The average time, \bar{U} , during which useful data is transmitted is also affected. Results for MultiACK with hidden nodes $Q=3$ are shown in Figure 4.2. The results show that the throughput improvement with $Q=3$ is higher than the results with $Q=0$ hidden nodes. For example for BER 10^{-3} , $T_{data}=1$ and DATA packet size of 100 bits, throughput improvement with $Q=3$ is 0.95% with 16 nodes while for $Q=0$ it is 0.82%. For $T_{data}=3$, the minimum throughput improvement for 2 nodes is 2.63% and the maximum is 5.26%. For $T_{data}=15$ and 30 slots, the throughput improvement remains at 10.52%. For lower BERs, shown in Figure 4.2(c) to (f) the throughput improvement drops as BER decreases. In summary, $Q=0$ increases P_s , while $Q=3$ decreases P_s . The parameters which increase with $Q=0$ are P_s , T_{succ} and \bar{U} , while T_{fail} and T_{defer} decrease. With $Q=3$, P_s , $T_{success}$ and \bar{U} decrease while T_{fail} and T_{defer} increase. The throughput improvement is higher for $Q=3$ than for $Q=0$. Values are shown in Table 4.3.

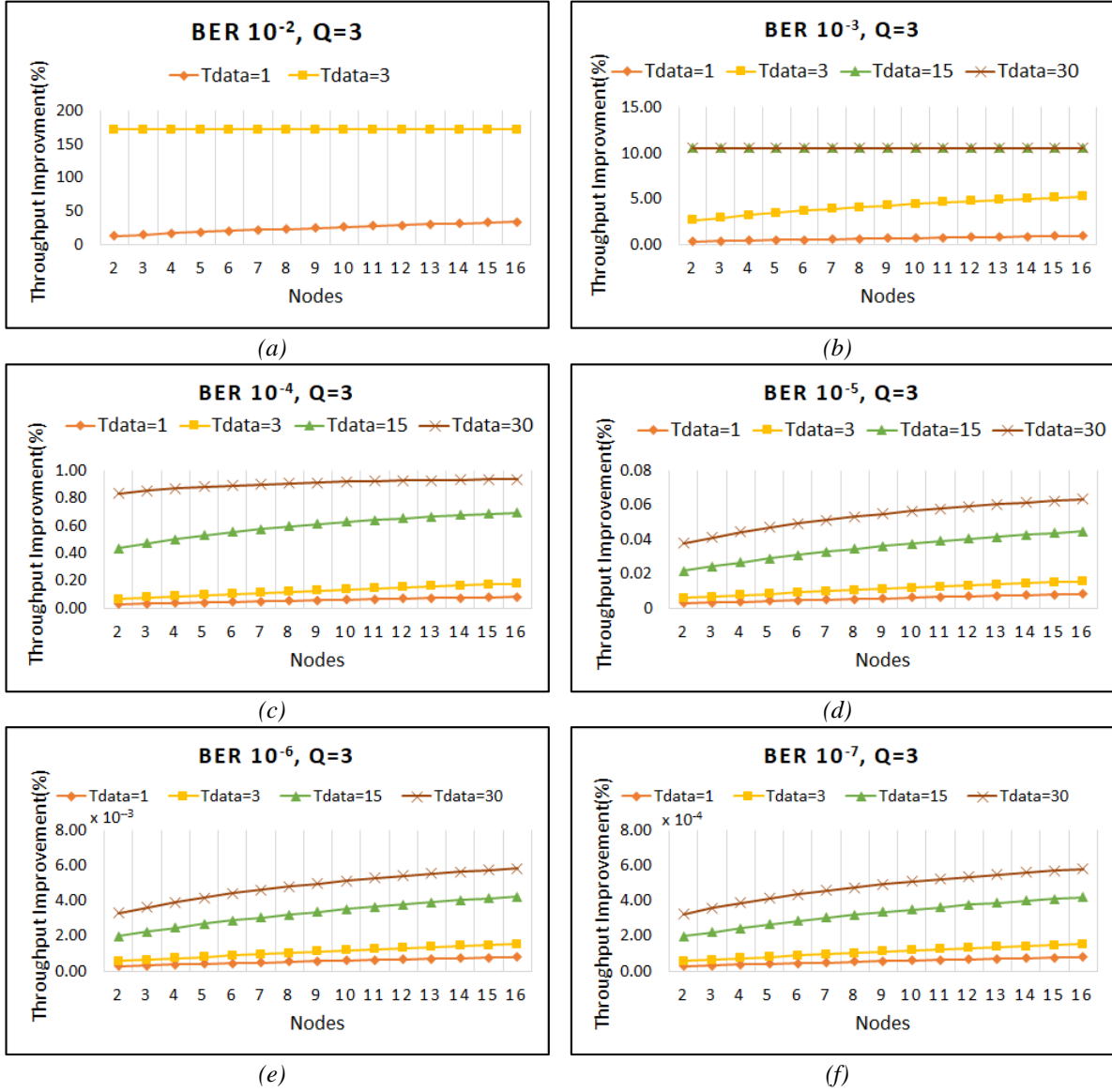


Figure 4.2: Throughput Improvement vs. Number of nodes, MultiACK Scenario-I, for: (a) $BER 10^{-2}$ (b) $BER 10^{-3}$ (c) $BER 10^{-4}$ (d) $BER 10^{-5}$ (e) $BER 10^{-6}$ (f) $BER 10^{-7}$, for $Q=3$ nodes.

Table 4.3: Impact of Hidden nodes (Q) on throughput Improvement, for $T_{data}=1$ and 16 nodes

BER	Throughput Improvement (%)		Analysis
	Q=3	Q=0	
10^{-2}	33.99	29.96	Throughput improvement is lower for $Q=0$ than for $Q=3$. It decreases as the BER decreases.
10^{-3}	0.95	0.82	
10^{-4}	0.08	0.07	
10^{-5}	8.2×10^{-3}	7.1×10^{-3}	
10^{-6}	8.2×10^{-4}	7.1×10^{-4}	
10^{-7}	8.2×10^{-5}	7.1×10^{-5}	

The impact of hidden nodes on the parameters, P_s , $T_{success}$, T_{fail} and T_{defer} , S , S_{M-1} and throughput improvement is shown in Table 4.4 for $BER 10^{-3}$. The impact on P_s , $T_{success}$, T_{fail} and T_{defer} is

shown in the form of mathematical values obtained from MATLAB. P_s and T_{success} are greater for $Q=0$ than for $Q=3$, while T_{fail} and T_{defer} are greater for $Q=3$ than $Q=0$. The throughput improvement is 0.95% with hidden nodes while for no hidden nodes it is 0.82%.

Table 4.4: Quantitative Analysis on Impact of Hidden nodes (Q) on throughput Improvement, for $T_{\text{data}}=1$ and 16 nodes, $BER 10^{-3}$

Q=3		Q=0	
Parameters	Values	Parameters	Values
P_s	0.9526	P_s	0.9599
T_{success}	3.245	T_{success}	3.27
T_{fail}	4.28×10^{-3}	T_{fail}	3.62×10^{-3}
T_{defer}	5.422	T_{defer}	0.058
S	3.43×10^{-4}	S	3.51×10^{-4}
S_{M-1}	3.47×10^{-4}	S_{M-1}	3.54×10^{-4}
Throughput Improvement	0.95%	Throughput Improvement	0.82%

4.1.1.2 Analysis as a function of BER

Figure 4.3 illustrates the MultiACK performance with varying BER and varying DATA packet sizes. The analysis shows that at higher BER, the improvement is better than at lower BERs. As explained earlier the throughput improvement varies directly with the BER and the DATA packet size (4.4). The throughput improvement is very low at $BER 10^{-7}$, 10^{-6} and 10^{-5} and tends to increase as BER increases to 10^{-4} and 10^{-3} . For example at $BER 10^{-7}$ the throughput improvement is 7.13×10^{-5} and increases to 0.82% at $BER 10^{-3}$ for $T_{\text{data}} = 1$ slot. The impact of increasing DATA packet size is also seen in Table 4.5. Values of the percentage improvement in throughput are shown in Table 4.5.

Table 4.5: MultiACK-Scenario-I, Performance Analysis as a function of BER.

BER	Tdata=1	Tdata=3	Tdata=15	Tdata=30
10^{-7}	7.13×10^{-5}	1.35×10^{-4}	3.84×10^{-4}	5.43×10^{-4}
10^{-6}	7.13×10^{-4}	1.35×10^{-3}	3.87×10^{-3}	5.48×10^{-3}
10^{-5}	7.13×10^{-3}	1.57×10^{-2}	4.48×10^{-2}	6.34×10^{-2}
10^{-4}	7.23×10^{-2}	1.57×10^{-1}	6.62×10^{-1}	9.28×10^{-1}
10^{-3}	0.82	4.85	10.5	10.5

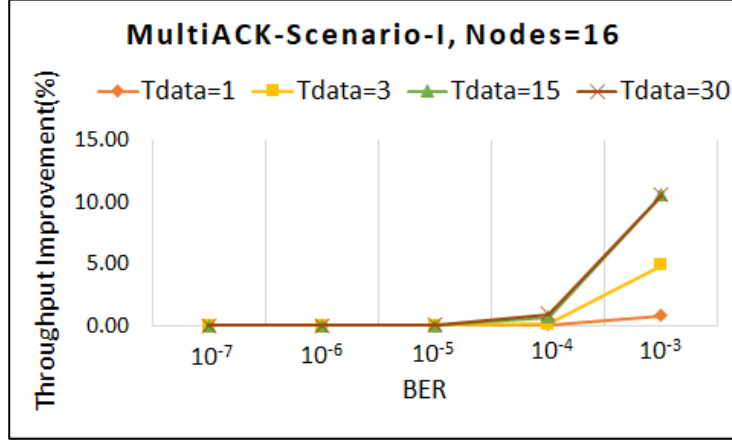


Figure 4.3: Throughput Improvement vs. BER, MultiACK Scenario-I, for BER= 10^{-7} to 10^{-3} .

Values of throughput improvement at BER 10^{-7} and 10^{-6} are almost flat, for all values of T_{data} . As the packet error rate (PER) varies directly with the BER and the packet size, the impact of varying T_{data} is seen. As T_{data} increases it increases T and T_{M-1} . Also, a high BER lowers the amount of successful transmissions.

The improvement in throughput increases as BER increases. This is because, due to MultiACK mechanism, the probability that at least one ACK is received increases. This increases the efficiency of the protocol. PER in MultiACK-SFAMA is less than that of S-FAMA. The ratio P_{eM}/P_e being less than 1 indicates that PER in S-FAMA is higher than in MultiACK. Also $T_{M-1} < T$, and $T_{Tot-M-1} < T_{Tot}$. The ratio S_{M-1}/S , which varies directly with T_{Tot} and inversely with $T_{Tot-M-1}$, is greater than 1. The throughput improvement is larger at higher BER and degrades at lower BERs.

4.1.1.3 Analysis as a function of the data length

Figure 4.4 depicts the average throughput improvement vs the data length (T_{data}) for BER 10^{-5} . As shown in the figure, the throughput improvement increases as T_{data} increases; the larger the size of the DATA packet the larger the throughput improvement. The values are shown in Table 4.6.

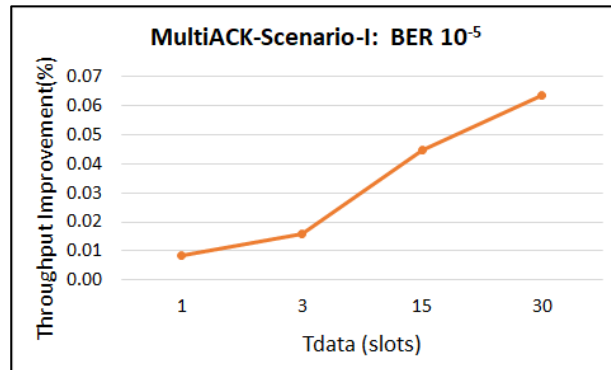


Figure 4.4: Throughput Improvement vs T_{data}

Table 4.6: Analysis as a function of data length at BER 10^{-5}

Tdata (slot)	1	3	15	30
Throughput Improvement (%)	0.007	0.013	0.041	0.060

4.1.1.4 Analysis as a function of the transmission range

Results are plotted in Figure 4.5 for a transmission range varying from 100m to 3000m, Tdata= 1, 3, 15 & 30 slots , BER from 10^{-2} to 10^{-7} and Q=0.

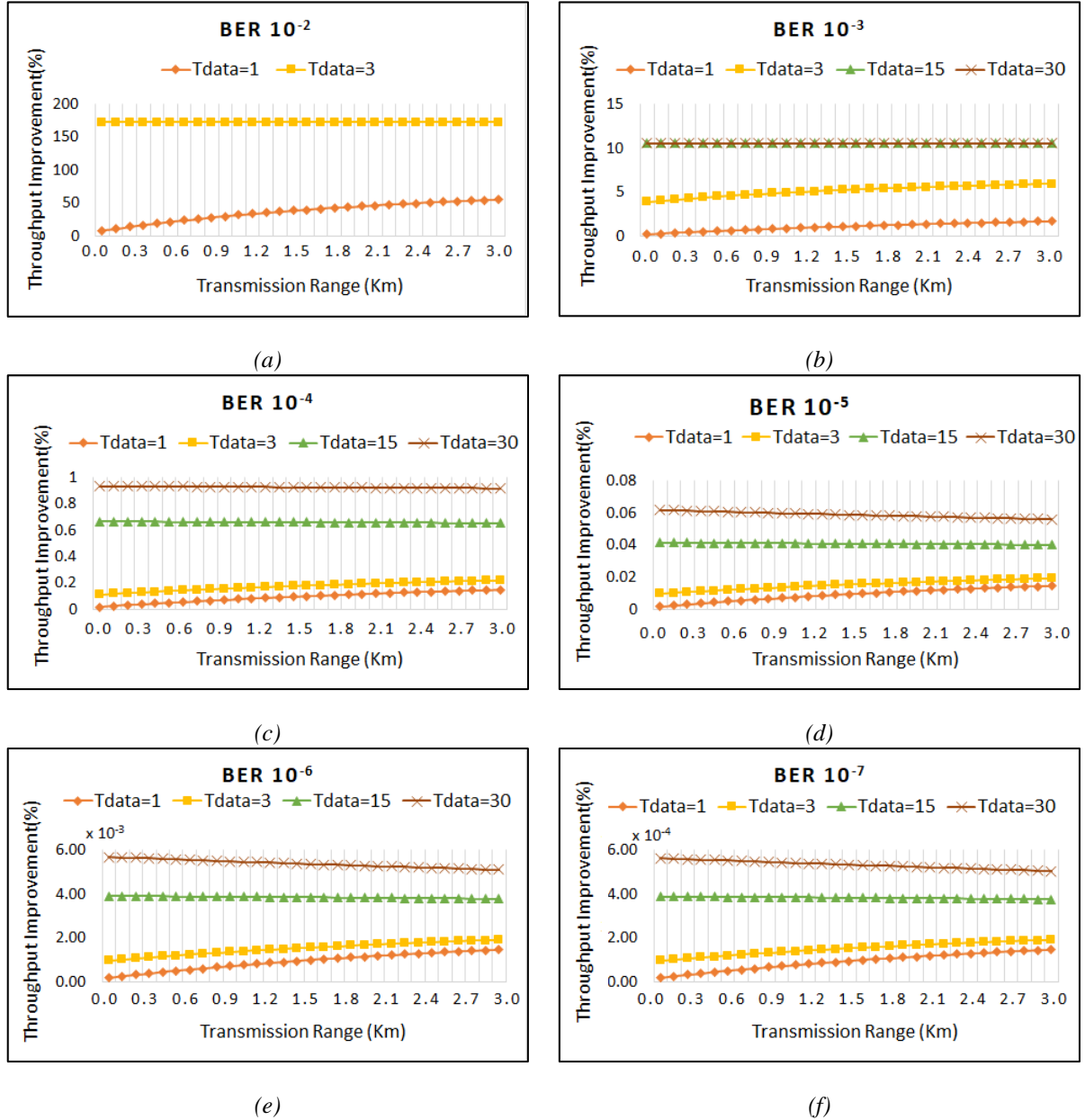


Figure 4.5: Performance of MultiACK as a function of Transmission range and Tdata= 1, 3, 15 and 30 slots for (a) BER 10^{-2} (b) BER 10^{-3} (c) BER 10^{-4} (d) BER 10^{-5} (e) BER 10^{-6} (f) BER 10^{-7}

The results show that the throughputs of S-FAMA and MultiACK decrease as the transmission range increases for the same length of data. Table 4.7 shows values of throughput improvement for a selected range of 100 m to 500 m. From Table 4.7, it is seen that MultiACK throughput is larger compared to the throughput of S-FAMA, also the throughput improvement (S_{M-1}/S) is seen to increase with the distance. This is because as the distance increases, it increases the propagation delay and hence T_{slot} . This has a direct impact on T_{Tot} and $T_{Tot-M-1}$, which also increase. The throughput improvement (4.4) varies directly with T_{Tot} and inversely with $T_{Tot-M-1}$. Since the throughput S and S_{M-1} , varies inversely with T_{Tot} and $T_{Tot-M-1}$ respectively, the throughputs decrease but the ratio of ' S_{M-1}/S ' increases with distance because $S < S_{M-1}$ and $T_{Tot-M-1} < T_{Tot}$.

Table 4.7: Analysis as a function of Transmission range at BER 10^{-3}

$T_{data}=1$	$Q=0$	BER 10^{-3}	Nodes=16	Throughput Improvement (TI)	
Distance	S	S_{M-1}	S_{M-1}/S	$(S_{M-1}/S)-1$	TI%
100	0.001903	0.001907	1.002094	0.002094	0.21
200	0.001333	0.001337	1.002878	0.002878	0.29
300	0.001017	0.001021	1.003633	0.003633	0.36
400	0.000817	0.000820	1.004362	0.004362	0.44
500	0.000679	0.000682	1.005064	0.005064	0.51

Figure 4.5 (a) to (f) also depicts the impact of transmission range on throughput improvement with different lengths of data and varying BERs. The length of data is directly affected by transmission range as it is a measure of the duration of all slot needed by the DATA packet. The increase in transmission range increases T_{slot} and hence T_{data} which in turn increases T_{Tot} . It is observed that for a given transmission range, throughput improvement tends to be lower at lower BERs. This is because T_{Tot} varies directly with the distance and inversely with ' $1-P_e$ '. Lower BERs, increases ' $1-P_e$ ' and decreases T_{Tot} and hence decreases the throughput improvement for a given transmission range.

The throughput improvement for $T_{data}=3$ slots is in hundreds (172.53%) at a range of 3000m for BER 10^{-2} and is below tens (5.93%) for BER 10^{-3} . Further, increasing the length of data to 15 and 30 slots shows no results for BER 10^{-2} . This is because P_e tends to 1. The impact of transmission range on the throughput improvement for BER 10^{-3} to 10^{-7} shows throughput improvement for larger DATA packets. However, the improvement degrades with increasing distance. The percentage improvement at these values is very low.

In S-FAMA, low transmission ranges involve low competition to acquire the channel but a higher number of hops through the network and lower connectivity. This degrades performance. A situation of isolated nodes occurs when one or more pairs of nodes cannot be connected through any path.

For high transmission ranges the throughput performance degrades because of the increase in neighboring nodes causing an increase in the overheard traffic. It becomes difficult to acquire a channel due to large number of RTS collisions. In our results it is clearly seen that the improvement is achieved at all transmission ranges. This is due to the better performance of MultiACK compared to S-FAMA.

4.1.1.4.1 Impact of hidden nodes

The presence of hidden nodes in S-FAMA impacts P_s (the probability of no collision). This further affects T_{success} , T_{fail} and T_{defer} . From the results and analysis of parameters it is observed that P_s is higher with no hidden nodes ($Q=0$) and reduces in the presence of hidden nodes ($Q=3$). When P_s increases, T_{success} and channel utilization is high. T_{fail} and T_{defer} are low. In the presence of hidden nodes ($Q=3$), P_s decreases, T_{fail} and T_{defer} increase and T_{success} and channel utilization decrease. The effects of hidden nodes are shown in Figure 4.6. It is seen that at $T_{\text{data}}=1$ and 3, the throughput improvement increases with the increase in range. For larger DATA packets, $T_{\text{data}}=15$ and 30, it tends to decrease with the increase in range. At lower BER the throughput improvement is very low. The comparative analysis is shown in Table 4.8.

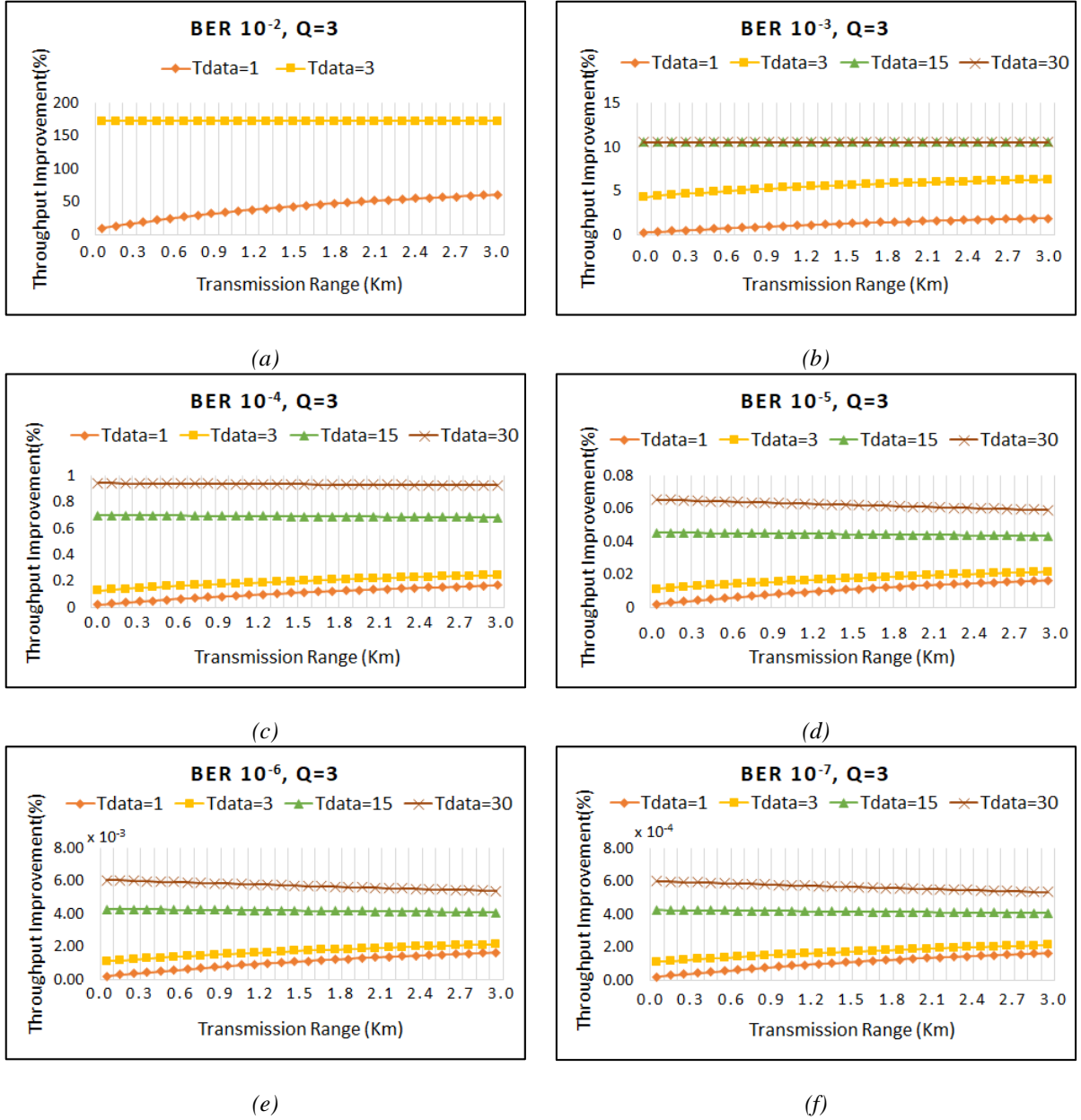


Figure 4.6: Performance of MultiACK Scenario-I as a function of Transmission range and $T_{\text{data}} = 1, 3, 15$ and 30 slots for (a) BER 10^{-2} (b) BER 10^{-3} (c) BER 10^{-4} (d) BER 10^{-5} (e) BER 10^{-6} (f) BER 10^{-7} with hidden nodes ($Q=3$).

Table 4.8: MultiACK-Scenario-I, Performance Analysis with $Q=0$ and $Q=3$ hidden nodes and $T_{data}=1$ slot and 16 nodes.

	Q=0		Q=3	
	Transmission Range		Transmission Range	
BER	100m	3000m	100m	3000m
10^{-3}	0.21	1.68	0.25	1.89
10^{-4}	0.02	0.15	0.02	0.17
10^{-5}	1.80×10^{-3}	1.47×10^{-2}	2.11×10^{-3}	1.65×10^{-2}
10^{-6}	1.80×10^{-4}	1.47×10^{-3}	2.11×10^{-4}	1.65×10^{-3}
10^{-7}	1.80×10^{-5}	1.47×10^{-4}	2.11×10^{-5}	1.65×10^{-4}

4.1.1.5 Analysis as a function of the Offered Load

The throughput performance of S-FAMA and MultiACK has been analyzed using (3.15) and (3.24). Graphs for throughput versus offered load, for $BER = 10^{-5}$ and 16 nodes, are presented in Figure 4.7. The curves show that S-FAMA has a maximum throughput of 0.00104 bps for $T_{data}=1$ and λ ranging from 0.03481 to 0.03871 packets/second. For $T_{data}=3$, the maximum throughput of S-FAMA is 0.0124 for λ ranging from 0.0273 to 0.0292 packets/second.

Figure 4.7 also shows that MultiACK has a maximum throughput of 0.001045bps for $T_{data}=1$ and $\lambda=0.03581$ -0.03791 packets/second. Thus, the improvement in throughput of MultiACK is 0.0256%.

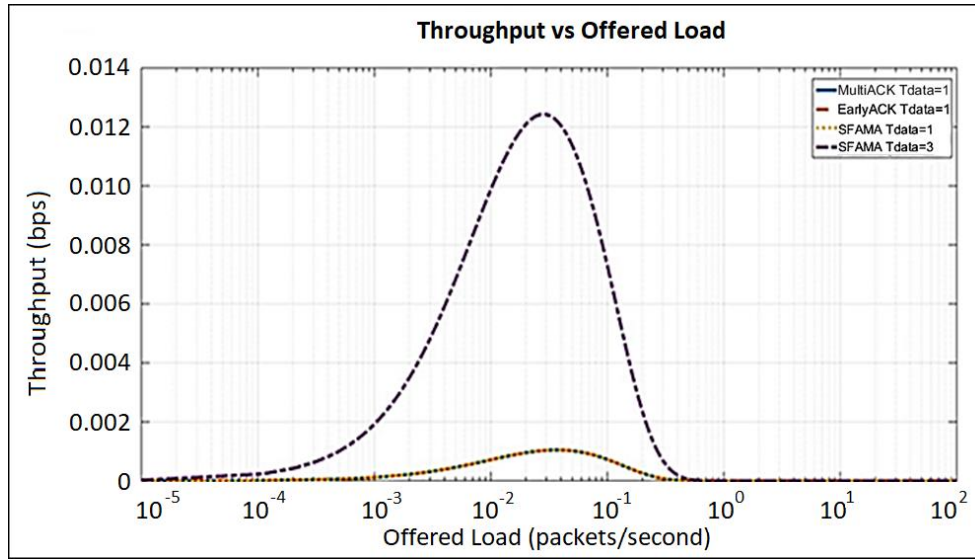


Figure 4.7: Throughput (bps) vs offered Load (packets/second) for S-FAMA, $T_{data}=1$ & 3 slots, MultiACK with $T_{data}=1$ slot and EarlyACK with $T_{data}=1$ slot

Figure 4.8 shows a comparison for MultiACK Scenario-I with $T_{data} = 1$ & 3 slots. The maximum throughput improvement for $T_{data} = 1$ slot is 0.0256 bps at an offered load of 0.03561-0.03811 packets/seconds. With $T_{data} = 3$ slots, the throughput improvement is 0.0385 at an offered load of 0.02811 to 0.02841 packets/sec. It is seen that with $T_{data}=3$ slots throughput improvement increases by 50.39% compared to that of $T_{data}=1$ slot. Thus, for the given range of offered load, increasing the size of T_{data} increases the throughput improvement.

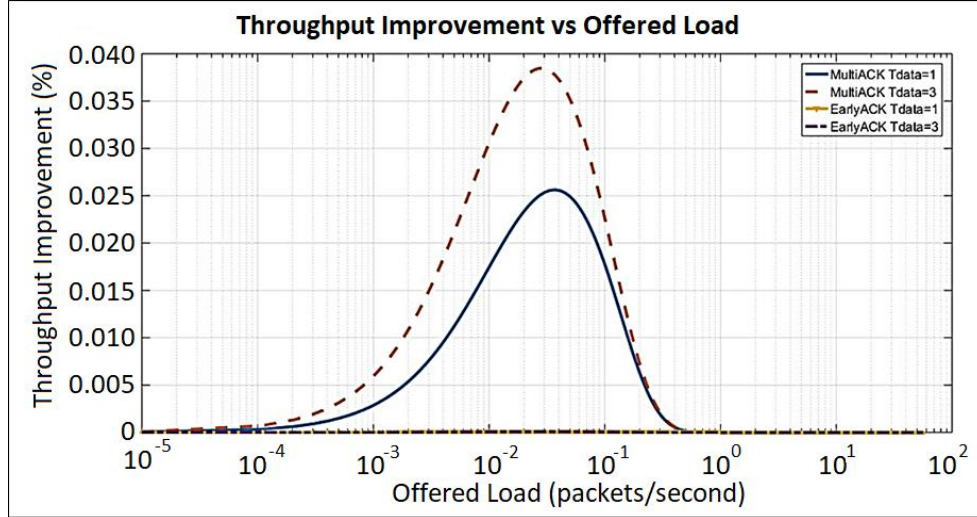


Figure 4.8: Throughput Improvement vs offered Load with MultiACK-Scenario-I, and EarlyACK

4.1.2 Scenario-II

In Scenario-II we have used the same value of T_{ACK} (0.025seconds) as in Scenario-I to compare the throughputs of both scenarios. The number of ACKs in this case is $i = 36$ ACKs and $L_{ACK} = 25$ bits. In the simulations we have used the parameters given in Table 4.9. Throughput improvement curves have been plotted for $BER = 10^{-2}$ to 10^{-7} . In this scenario the results were not positive.

Table 4.9: Parameters used in MutliACK: Scenario-II

Parameter	Values
T_{slot}	$\tilde{D} + T_{CTS}$
T_{CTS}	(L_{CTS}/R) (0.1)
L_{CTS} (RTS/CTS packet size)	100 bits
T_{ACK}	0.025 s
i	36
N	2-16
Q (hidden nodes)	0 and 3
R (Bitrate)	1000 bps
Propagation speed	1500 m/s
\tilde{D} (Propagation Delay)	(Distance/Speed)
DATA packet size	100, 1700, 11300, 23300 bits
T_{data}	1, 3, 15 & 30 slots
L_{ACK}	25 bits
Distance (Range)	1000m (w.r.t. nodes) 100m to 3000m (w.r.t transmission range)

4.1.2.1 Analysis as a function of the number of Nodes

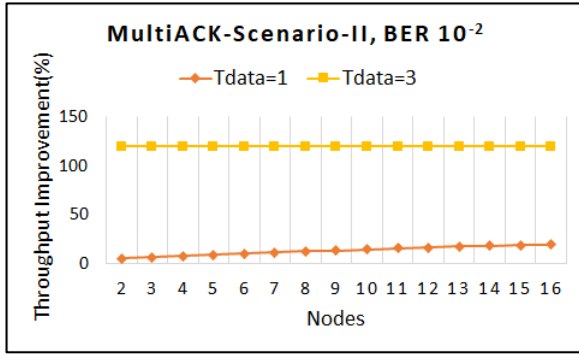
The curves for the throughput improvement vs the number of nodes have been plotted for $T_{data} = 1, 3, 15, 30$ and $BER = 10^{-2}$ to 10^{-7} . Results obtained are shown in Figure 4.9. The curves show

improvement in throughput of S-FAMA with MultiACK Scenario-II, for BER 10^{-2} , where the minimum is 4.76% and the maximum is 19.51% for 2 and 16 nodes, respectively.

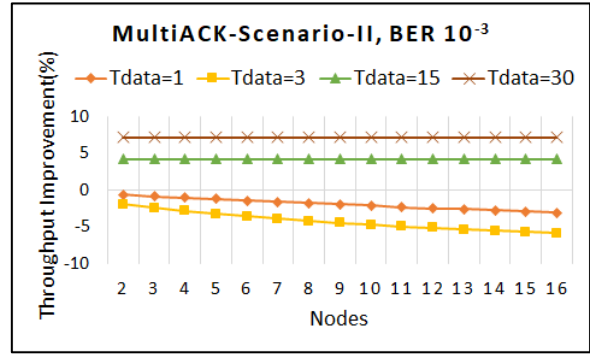
For BER 10^{-3} the results show positive improvement for $T_{\text{data}}=15$ and 30 slots. For $T_{\text{data}}=15$, the throughput improvement remains almost constant at 4.25%. For $T_{\text{data}}=30$, the same happens at 7.20%.

The results for BER 10^{-4} to 10^{-7} show no improvement. In fact, they show that this hypothesis degrades the throughput of S-FAMA. This is because the increase in the duration of the MultiACK packet to $2T_{\text{slot}}$ increases T_{M-2} , the time between the start of DATA packet and successful reception of an ACK; this, in turn, increases $T_{\text{Tot-M-2}}$ (3.27) which further increases $T_{\text{success-M-2}}$ (3.28) and $T_{\text{defer-M-2}}$ (3.29). The throughput S_{M-2} varies inversely with $T_{\text{Tot-M-2}}$, $T_{\text{success-M-2}}$ and $T_{\text{defer-M-2}}$; thus, throughput decreases. The mathematical expression derived for the second scenario of MultiACK is shown in (4.5).

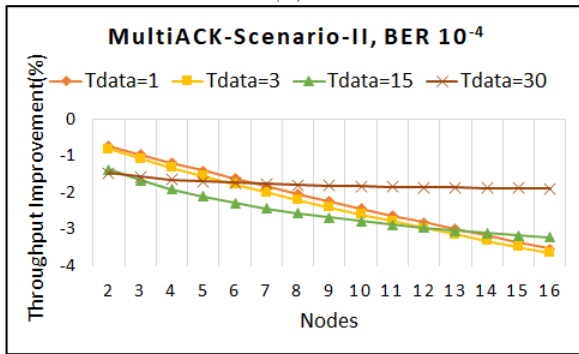
$$\frac{S_{M-2}}{S} = \frac{(N+1)P_s T_{\text{Tot}} + 2T_{\text{slot}}(1-P_s) + (T_{\text{data}} + T_{\text{slot}}) \left(\left(\frac{QP_s}{(1-P_e)} \right) + N(1-P_s) \right) + \frac{1}{\lambda}}{(N+1)P_s T_{\text{Tot-M-2}} + 2T_{\text{slot}}(1-P_s) + (T_{\text{data}} + 2T_{\text{slot}}) \left(\left(\frac{QP_s}{(1-P_{eM})} \right) + N(1-P_s) \right) + \frac{1}{\lambda}} \quad (4.5)$$



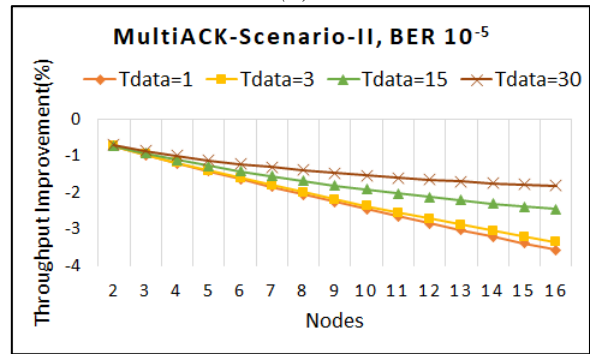
(a)



(b)



(c)



(d)

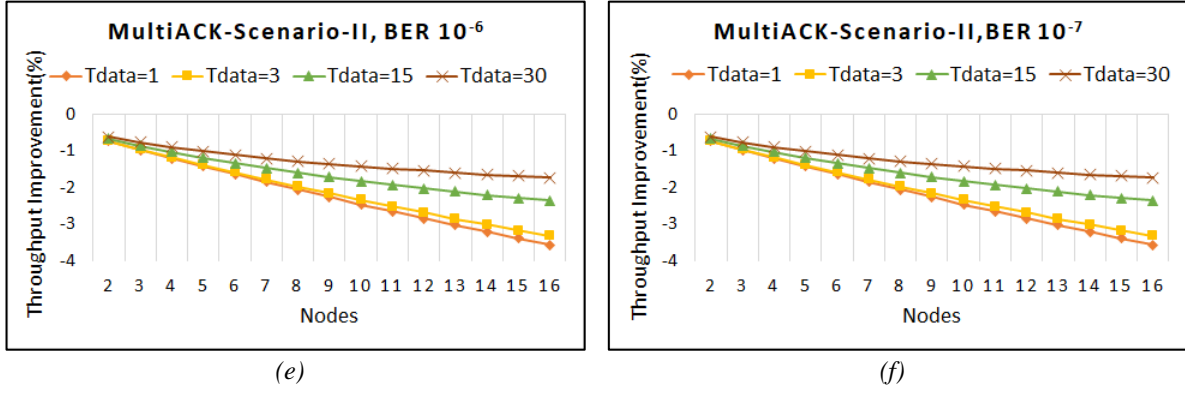


Figure 4.9: MultiACK Scenario-II.: Throughput Improvement vs. Number of nodes for: (a) BER 10^{-2} (b) BER 10^{-3} (c) BER 10^{-4} (d) BER 10^{-5} (e) BER 10^{-6} (f) BER 10^{-7}

4.1.2.2 Analysis as a function of BER

Figure 4.10 illustrates the performance as a function of BER from 10^{-7} to 10^{-3} . The throughput degradation at $T_{\text{data}}=1$ and 3 slots is -3.10% and -5.85%, it is seen to increase to 4.25% at $T_{\text{data}}=15$ slots and at 30 slots it is 7.20% for BER = 10^{-3} . The throughput improvement is negative except for $T_{\text{data}}=15$ and 30 slots at BER 10^{-3} . Results are shown in Table 4.10 with 16 nodes.

Table 4.10: MultiACK-Scenario-II, Performance Analysis as a function of BER.

Comparative Analysis: Throughput Improvement (%) vs BER				
BER	Tdata=1	Tdata=3	Tdata=15	Tdata=30
10^{-7}	-3.57	-3.33	-2.36	-1.73
10^{-6}	-3.57	-3.33	-2.36	-1.73
10^{-5}	-3.57	-3.36	-2.46	-1.82
10^{-4}	-3.53	-3.65	-3.22	-1.89
10^{-3}	-3.10	-5.85	4.25	7.20

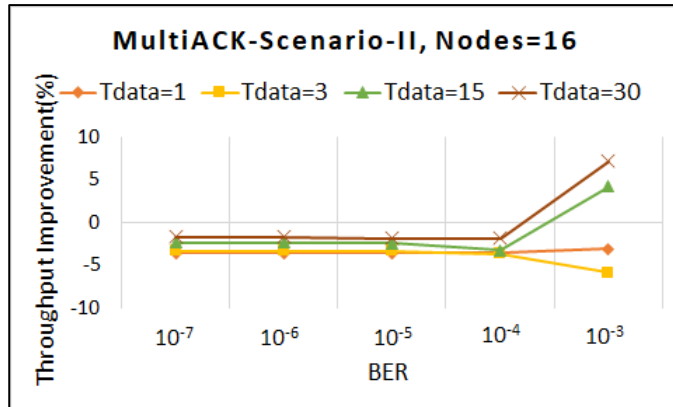


Figure 4.10: Throughput Improvement vs. BER, MultiACK Scenario-II.

4.1.2.3 Analysis as a function of the Transmission Range

Figure 4.11 presents the performance results of MultiACK Scenario-II. For BER 10^{-2} results show that for $T_{data}=1$ throughput improvement increases with the increase in range. With $T_{data}=3$, the improvement is there but decreases with the distance. With larger DATA packets, T_{data} equal 15 and 30, it gives no results. This is because T_{Tot} and $T_{Tot-M-2}$ are infinite, because P_e and P_{eM-2} are 1. In Figure 4.11 (b), with BER 10^{-3} and $T_{data}=1$ slot, there is no improvement in throughput. For $T_{data}=3$ slots, 0.67% improvement is observed only for 100m range. For a transmission range from 200m to 3000m the results also show no improvement. For $T_{data}=15$ slots, there is an improvement in throughput at 100m (8.95%) which tends to reduce to 2000m (0.30%). From 2000m to 3000m there is no improvement. For $T_{data}=30$ slots, improvement is seen, which tends to reduce with the distance between 100m (9.75%) and 3000m (2.66%).

For BER 10^{-4} , $T_{data}=1, 3$ and 15 slots, no improvement is seen. $T_{data}=30$ slots gives improvement for transmission ranges between 100m (0.27%) and 200m (0.02%). From 400m to 3000m no improvement is seen. For BER 10^{-5} to 10^{-7} , there is no improvement in throughput.

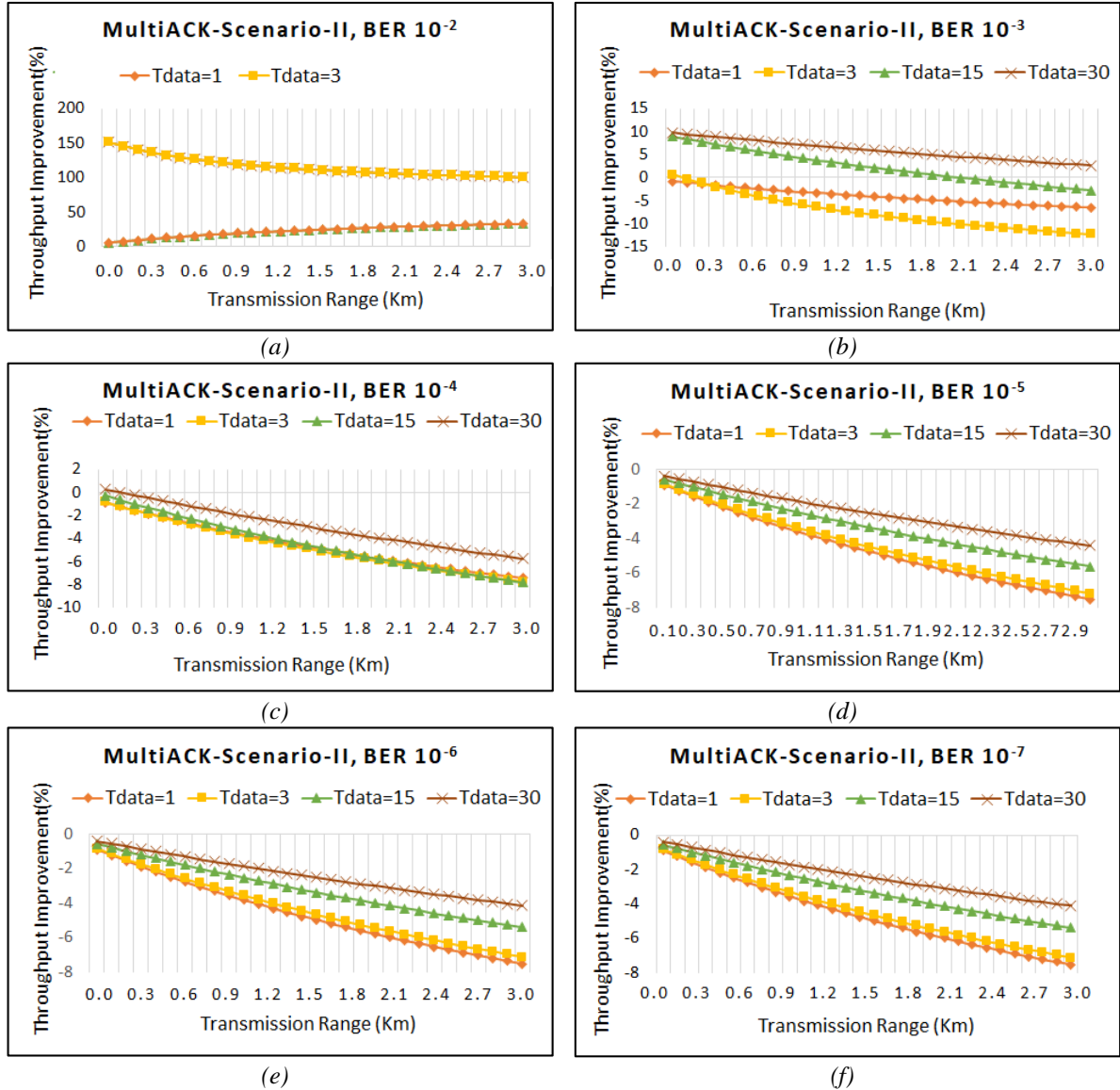


Figure 4.11: MultiACK Scenario-II.: Throughput Improvement (%) vs. Transmission range, (a) BER 10^{-2} (b) BER 10^{-3} (c) BER 10^{-4} (d) BER 10^{-5} (e) BER 10^{-6} (f) BER 10^{-7} .

4.1.2.4 Analysis as a function of the data length

Figure 4.12 shows that the throughput improvement versus the length of data gives negative results. Table 4.11 depicts the behavior for BER 10^{-5} .

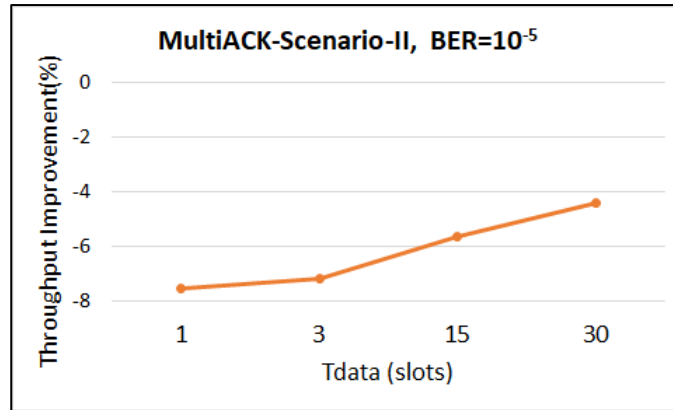


Figure 4.12: Throughput Improvement vs. Tdata, MultiACK Scenario-II, with 16 nodes.

Table 4.11: Analysis Throughput Improvement vs. Tdata, MultiACK Scenario-II

	Tdata			
BER	1	3	15	30
10^{-5}	-7.52865	-7.18986	-5.64278	-4.41969

4.1.3 Comparative Analysis

The performance of MultiACK Scenario-I, in terms of throughput is better with respect to varying nodes, transmission range, BER, and for varying length of data. Table 4.12 depicts the comparative analysis of MultiACK Scenarios I and II. The MultiACK Scenario-I mechanism improves efficiency of S-FAMA and increases the probability of successful reception of an ACK packet.

Table 4.12: MutliACK Scenario-I & II, Performance Analysis

Throughput Improvement vs Number of Nodes for 16 nodes and BER= 10^{-5}				
MultiACK	T _{data} =1	T _{data} =3	T _{data} =15	T _{data} =30
Scenario-I	7.14×10^{-3}	13×10^{-3}	41×10^{-3}	60×10^{-3}
Scenario-II	-3.57	-3.36	-2.46	-1.82

If we compare the throughput improvement performance of MultiACK Scenarios I and II, we can see that the results for Scenario-II are worse as compared not only to Scenario-I, but also to S-FAMA itself. Table 4.13 and Table 4.14 depicts the comparative analysis of both scenarios.

Table 4.13: MutliACK Scenario-I & II, Comparative Analysis of throughput improvement at BER 10^{-3}

Throughput Improvement (%) vs BER					
Nodes=16	BER= 10^{-3}	$T_{data}=1$	$T_{data}=3$	$T_{data}=15$	$T_{data}=30$
Scenario-I		0.82	4.85	10.52	10.52
Scenario-II		-3.10	-5.85	4.25	7.20

Table 4.14: Comparative Analysis: Throughput Improvement vs Transmission Range for $T_{data}=1$ slot.

BER	Improvement %		Improvement %	
	MultiACK Scenario-I		MultiACK Scenario-II	
	At 100m	At 3000m	At 100m	At 3000m
10^{-2}	8.27	55.22	5.74	33.20
10^{-3}	0.21	1.68	-0.79	-6.53
10^{-4}	0.018	0.149	-0.89	-7.45
10^{-5}	1.81×10^{-3}	1.47×10^{-2}	-0.90	-7.53
10^{-6}	1.81×10^{-4}	1.47×10^{-3}	-0.90	-7.53
10^{-7}	1.81×10^{-5}	1.47×10^{-4}	-0.90	-7.53

4.2 EarlyACK

This section presents the results obtained for EarlyACK. The analysis has been done using the parameters shown in Table 4.15. The throughput improvement was calculated using expression (4.6).

Table 4.15: Parameters for analysis of EarlyACK

Parameter	Values
T_{slot}	$\tilde{D} + T_{CTS}$
T_{CTS}	(L_{CTS}/R) 0.1s
L_{CTS} (RTS/CTS packet size)	100 bits
T_{ACK}	0.025s
n	1
N	2-16
Q (hidden nodes)	0
R (Bitrate)	1000bps
Propagation speed	1500 m/s
\tilde{D} (Propagation Delay)	Distance/Speed
DATA packet size	100, 1700, 11300, 23300 bits
T_{data}	1, 3, 15 & 30 slots(s)
L_{ACK}	25 bits
Distance (Range)	1000m (w.r.t. nodes) 100m to 3000m (w.r.t transmission range)

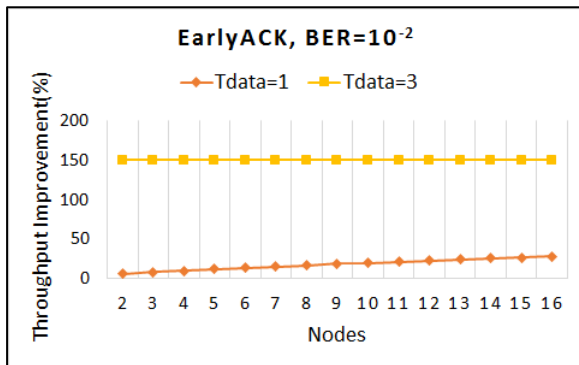
$$\frac{S_{EA}}{S} = \frac{(N+1)P_s T_{Tot} + 2T_{slot}(1-P_s) + (T_{data} + T_{slot}) \left(\left(\frac{QP_s}{(1-P_e)} \right) + N(1-P_s) \right) + \frac{1}{\lambda}}{(N+1)P_s T_{Tot-EA} + 2T_{slot}(1-P_s) + (T_{data} + T_{slot}) \left(\left(\frac{QP_s}{(1-P_{eEA})} \right) + N(1-P_s) \right) + \frac{1}{\lambda}} \quad (4.6)$$

4.2.1 Analysis as a function of the number of Nodes

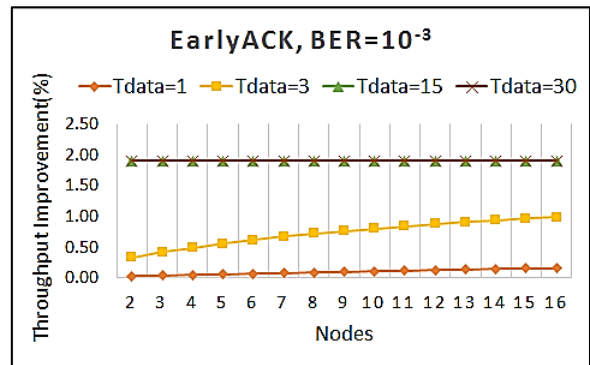
Graphs for the throughput improvement vs the number of nodes are shown in Figures 4.13 (a) to (f). The analysis has been made for $BER=10^{-2}$ to 10^{-7} for different values of T_{data} and no hidden nodes ($Q=0$). The number of bits in the DATA packet (L_{DATA}) has been 100, 1700, 11,300 and 23,300 bits. It can be seen from the results that the improvement for $BER 10^{-2}$, $T_{data}=1$ and 3 is very high as compared to those of low BER. The minimum and maximum throughput improvement for $T_{data}=1$ is 6.56% and 28.41%, respectively. The highest throughput improvement is 149.99%, and it occurs for $T_{data}=3$. This is because at high BER, the packet error rate is also high. For example at $BER 10^{-2}$ and 100 bits DATA packet, the packet error rate P_e is 1, this makes T_{Tot} infinite and the throughput goes to zero.

For $BER 10^{-3}$, the throughput improvement increases as the number of nodes increases. The effect of the data packet size is also significant. The throughput is seen to increase with the packet size, as shown for $T_{data}=1$. As the packet size increases, the improvement grows. For $T_{data}=15$ and 30 slots, the throughput improvement is 1.91%.

In Figure 4.13 (c) to (f) it is observed that as BER decreases from 10^{-4} to 10^{-7} , throughput improvement also lowers. Though the variation with the increase of the packet size is positive in terms of throughput improvement, it is however very marginal. For example, in Figure 4.13(c) the minimum at number of nodes=2 for $T_{data}=1$ slot is 3.1×10^{-4} % and the maximum at 16 nodes, for $T_{data}=30$, is 1.87×10^{-2} %. The same can be observed for $BER=10^{-5}$, where for $T_{data}=30$ slots the minimum throughput improvement is 5.65×10^{-5} % and the maximum is 1.31×10^{-4} %. It continues to lower for $BER=10^{-6}$ and $BER=10^{-7}$ where the maximum throughput improvement for $T_{data}=30$ slots at 16 nodes is 12.1×10^{-7} % and 12.1×10^{-9} %, respectively.



(a)



(b)

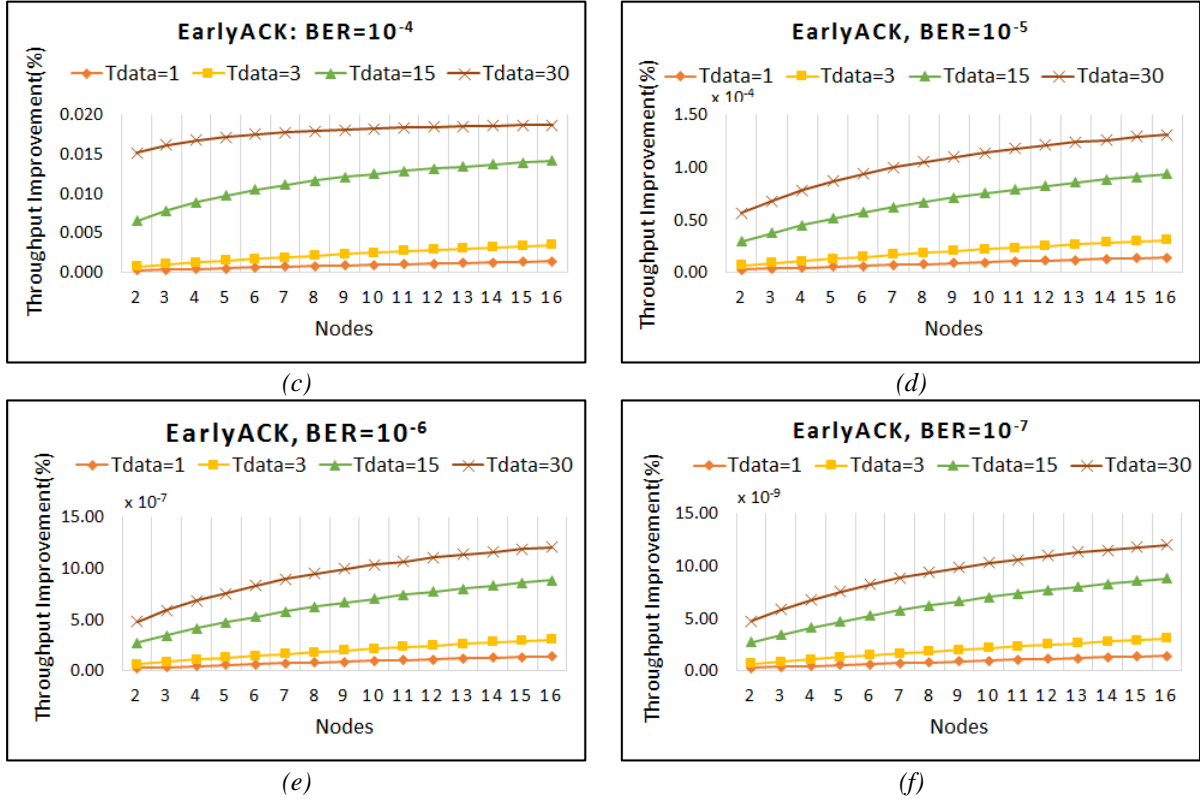


Figure 4.13: Throughput Improvement (%) vs. Number of nodes in EarlyACK for (a) BER 10^{-2} (b) BER 10^{-3} (c) BER 10^{-4} (d) BER 10^{-5} (e) BER 10^{-6} (f) BER 10^{-7}

The curves show that this mechanism performs marginally better in terms of throughput, and assures that no retransmission of DATA takes place in case of ACK loss. As the cost of losing an ACK is very significant in underwater communication, this EarlyACK mechanism saves cost in such scenarios by preventing the repetition of the data transmission cycle, thus resulting in energy saving.

4.2.1.1 Impact of Hidden Nodes

Graphs for the throughput improvement vs the number of nodes for $Q=3$ are shown in Figures 4.14 (a) to (f). The analysis has been made for BER= 10^{-2} to 10^{-7} for different values of T_{data} . The number of bits in the DATA packet (L_{DATA}) has been 100, 1700, 11,300 and 23,300 bits. It can be seen from the results that the improvement for BER 10^{-2} , $T_{data}=1$ and 3 is very high as compared to those of low BER. The minimum and maximum throughput improvement for $T_{data}=1$ is 13.95 (for $Q=0$ it was 6.56%) and 35.32% (it was 28.41% for $Q=0$), respectively. The highest throughput improvement is 149.99% (same as with $Q=0$), and it occurs for $T_{data}=3$. This is because at high BER, the packet error rate is also high. For example, at BER 10^{-2} and 100 bits DATA packet, the packet error rate P_e is 1 and the throughput goes to zero. The impact on the throughput improvement, with and without hidden nodes is realized from the analysis. The parameters which increase with $Q=0$ are P_s , $T_{success}$ and \bar{U} , while T_{fail} and T_{defer} decrease. With $Q=3$, P_s , $T_{success}$ and \bar{U} decrease while T_{fail} and T_{defer} increase. The throughput improvement is higher for $Q=3$ than for $Q=0$.

For BER 10^{-3} , the throughput improvement increases as the number of nodes increases. The effect of the data packet size is also significant. The throughput is seen to increase with the number of nodes, as shown for $T_{data}=1$. As the packet size increases, the improvement grows.

For $T_{\text{data}}=15$ and 30 slots, the throughput improvement is 1.91% which is the same as with $Q=0$.

In Figure 4.14 (c) to (f) it is observed that as BER decreases from 10^{-4} to 10^{-7} , throughput improvement also lowers. Though the variation with the increase of the packet size is positive in terms of throughput improvement, it is however very marginal. For example, in Figure 4.14(c) the minimum at number of nodes=2 for $T_{\text{data}}=1$ slot is 6.7×10^{-4} % which is higher compared to 3.1×10^{-4} % for $Q=0$ and the maximum at 16 nodes, for $T_{\text{data}}=30$ is 1.89×10^{-3} %, which is lower than 1.87×10^{-2} % that occurred at $Q=0$. The same can be observed for $\text{BER}=10^{-5}$, where for $T_{\text{data}}=30$ slots, the minimum throughput improvement is 8.59×10^{-5} % (it was 5.65×10^{-5} % for $Q=0$) and maximum is 1.36×10^{-4} % which is close to 1.31×10^{-4} % that occurred at $Q=0$. It continues to lower for $\text{BER}=10^{-6}$ and $\text{BER}=10^{-7}$ where the maximum throughput improvement for $T_{\text{data}}=30$ slots at 16 nodes is 12.7×10^{-6} %, which is higher compared to 12.1×10^{-7} % at $Q=0$ and 12.6×10^{-9} %, compared to 12.1×10^{-9} % at $Q=0$.

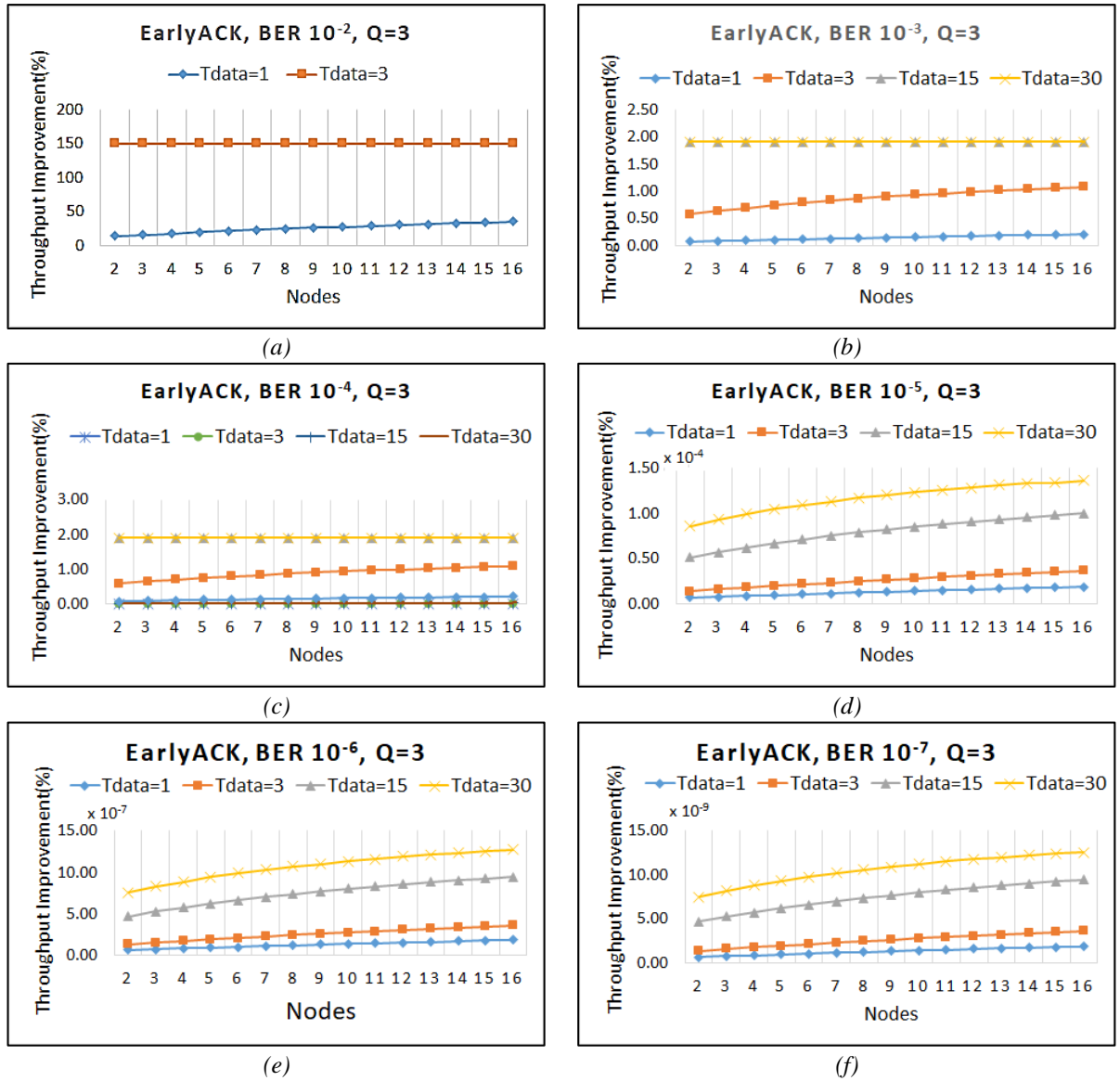


Figure 4.14: Throughput Improvement (%) vs. Number of nodes in EarlyACK for $Q=3$,
(a) $\text{BER } 10^{-2}$ (b) $\text{BER } 10^{-3}$ (c) $\text{BER } 10^{-4}$ (d) $\text{BER } 10^{-5}$ (e) $\text{BER } 10^{-6}$ (f) $\text{BER } 10^{-7}$

4.2.2 Analysis as a function of BER

Figure 4.15 illustrates the EarlyACK performance with varying BER. The improvement in throughput at BER 10^{-3} and $T_{\text{data}}=1\text{slot}$ is 0.16% and is seen to increase to 0.99% at $T_{\text{data}}=3$ slots. Further increase in T_{data} to 15 and 30 slots increases the improvement to 1.908262% to 1.908323%, respectively. This is because $T_{\text{Tot-EA}}$ varies directly with the data packet size and inversely with $(1-P_{\text{eEA}})$. For example for BER= 10^{-3} and $T_{\text{data}}=1\text{slot}$, $T_{\text{Tot-EA}}$ is 3.77s and for $T_{\text{data}}=3\text{slots}$ it increases to 24.26s. The larger the packet size, the larger the $T_{\text{Tot-EA}}$ and hence the throughput improvement. Also the higher the BER, the higher the improvement. The throughput varies directly with the DATA packet size. As shown in (3.41), throughput varies directly with δ , the normalized DATA transmission time, which depends on L_{DATA} (3.42). Increasing the packet size, increases the throughput. For example, for BER= 10^{-3} , $T_{\text{data}}=1\text{slot}$, L_{DATA} is 100bits and the throughput is 35.05×10^{-5} for S-FAMA and 35.11×10^{-5} for EarlyACK. When T_{data} is increased to 3 slots, L_{DATA} is 1700 bits, the throughput of S-FAMA is 3.09×10^{-3} while for EarlyACK it is 3.12×10^{-3} , which gives an improvement of 0.99%.

It is also observed that, for a given BER, $T_{\text{Tot-EA}}$ and PER increase with increasing DATA packet size. For example, at BER 10^{-4} , we observe that the variation in $T_{\text{Tot-EA}}$ at the same BER 10^{-4} shows an increase from 3.44 to 6.15 as T_{data} increases from 1 slot to 3 slots. The PER also increases from 0.02 to 0.16. Further increase to $T_{\text{data}}=15$ and 30 slots increases the throughput improvement to 0.68% and 0.90%.

We see that the improvement is low and tends to increase as T_{data} increases from 1 to 30 slots. Values are shown in Table 4.16. As BER decreases $T_{\text{Tot-EA}}$ decreases. T_{Tot} and $T_{\text{Tot-EA}}$ vary inversely with $1-P_e$ and $1-P_{\text{eEA}}$. For BER 10^{-3} , $T_{\text{data}}=1$ slot, $1-P_e$ is 0.8186 while $1-P_{\text{eEA}}$ is 0.8134. This gives T_{Tot} as 3.799 and $T_{\text{Tot-EA}}$ as 3.765. Since $T_{\text{Tot-EA}}$ is less than T_{Tot} , the throughput improvement increases, as it varies directly with T_{Tot} and inversely with $T_{\text{Tot-EA}}$.

Table 4.16 shows the comparative analysis of throughput improvement for Early ACK, for varying DATA packet sizes. From the results it can be seen that at higher BER the improvement is higher. The throughput shows improvement for BER 10^{-2} to 10^{-7} . By sending an early ACK in case of ACK loss the probability of successful reception of ACK increases the effectiveness of the mechanism and saves energy and cost. Thus, the proposed mechanism would be useful in case of ACK loss.

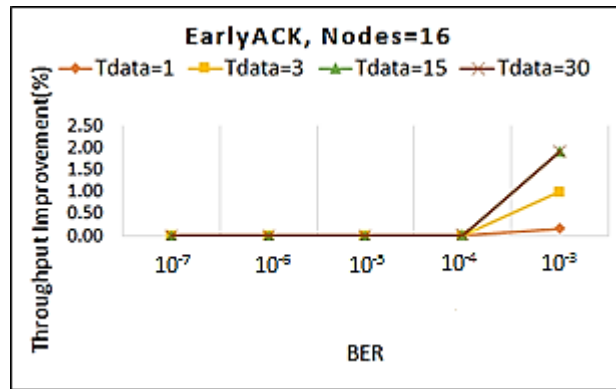


Figure 4.15: EarlyACK: Throughput Improvement (%) vs. BER

Table 4.16: EarlyACK, Comparative Analysis as a function of BER, with 16 nodes

BER	Tdata=1	Tdata=3	Tdata=15	Tdata=30
10^{-7}	1.45×10^{-9}	3.08×10^{-9}	8.81×10^{-9}	12×10^{-9}
10^{-6}	1.45×10^{-7}	3.08×10^{-7}	8.86×10^{-7}	12.1×10^{-7}
10^{-5}	1.45×10^{-5}	3.12×10^{-5}	9.37×10^{-5}	1.31×10^{-4}
10^{-4}	1.47×10^{-3}	3.56×10^{-3}	1.4×10^{-2}	1.87×10^{-2}
10^{-3}	1.64×10^{-1}	9.91×10^{-1}	1.91	1.91
10^{-2}	28.4	149.99	---	---

4.2.3 Analysis as a function of the Transmission Range

The throughput improvement results are plotted in Figure 4.16 as the transmission range varies from 100m to 3000m for $T_{data}=1, 3, 15$ & 30 slots and BER ranging from 10^{-2} to 10^{-7} , with no hidden nodes.

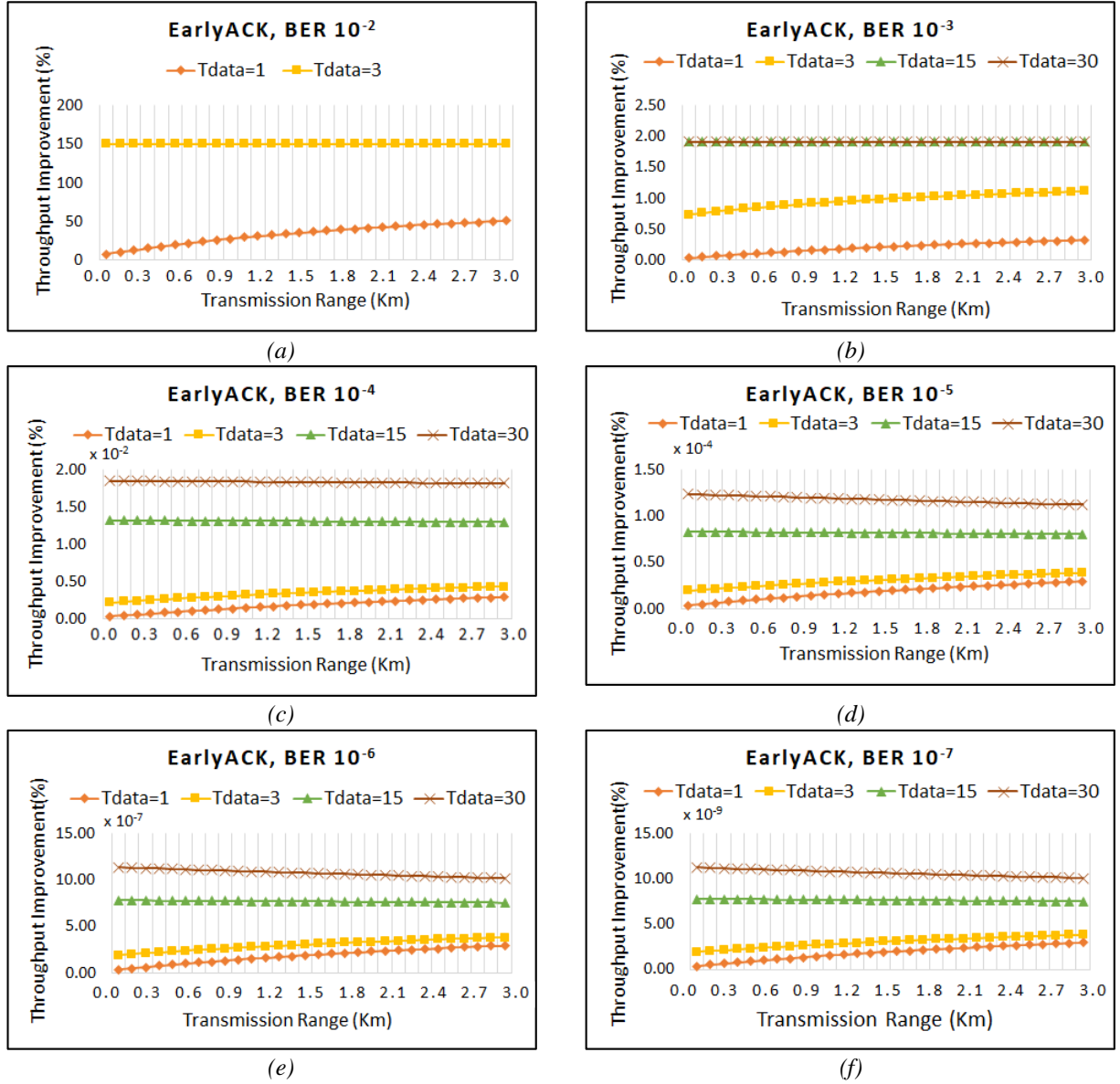
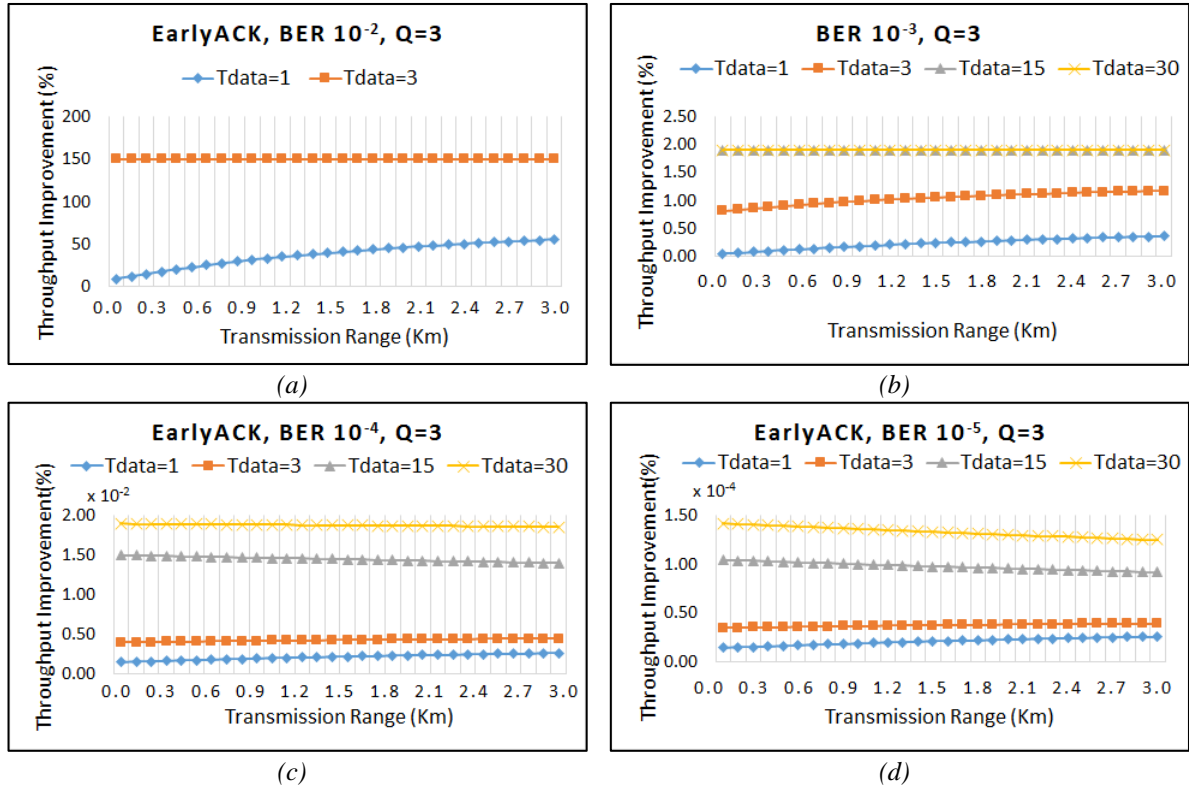


Figure 4.16: EarlyACK: Throughput Improvement vs Transmission Range for: (a) BER 10^{-2} (b) BER 10^{-3} (c) BER 10^{-4} (d) BER 10^{-5} (e) BER 10^{-6} (f) BER 10^{-7}

The analysis was done with 16 nodes. It shows that at $\text{BER}=10^{-2}$ the minimum improvement is 9.08% and the maximum is 55.73% for $T_{\text{data}}=1$ slot. For $T_{\text{data}}=3$, the minimum is 7.80% at 100m and 50.87% at 3000m. For $\text{BER } 10^{-3}$, improvement is seen to increase with larger DATA size and increasing range. The improvement is seen to reduce for lower BERs from 10^{-4} to 10^{-7} for $T_{\text{data}}=15$ and 30 slots with increasing transmission range. This is due to the increase in propagation delay, which tends to increase $T_{\text{Tot-EA}}$ and reduces the throughput improvement, which varies inversely with $T_{\text{Tot-EA}}$.

4.2.3.1 Impact of hidden nodes

Results for throughput improvement as a function of transmission range are plotted for $Q=3$ hidden nodes in Figure 4.17. At a range of 100 m the throughput improvement is 9.08% for $T_{\text{data}}=1$ slot. This is higher as compared to the improvement at $Q=0$ hidden nodes, where it is 7.80%. The maximum occurs at 3000m, where it is 55.73% for $Q=3$ nodes and 50.86% for $Q=0$ nodes. For $T_{\text{data}}=3$ slots, the throughputs of S-FAMA and EarlyACK become very low, 3.67×10^{-9} and 9.17×10^{-9} , respectively, for $Q=3$. The throughput improvement increases to 149.99%. Comparing with the throughputs of S-FAMA and EarlyACK at $Q=0$, $S=4.32 \times 10^{-9}$ and $S_{\text{EA}}=1.08 \times 10^{-8}$, the improvement is 149.99%. Larger DATA packet sizes of 15 and 30 slots gives no improvement. At $T_{\text{data}}=15$ and 30, $P_{\text{e}}=1$ and $P_{\text{eEA}}=1$. This makes T_{Tot} and $T_{\text{Tot-EA}}$ infinite and S and S_{EA} become 0. Comparison of throughput improvement for EarlyACK with and without hidden nodes is summarized in Table 4.17.



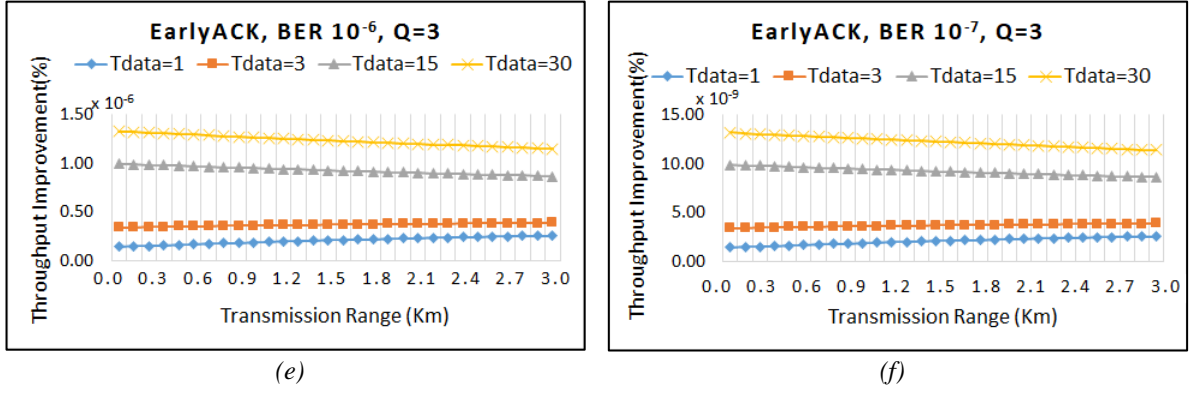


Figure 4.17: EarlyACK: Throughput Improvement vs Transmission Range for: (a) BER 10^{-2} (b) BER 10^{-3} (c) BER 10^{-4} (d) BER 10^{-5} (e) BER 10^{-6} (f) BER 10^{-7}

Table 4.17: EarlyACK comparative analysis of throughput improvement (%) for $Q=0$ and $Q=3$ at BER 10^{-3} .

T_{data}	Distance (Km)	$Q=0$	$Q=3$
1	0.1	0.04	0.05
	0.3	0.33	0.37
3	0.1	0.74	0.81
	0.3	1.11	1.18
15	0.1	1.91	1.91
	0.3	1.91	1.91
30	0.1	1.91	1.91
	0.3	1.91	1.91

4.2.4 Analysis as a function of the length of data

Figure 4.18 depicts the throughput improvement for $T_{data} = 1, 3, 15$ and 30 slots for BERs ranging from 10^{-6} to 10^{-3} . The throughput varies inversely as the size of the DATA packet increases. Table 4.18 gives the comparative analysis of throughput improvement. From the table it is seen that the improvement varies directly with DATA packet size.

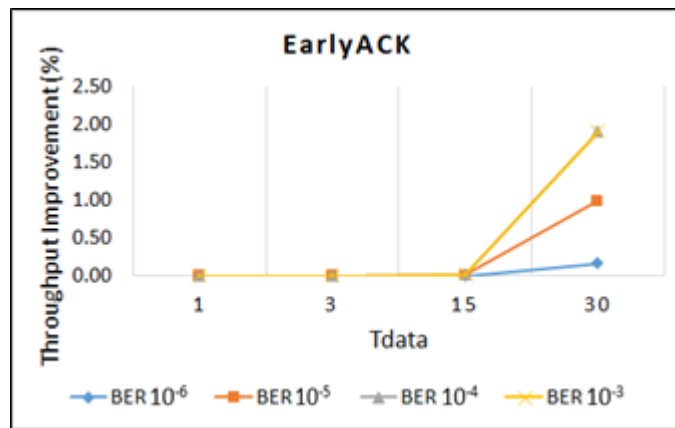


Figure 4.18: Throughput Improvement vs T_{data} for EarlyACK, with 16 nodes.

Table 4.18: EarlyACK Comparative Analysis of Throughput Improvement vs Tdata

T _{data}	BER			
	10 ⁻³	10 ⁻⁴	10 ⁻⁵	10 ⁻⁶
1	16.4x10 ⁻²	1.47x10 ⁻³	1.45x10 ⁻⁵	1.45x10 ⁻⁶
3	99.13x10 ⁻²	3.56x10 ⁻³	3.12x10 ⁻⁵	3.08x10 ⁻⁷
15	1.9082622	14.15x10 ⁻³	9.37x10 ⁻⁵	3.08x10 ⁻⁷
30	1.9083234	18.70x10 ⁻³	1.31x10 ⁻⁴	1.20x10 ⁻⁶

4.2.5 Analysis as a function of the Offered Load

Graphs for throughput improvement against offered load for EarlyACK have been shown in Figure 4.8 for comparison with MultiACK. Throughput Improvement curves are plotted for T_{data}=1 and T_{data}=3, BER= 10⁻⁵, N=16, n=1. The curve shows a very marginal improvement in the throughput with EarlyACK as compared to MultiACK. For T_{data}=1 slot, the maximum improvement is 5.12× 10⁻⁵ at an offered load $\lambda = 0.03621$ to 0.03751 packets/second. The maximum throughput improvement in EarlyACK with T_{data}=3slots is 7.69× 10⁻⁵ at λ equal 0.02771-0.02881 packets/seconds.

4.3 Energy Consumption

In underwater acoustic sensor networks, MAC protocols must be designed to save energy. In such networks a node consumes energy not only in transmission and reception but also overhearing, and collisions also unnecessarily waste energy of the nodes. These problems are more common in handshake based protocols where the control traffic is high. The energy waste in underwater acoustic networks is very critical as it is not easy to recharge sensor nodes. Further, the high bit error rate adds to the energy waste. Hence, a primary objective of MAC protocol must be energy efficiency without compromising the throughput [80]. In this section we analyze the energy consumption in S-FAMA, MultiACK (with i=4) and EarlyACK.

The energy consumed during transmission for one hop can be calculated using (3.43), (3.44) and (3.45) [81, 82].

The number of hops N is taken as 5, 10, 15 and 20. Other parameters used are the Signal to Noise ratio (SNR) of 20 dB, the ambient noise level of 70 dB, the Directivity index of 3 dB and depth of 75 m. The number of packets, K, is taken as 1000, DATA transmission time T_{tx} is 125ms and a transmission power of 2 W related to the acoustic modems and hydrophones is considered [81, 82].

Table 4.19: Parameters for Energy Consumption per node

Parameters	Description	Value
N	Number of hops	5, 10, 15, 20
T _{Tx}	Transmission time taken by one packet	0.125s
K	Number of Packets each node transmits	1000
P	Transmission Power	2 W
L _{DATA}	Data Packet size	100 bits
L _{ACK}	ACK Packet size	100 bits (25*4)
BER	Bit Error Rate	10 ⁻⁵
Pe	Packet error rate in S-FAMA	19.98 x 10 ⁻⁴
PeM	Packet error rate in MultiACK-SFAMA	9.9951x 10 ⁻⁴
PeEA	Packet error rate in EarlyACK-SFAMA	19.96 x 10 ⁻⁴

Using (3.46) and parameters in Table 4.19, the total transmission energy wasted in unsuccessful transmissions in MultiACK compared with that of S-FAMA (4.8) shows a saving of 50%, shown in Figure 4.19.

$$\frac{E_{w-MA}}{E_{w-SF}} = \frac{9.995 \times 10^{-4}}{0.0020} \quad (4.7)$$

$$\frac{E_{w-MA}}{E_{w-SF}} = 0.49995 \approx 0.50 \approx 50\% \quad (4.8)$$

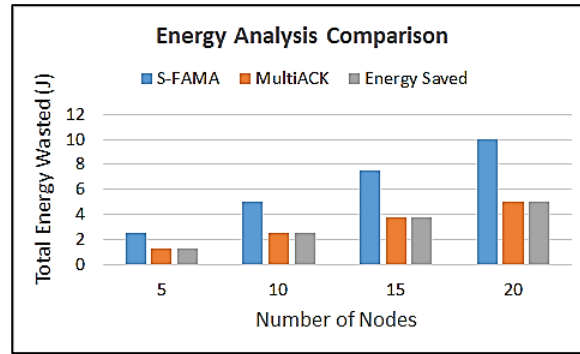


Figure 4.19: Analysis of transmission energy wasted in S-FAMA & MultiACK-SFAMA for BER 10^{-5} .

A comparison of the total energy used during successful transmission in S-FAMA (E_{T1}), MultiACK (E_{T2}) and EarlyACK (E_{T3}) is calculated using (3.49), (3.50) and (3.51):

$$E_{T1} = N \times T_{Tx} \times K \times P \times (1-P_e) = 5 \times 0.125 \times 1000 \times 2 \times (1-0.002) = 1247.5 \text{ J} \quad (4.9)$$

$$E_{T2} = N \times T_{Tx} \times K \times P \times (1-P_{eM}) = 5 \times 0.125 \times 1000 \times 2 \times (1-9.995 \times 10^{-4}) = 1248.75 \text{ J} \quad (4.10)$$

$$E_{T3} = N \times T_{Tx} \times K \times P \times (1-P_{eEA}) = 5 \times 0.125 \times 1000 \times 2 \times (1-0.002) = 1247.5 \text{ J} \quad (4.11)$$

Improvement in total energy used during successful transmission for MutliACK and EarlyACK is obtained using (3.52) and (3.53) respectively. The ratio E_{T2}/E_{T1} (4.12) is greater than 1, indicating improvement by 0.1% in total energy used during successful transmission with MutliACK. The ratio E_{T3}/E_{T1} is greater than 1 (4.13), indicating improvement, but marginal, by $2 \times 10^{-4} \%$ for EarlyACK.

$$\frac{E_{T2}}{E_{T1}} = \frac{1 - 9.995 \times 10^{-4}}{1 - 0.0020} = 1.001 \quad (4.12)$$

$$\frac{E_{T3}}{E_{T1}} = \frac{1 - 0.001996}{1 - 0.001998} = 1.000002 \quad (4.13)$$

The energy efficiency for MultiACK is calculated using (3.54). In total, the percentage of energy transmission in MultiACK is 0.1% larger than in S-FAMA, showing improvement in transmission (4.14). The energy efficiency for EarlyACK is calculated using (3.55). In total, the amount of energy transmitted in EarlyACK is $2 \times 10^{-4} \%$ larger, showing only marginal improvement in energy efficiency.

$$\eta_{MA} = \left(\frac{0.999 - 0.998}{0.998} \right) \times 100 = 0.10 \% \quad (4.14)$$

Figure 4.20 shows the improvement in transmission energy for MultiACK for varying BER from 10^{-6} to 10^{-2} . The improvement can be seen as the energy waste is reduced by almost 50% for BER from 10^{-6} to 10^{-4} . At 10^{-3} it is 52% and increases to 80% for BER 10^{-2} (see Table 4.20).

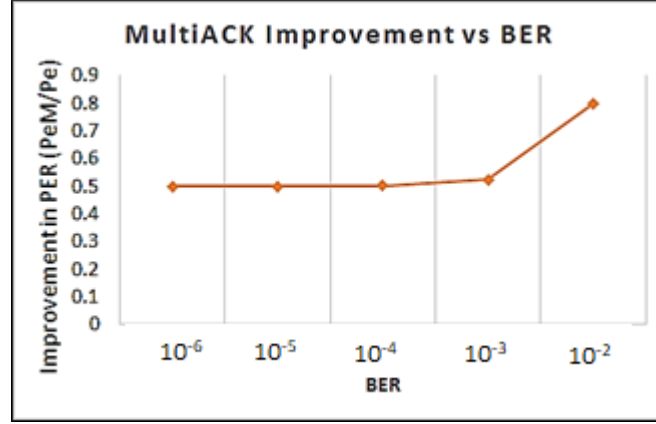


Figure 4.20: MultiACK energy transmission improvement at different BERs. (10^{-6} to 10^{-2})

Figure 4.21 confirms that MultiACK outperforms EarlyACK in saving energy at all BERs by almost 50%, except for 10^{-3} and 10^{-2} . A comparative analysis of the reduction in the total transmission energy wasted during unsuccessful transmission in S-FAMA, MultiACK and EarlyACK is shown in Table 4.20. In case of EarlyACK, the PER for low BER is almost the same as the packet error rate of S-FAMA. Thus, at low BERs, 10^{-6} and 10^{-5} , EarlyACK gives no improvement in the transmit energy waste reduction. Very little improvement is seen in EarlyACK at higher BER 10^{-4} to 10^{-2} due to close values of PER with S-FAMA. MultiACK outperforms S-FAMA and EarlyACK.

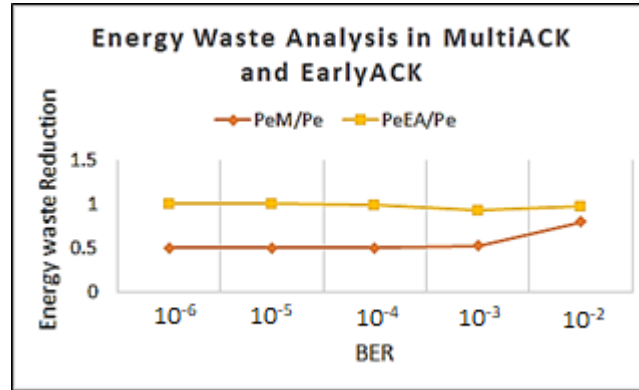


Figure 4.21: Comparative analysis of transmission energy wasted in unsuccessful transmission in MultiACK and EarlyACK.

Table 4.20: Analysis of Total Transmission Energy Wasted in S-FAMA, MultiACK & EarlyACK at BER 10^{-5}

Nodes	S-FAMA	MultiACK-SFAMA	EarlyACK-SFAMA
	E_{w-SF} (J)	E_{w-MA} (J)	E_{w-EA} (J)
5	2.5	1.25	2.5
10	5	2.5	5
15	7.49	3.75	7.5
20	10	5	10

Analysis of Packet Error Rates and improvement in Total Energy waste in MultiACK & EarlyACK is shown in Table 4.21.

Table 4.21: Analysis of Packet Error Rates and Improvement in Total Energy waste in MultiACK & EarlyACK

BER	Pe	PeM	PeEA	E_{w-MA}/E_{w-SF}	E_{w-EA}/E_{w-SF}
10^{-6}	0.0002	0.0001	0.0002	0.50	1
10^{-5}	0.002	0.001	0.002	0.50	1
10^{-4}	0.02	0.01	0.0196	0.51	0.99
10^{-3}	0.18	0.095	0.17	0.53	0.93
10^{-2}	0.87	0.69	0.84	0.80	0.97

Table 4.22, shows the comparison of the total energy consumption during successful transmissions in MultiACK (E_{C-MA}) and S-FAMA (E_{C-SF}). The analysis shows that in MultiACK the total percentage of energy successfully used is 0.1% larger.

Table 4.22: Energy Consumption Analysis at BER 10^{-5}

Nodes	S-FAMA		MultiACK-SFAMA		
	E_{C-SF} (J)	E_{w-SF} (J)	E_{C-MA} (J)	E_{w-MA} (J)	Energy Enhanced %
5	1247.50	2.50	1248.75	1.25	0.10
10	2495.01	5.00	2497.50	2.50	0.10
15	3742.51	7.49	3746.25	3.75	0.10
20	4990.01	9.99	4995.00	4.998	0.10

4.4 Improvement Analysis

4.4.1 MultiACK

This section summarizes the improvement obtained by using MultiACK. The impact on the throughput is shown in Table 4.23. For all BERs, 10^{-2} to 10^{-6} , MultiACK shows improvement. At higher BERs, the improvement is higher. The mechanism improves efficiency of S-FAMA by increasing the probability that an ACK would be received, and is useful in scenarios of ACK loss. The impact on delay for Scenario-I is calculated using the expressions for $T_{Tot-M-1}$ and T_{Tot} . We found that $T_{Tot-M-1}$ is 4.65 secs while T_{Tot} for S-FAMA is 6.51secs. Thus, MultiACK mechanism reduces delay in S-FAMA by 28.59%. The analysis on energy at BER 0.005, 100 bits DATA packet shows that using MultiACK reduces the energy waste by 35.41%. The impact on transmission energy consumed during successful transmission is found to be 61.09%

compared to that of S-FAMA. This shows that the improvement is higher at high BER because total energy waste in S-FAMA and MultiACK varies directly with PER which varies directly with BER.

Table 4.23: Impact of Improvement Factor on Throughput

Impact of Improvement Factor on Throughput		
BER	MultiACK	EarlyACK
10^{-2}	1.186	1.175
10^{-3}	1.005	1.001
10^{-4}	1.0005	1.00001
10^{-5}	1	1
10^{-6}	1	1

4.4.2 EarlyACK

This section summarizes the improvement obtained by using EarlyACK. The impact on the throughput is shown in Table 4.24. For BER 10^{-2} , the improvement is 17.5%; for lower BERs 10^{-4} to 10^{-6} , the improvement is negligible. The difference in the throughputs of S-FAMA, MultiACK and EarlyACK is marginal. The analysis on delay shows that, for BER=0.005 and an ACK packet 100 bits long, T_{Tot-EA} is 4.72secs, while T_{Tot} for S-FAMA is 6.51secs. Thus, EarlyACK shows a reduction in delay by 27.50 %. For the same parameters, the transmission energy wasted is reduced by 23.87%. The energy consumed in successful transmissions is found to be 41.17 % more. In this regard, the impact of MultiACK is higher than EarlyACK.

Table 4.24: Impact of Improvement Factor on Delay and Throughput for MultiACK and EarlyACK

BER	S-FAMA			MultiACK				EarlyACK			
	PER (P_e)	Delay (T_{Tot})	Throughput (S)	PER (P_{e-M})	Delay (T_{Tot-M})	Throughput (S_{M-I})	% Improvement	PER (P_{e-EA})	Delay (T_{Tot-EA})	Throughput (S_{EA})	% Improvement
10^{-2}	0.87	15.03	3.03×10^{-4}	0.69	7.47	3.59×10^{-4}	18.48	0.84	12.79	3.56×10^{-4}	17.5
10^{-3}	0.18	3.80	3.83×10^{-4}	0.10	3.59	3.84×10^{-4}	0.52	0.17	3.77	3.84×10^{-4}	0.26
10^{-4}	0.02	3.44	3.86×10^{-4}	0.01	3.42	3.86×10^{-4}	0	0.02	3.44	3.86×10^{-4}	0
10^{-5}	2×10^{-3}	3.40	3.86×10^{-4}	10^{-3}	3.40	3.86×10^{-4}	0	2×10^{-3}	3.40	3.86×10^{-4}	0
10^{-6}	2×10^{-4}	3.40	3.86×10^{-4}	10^{-4}	3.40	3.86×10^{-4}	0	2×10^{-4}	3.40	3.86×10^{-4}	0

4.5 Comparative Analysis

The comparative analysis at BER 10^{-5} , summarized in Table 4.25 and Table 4.26, shows that the improvement in Early ACK is less than in Scenario-I of MultiACK. The analysis shows highest performance for MultiACK Scenario-I. The EarlyACK improvement is second and for MultiACK Scenario-II there is no improvement.

Table 4.25: MutliACK & EarlyACK Comparative Analysis of Throughput Improvement vs Tdata

Comparison of Throughput Improvement(%) vs Tdata, for MultiACK-Scenario-I & II and EarlyACK for BER=10 ⁻⁵ , Nodes=16			
T _{data}	Scenario-I	Scenario-II	EarlyACK
1	7.13x10 ⁻³	-3.57	1.45x10 ⁻⁵
3	1.37x10 ⁻²	-3.36	3.12x10 ⁻⁵
15	4.11x10 ⁻²	-2.46	9.37x10 ⁻⁵
30	5.99x10 ⁻²	-1.82	1.31x10 ⁻⁴

Table 4.26: MutliACK & EarlyACK Comparative Analysis of Throughput Improvement for BER 10⁻⁵

Nodes=16	BER=10 ⁻⁵	Tdata=1	Tdata=3	Tdata=15	Tdata=30
MultiACK Scenario-I		8.23x10 ⁻³	1.57x10 ⁻²	4.48x10 ⁻²	6.34x10 ⁻²
MultiACK Scenario-II		-3.57	-3.36	-2.46	-1.82
EarlyACK		1.45x10 ⁻⁵	3.12x10 ⁻⁵	9.37x10 ⁻⁵	1.31x10 ⁻⁴

The throughput versus offered load for S-FAMA is shown in Figure 4.22 for BER = 10⁻⁵ and 16 nodes for T_{data}=1 slot and 3 slots. The throughput is larger for T_{data}=3. The throughput of S-FAMA may be compared with that of MultiACK and EarlyACK, shown in Figures 4.23 and 4.24 respectively.

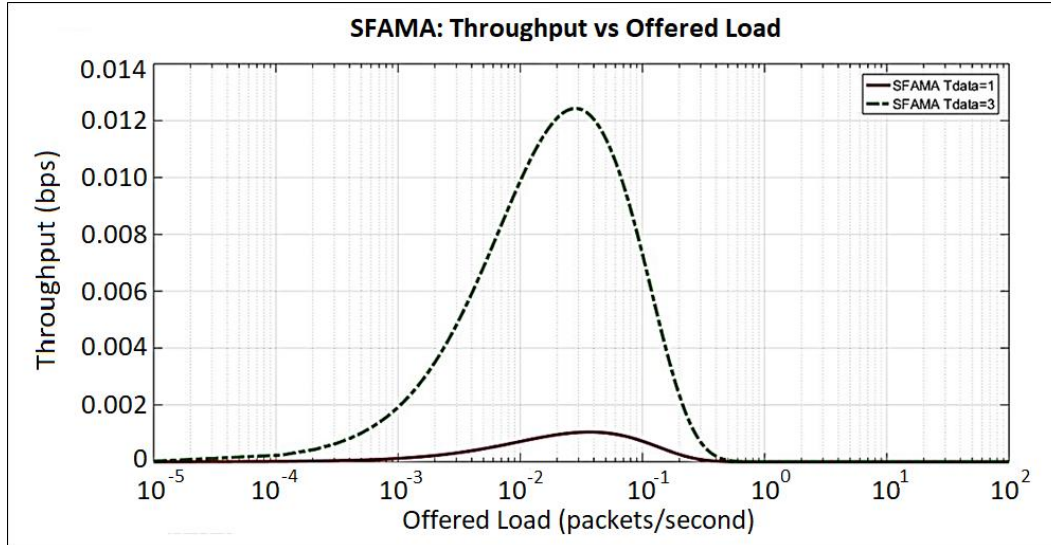


Figure 4.22: Comparison of Throughput vs Offered Load in S-FAMA for Tdata =1 and Tdata=3slots.

The curves for varying offered load in Figure 4.23 confirm that the proposed mechanism of MultiACK improves the throughput of S-FAMA, though marginally. The maximum improvement for T_{data}=1 is 0.026% at an offered load of λ ranging from 0.036-0.039 packets/second. The maximum throughput improvement with T_{data}=3 is 0.039% at λ ranging from 0.0281 to 0.0284.

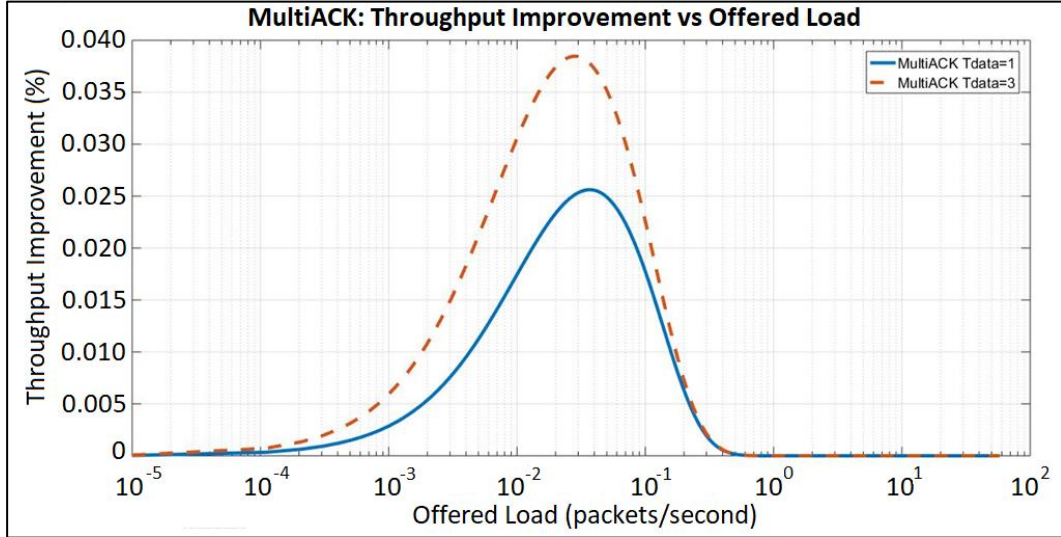


Figure 4.23: Comparison of Throughput Improvement vs Offered Load in S-FAMA with MultiACK for $T_{data}=1$ & 3 slots.

Throughput improvement in EarlyACK with $T_{data}=1$ and $T_{data}=3$, $BER=10^{-5}$, $N=16$, $n=1$ is shown in Figure 4.24. The curves show that the EarlyACK throughput is essentially that of S-FAMA. The maximum improvement for $T_{data}=1$ is $5.12 \times 10^{-5} \%$ at an offered load of λ ranging from 0.036-0.038 packets/second. The maximum throughput improvement with $T_{data}=3$ is $7.69 \times 10^{-5} \%$ at λ ranging from 0.028 to 0.029.

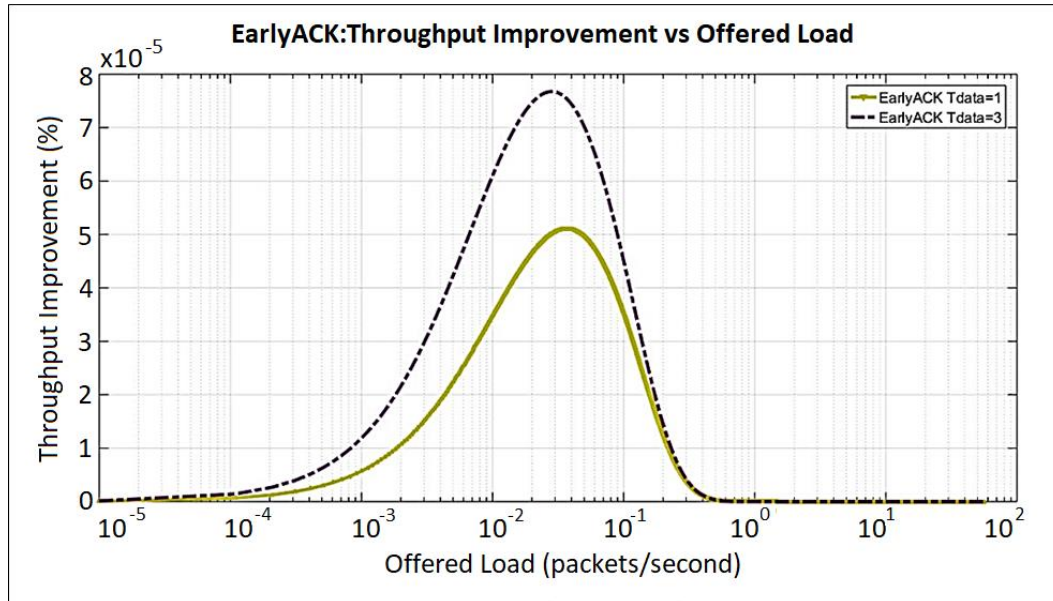


Figure 4.24: Comparison of Throughput Improvement vs Offered Load in S-FAMA with EarlyACK for $T_{data}=1$ & 3 slots.

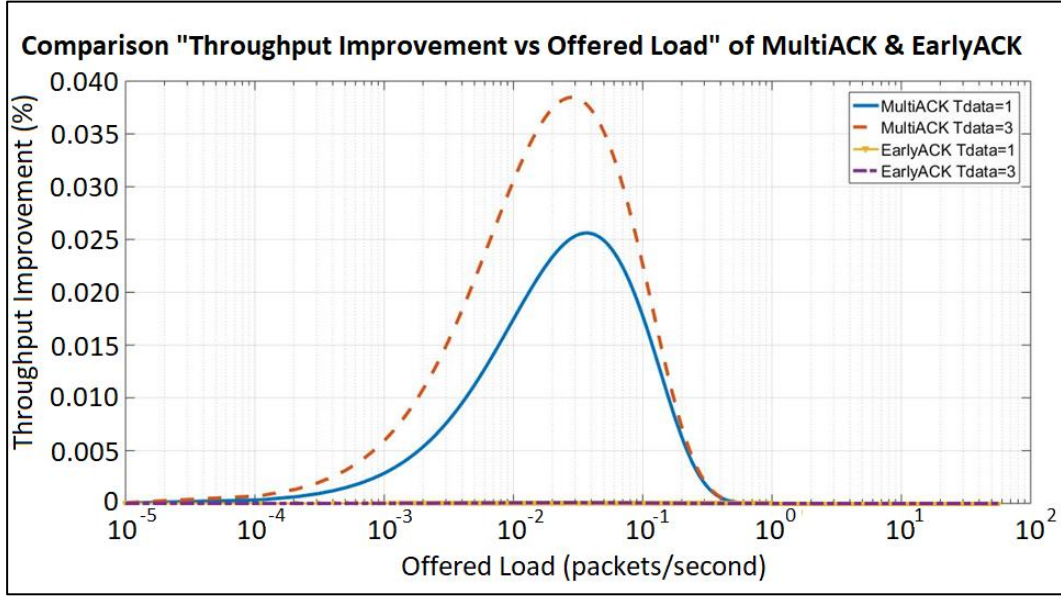


Figure 4.25: Comparison of Throughput Improvement vs Offered Load for MultiACK and EarlyACK for $T_{data}=1$ & 3 slots.

Comparison of MultiACK and EarlyACK performance with respect to offered load is shown in Figure 4.25. It can be clearly seen that MultiACK outperforms EarlyACK. EarlyACK throughput improvement compared to MultiACK is very low and appears almost flat in the figure. However, EarlyACK can be useful in preventing the repetition of the DATA retransmission in case of ACK loss.

Table 4.27 summarizes the analysis on the proposed variants. The computations are shown for $T_{data}=1$ and BER 10^{-3} to 10^{-6} . The results show that MultiACK performance is best in terms of packet error rate, delay, transmit energy, throughput and throughput improvement. The throughput improvement is 0.50% at BER 10^{-3} , whereas EarlyACK gives improvement of 0.1026%. MultiACK and EarlyACK both provide improvement in throughput but MultiACK outperforms EarlyACK. Thus, the MultiACK and EarlyACK mechanisms may be preferred over S-FAMA, as they are useful particularly in cases of ACK loss. They save energy and reduce cost by preventing the repetition of the entire RTS/CTS and DATA transmission cycle.

Table 4.27: Quantitative Analysis of S-FAMA, MultiACK and EarlyACK Protocols at BER 10^{-3} to 10^{-6} for Underwater Acoustic Networks

Protocol	BER	PER	Delay (s)	Transmit Energy waste (J)	Energy Waste Reduction %	Avg. Throughput (bps)	Throughput Improvement (%)
S-FAMA	10^{-3}	1.81×10^{-1}	3.80	226.75	0	3.83×10^{-4}	0
	10^{-4}	1.98×10^{-2}	3.44	24.75		3.86×10^{-4}	
	10^{-5}	2.00×10^{-3}	3.40	2.50		3.87×10^{-4}	
	10^{-6}	2.00×10^{-4}	3.40	0.25		3.87×10^{-4}	
MultiACK-SFAMA	10^{-3}	9.53×10^{-2}	3.59	119.13	47.46	3.85×10^{-4}	0.50
	10^{-4}	1.00×10^{-2}	3.42	12.50	49.50	3.87×10^{-4}	4.42×10^{-2}
	10^{-5}	9.99×10^{-4}	3.40	1.25	50.00	3.87×10^{-4}	4.37×10^{-3}
	10^{-6}	9.99×10^{-5}	3.40	0.13	48.00	3.87×10^{-4}	4.36×10^{-4}
EarlyACK-SFAMA	10^{-3}	1.69×10^{-1}	3.77	210.75	7.06	3.84×10^{-4}	0.10
	10^{-4}	1.96×10^{-2}	3.44	24.50	1.01	3.86×10^{-4}	9.20×10^{-4}
	10^{-5}	2.00×10^{-3}	3.40	2.50	0.	3.86×10^{-4}	9.08×10^{-6}
	10^{-6}	2.00×10^{-4}	3.40	0.25	0	3.86×10^{-4}	9.06×10^{-8}

4.6 Conclusion

In this chapter we have analyzed the performance of the two proposed variants of S-FAMA, namely MultiACK and EarlyACK, with respect to throughput, delay, BER, data packet size and energy consumption. Quantitative analysis was done using the results obtained from the analytical expressions derived in Chapter 3. In Scenario-I, the duration of the MultiACK packet was kept the same as the control packet, and T_{MultiACK} was one slot, while in Scenario-II the duration of the MultiACK packet is larger than the control packet and T_{MultiACK} is 2 time slots. In both scenarios the length of the ACK packet was shortened to 0.025s. Comparison of results show that Scenario-I outperforms original S-FAMA while Scenario-II shows improvement only for BER 10^{-2} , $T_{\text{data}}=1$ and 3 slots. For BER 10^{-3} , it shows improvement for $T_{\text{data}}=15$ and 30 slots only. There is no improvement seen for lower BERs. In Scenario-II, increasing T_{MultiACK} to 2 time slots increases $T_{\text{Tot-M-2}}$, which adds delay and reduces improvement.

The results of EarlyACK also show improvement. However, the comparative analysis of MultiACK and EarlyACK performance shows that MultiACK Scenario-I is better.

Overall the improvement factors for the MultiACK Scenario-I and EarlyACK show that both mechanisms outperform the original S-FAMA. Both variants may have practical usefulness in case of ACK loss, by saving energy and time in critical periods.

CHAPTER 5 : CONCLUSION

This chapter concludes the research work carried out for this thesis. This thesis was aimed to improve the S-FAMA protocol by providing additional features that enhance its operation. We started with the description of the underwater environment characteristics along with the challenges faced during underwater communication. Underwater acoustic communication is badly affected by factors such as temperature, density, path loss, noise, multi-path propagation, Doppler effect, propagation delay etc. Since the underwater environment is different from terrestrial environment, terrestrial MAC protocols are unsuitable and cannot be used directly for underwater communication.

Initial analysis was carried out on the existing MAC algorithms and protocols, to evaluate their performance. The performance was evaluated and compared as a function of throughput, delay, BER, varying DATA packet sizes and energy consumption. Simulations were performed to measure these performance metrics of existing MAC protocols under different parameter settings.

Based on the quantitative analysis of results of existing MAC protocols, five MAC protocols were selected, namely, ALOHA, CSMA, MACA, FAMA and S-FAMA for further evaluation. The performances in terms of throughput and delay were evaluated and compared.

S-FAMA, a variant of FAMA, was selected. Although S-FAMA avoids collisions and saves energy by slotting time, we identified from that, if an ACK is lost, the entire RTS/CTS and DATA cycle must be repeated. Retransmission of the entire cycle consumes a significant amount of energy. To solve this issue, we proposed two solutions, namely MultiACK and EarlyACK, to handle cases when an ACK packet fails to reach the transmitter.

In the MultiACK mechanism, instead of sending one ACK packet, we send i -ACK packets, an ACK-Train. Two scenarios were proposed for MultiACK. In the first scenario, Scenario-I, the duration of the ACK-Train ($i \times T_{ACK}$) is kept the same as that of the control packet (T_{CTS}); the size of the ACK packet is shortened to accommodate the train of ACK packets. In Scenario-II the duration of the ACK-Train ($i \times T_{ACK}$) is greater than one slot ($1T_{slot} + T_{CTS}$). We proved analytically that adding the features of MultiACK to the S-FAMA improves its throughput and efficiency in case of Scenario-I. The results for Scenario-II showed no improvement, because the additional time slot required offsets the benefits of the ACK-Train.

The second proposed mechanism, EarlyACK, prevents the repetition of the data transmission cycle if an ACK is lost. In the EarlyACK mechanism, when the receiver receives an RTS (with the same UID) it understands that the receiver has not received an ACK for the sent DATA. It sends an EarlyACK for the lost ACK instead of sending a CTS. We evaluated its performance as a function of number of nodes, transmission range, data length, BER and offered load. The results show that it improves the throughput improvement of original S-FAMA. Though the throughput increase is marginal, it increases reliability in terms of ACK loss. With a number of retries of 1 and 2 Early ACK enhances the throughput.

A comparative analysis of the three protocols, S-FAMA, MultiACK and EarlyACK has been discussed followed by the quantitative analysis. Both mechanisms would be useful in cases of

ACK loss and where energy savings in the sensor nodes is required, but MultiACK-Scenario-I outperforms EarlyACK.

The research has its innovation in terms of incorporating MultiACK and EarlyACK mechanisms in S-FAMA. We derived mathematical expressions for both of them and evaluated their performance. Though our proposed mechanism provides marginal improvement in throughput, its efficacy can be seen in case of ACK loss. As the cost of losing an ACK is very high, MultiACK saves both cost and energy. We also calculated the improvement factor, which shows that the probability of receiving an ACK correctly by using MultiACK is improved by 65.05%.

This is the first attempt and first approach of trying the two mechanisms of MultiACK and EarlyACK in S-FAMA without violation of S-FAMA algorithm. This unique approach was tested and validated using software tools. This research will help in academia as well as industry, by adopting these techniques to enhance the key features of existing MAC protocols for underwater communication.

REFERENCES

- [1] Noor Zaman, Khaled Ragab, Azween Bin Abdullah, "Wireless Sensor Networks and Energy Efficiency: Protocols, Routing and Management" IGI Global, 2012.
- [2] Ian F. Akyildiz, Mehmet Can Vuran, "Wireless Sensor Networks" – Ch: 16, pp 400-442, 2010- Technology & Engineering, John Wiley & Sons Ltd, USA.
- [3] Underwater Acoustic Sensor Networks (UWASNs), Project Description. [Online]. Available: <http://bwn.ece.gatech.edu/UWASN/work.html>, 10/23/2016 (accessed Oct. 23, 2016).
- [4] Ian F. Akyildiz, Dario Pompili, Tommaso Melodia, "Underwater acoustic sensor networks: research challenges", (www.elsevier.com/locate/adhoc) *Ad Hoc Networks* 3 (2005) 257–279
- [5] Dario Pompili, Ian F. Akyildiz, "Overview of Networking Protocols for Underwater Wireless Communications" *IEEE Communications Magazine* Jan 2009.
- [6] Mandar Chitre, Shiraz Shahabudeen, Milica Stojanovic, "Underwater Acoustic Communications and Networking: Recent Advances and Future Challenges" *Marine Technology Society Journal*, Volume 42, Number 1, 2008.
- [7] L. Kleinrock and F. A. Tobagi, Packet switching in radio channels: part I carrier sense multiple-access modes and their throughput-delay characteristics, *IEEE trans. on commun.* Vol. COM-23, pp. 1400–1416, 1975.
- [8] P. Karn, "MACA: A new channel access method for packet radio," in *Proc. 9th Computer Networking Conf.*, pp. 134–140, Sept. 1990.
- [9] C. L. Fullmer and J.J. Garcia-Luna-Aceves, "Floor acquisition multiple access (FAMA) for packet-radio networks," *ACM SIGCOMM, Computer Communication Review*, vol. 25 no. 4, pp. 262-273, Oct. 1995.
- [10] S. Climent, A. Sanchez, J. V. Capella, N. Meratnia, and J. J. Serrano, "Underwater acoustic wireless sensor networks: Advances and future trends in physical, MAC and routing layers," *Sensors*, vol. 14, no. 1, pp. 795–833, Jan. 2014.
- [11] Dario Pompili, "Efficient Communication Protocols for Underwater Acoustic Sensor Networks", Georgia Institute of Technology, August, 2007.
- [12] Jiejun, K., C. Jun-hong, W. Dapeng and M. Gerla. 2005. Building underwater ad-hoc networks and sensor networks for large scale real-time aquatic applications. *IEEE Military Communications Conference*, 2005. MILCOM 2005
- [13] Heidemann, J., Y. Wei, J. Wills, A. Syed and L. Yuan, 2006, Research challenges and applications for underwater sensor networking, *IEEE Wireless Communications and Networking Conference*, 2006, WCNC 2006.
- [14] Novikov, A.; Bagtzoglou, A.C. Hydrodynamic model of the lower Hudson River estuarine system and its application for water quality management. *Water Resour. Manag.* 2006, 20, pp(s): 257–276.
- [15] Deven Makhija, Kumaraswamy P, Rajarshi Roy, "CHALLENGES AND DESIGN OF MAC PROTOCOL FOR UNDERWATER ACOUSTIC SENSOR NETWORKS", 2006 4th International Symposium on Modeling and Optimization in Mobile, Ad Hoc and Wireless Networks, *IEEE Conference Publications*, © 2006 IEEE
- [16] I. F. Akyildiz, D. Pompili, and T. Melodia, "State-of-the-art in protocol research for underwater acoustic sensor networks," in *ACM International Workshop on Underwater Networks (WUWNet)*, Los Angeles, USA, 2006.
- [17] Qichao Zhao ; Lambert, A. ; Benson, C.R. , "The problem of multi-user access in undersea networks", *Communications and Information Systems Conference*, 2012 Military DOI: 10.1109/MilCIS.2012.6380676 *IEEE CONFERENCE PUBLICATIONS* Publication Year: 2012, pp(s): 1 – 6.
- [18] M. Stojanovic, "Acoustic (underwater) communications," in *Encyclopedia of Telecommunications*, J. G. Proakis, Ed. John Wiley and Sons, 2003.
- [19] J. Proakis, J. Rice, E. Sozer and M. Stojanovic, "Shallow water acoustic networks," in *Encyclopedia of Telecommunications*, J. G. Proakis, Ed. John Wiley and Sons, 2003.
- [20] V.O. Knudsen, R.S. Alford and J.W. Emling, Digital communications. *Journal of Marine Research* 7(12): 410, 1948.
- [21] Underwater Acoustic Sensor Networks (UW-ASN): Overview, <http://bwn.ece.gatech.edu/UWASN/index.html>, (Accessed Oct. 23, 2016).

- [22] Rony Hasinur Rahman, Craig Benson, Michael Frater, "Routing Protocols for Underwater Ad Hoc Networks," IEEE CONFERENCE PUBLICATIONS, 978-1-4577-2091-8/12©2011 IEEE, Publication Year: 2012, pp(s): 1 – 7.
- [23] Said Lmai, Mandar Chitre., Christophe Laot, and Sebastien Houcke, "Throughput-Efficient Super-TDMA MAC Transmission Schedules in Ad Hoc Linear Underwater Acoustic Networks" , IEEE JOURNAL OF OCEANIC ENGINEERING, VOL. 42, NO. 1, JANUARY 2017.
- [24] Zhang, S., Li, D., & Chen, J. A link-state based adaptive feedback routing for underwater acoustic sensor networks. IEEE Sensors Journal, 13(11), 4402–4412, 2013.
- [25] William S. Burdic, Underwater Acoustic Systems Analysis. Prentice-Hall, 1984.
- [26] U. Devee Prasan, Dr. S. Murugappan, "Underwater Sensor Networks: Architecture, Research Challenges and Potential Applications", International Journal of Engineering Research and Applications (IJERA) ISSN: 2248-9622 Vol. 2, Issue 2, Mar-Apr 2012, pp.251-256.
- [27] Rom, R., & Sidi, M., "Multiple Access Protocols, Performance and Analysis," New York: Springer, June 1989.
- [28] Code Division Multiple Access (CDMA), [Online]. Available: https://www.clear.rice.edu/elec301/Projects01/cdma_dominate/cdma.htm (Accessed Oct 28, 2016).
- [29] Jim Partan, Jim Kurose, and Brian Neil Levine, "A Survey of Practical Issues in Underwater Networks" WUWNet'06, September 25, 2006, Los Angeles, California, USA.
- [30] L. Freitag, M. Stojanovic, M.Grund, and S.Singh, Acoustic Communications for Regional Under sea Observatories. In Proc. Oceanology Intl., Mar. 2002.
- [31] Dario Pompili, Tommaso Melodia, and Ian F. Akyildiz, "A CDMA-Based Medium Access Control for Underwater Acoustic Sensor Networks", IEEE TRANSACTIONS ON WIRELESS COMMUNICATIONS, VOL. 8, NO. 4, APRIL 2009.
- [32] S. Han, Y. Noh, U. Lee, and M. Gerla, "M-FAMA: A multi-session MAC protocol for reliable underwater acoustic streams," in Proc. INFOCOM, pp. 665–673, Apr. 2013.
- [33] Chao Li, Yongjun Xu, Qi Wang, Boyu Diao, Zhulin An, Zhao Chen, and Zuying Luo, "FDCA: A Full-Duplex Collision Avoidance MAC Protocol for Underwater Acoustic Networks", IEEE Sensors Journal, Vol. 16, No. 11, pp(s):4638-4647, June 1, 2016.
- [34] C. L. Fullmer and J. J. Garcia-Luna-Aceves, "Solutions to hidden terminal problems in wireless networks," ACM SIGCOMM Comput. Commun. Rev., vol. 27, no. 47, pp. 39–49, Oct. 1997.
- [35] Youngtae Noh, Uichin Lee, Seongwon Han, Paul Wang, Dustin Torres, Jinwhan Kim, and Mario Gerla, "DOTS: A Propagation Delay-aware Opportunistic MAC Protocol for Mobile Underwater Networks" , IEEE Transactions on Mobile Computing, 1536-1233 (c) 2013 IEEE, pp(s): 1-14, 2013.
- [36] The TCP/IP Guide, [Online]. Available: http://www.tcpipguide.com/free/t_SimplexFullDuplexandHalfDuplexOperation-2.htm (Accessed Oct 28, 2016).
- [37] Xueyuan Su, Sammy Chan, and Masaki Bandai, "A Cross-Layer MAC Protocol for Underwater Acoustic Sensor Networks", IEEE Sensors Journal, Vol. 16, No. 11, pp(s): 4083-4091, June 1, 2016.
- [38] IT Policy and Ethics: Concepts, Methodologies, Tools, and Applications, edited by Management Association, Information Resources, USA.
- [39] Sozer, E. M., M. Stojanovic and J. G. Proakis, Underwater acoustic networks. IEEE J Ocean Eng. 25(1), pp(s):72-83, 2000.
- [40] Doukkali, H., L. Nuaymi and S. Houcke.2006. "Distributed MAC Protocols for Underwater Acoustic Data Networks", IEEE 64th Vehicular Technology Conference, VTC-2006 Fall.
- [41] Garcia-Luna-Aceves, J. J. and C. L. Fullmer, 1998. "Performance of floor acquisition multiple access in ad-hoc networks". Third IEEE Symposium on Computers and Communications, ISCC '98.
- [42] Molins, M. and M. Stojanovic. 2006, "Slotted FAMA: a MAC protocol for underwater acoustic networks", MTS/IEEE OCEANS. 2006- ASIA PACIFIC, May 2006, pp(s): 1-7.
- [43] Shahabudeen, S., M. Chitre and M. Motani, 2007. A multi-channel MAC protocol for AUV networks. IEEE Oceans' 07. Aberdeen, Scotland.
- [44] V. Bharghavan, A. Demers, S. Shenkar, and L. Zhang, "MACAW: A media access protocol for wireless LANs," in Proc. SIGCOMM'94 Conf. on Communications Architectures, Protocols and Applications, pp. 212–225. 1994.

- [45] Wen Lin, En Cheng, Fei Yuan, A MACA-based MAC protocol for Underwater Acoustic Sensor Networks, *Journal of Communications* ISSN 1796-2021 Volume 6, Number 2, April 2011, pp-179-184.
- [46] Y. Zhong; J. Huang ; J. Han, "A Delay-tolerant MAC Protocol with Collision Avoidance for Underwater Acoustic Networks," *Wireless Communications, Networking and Mobile Computing*, 2009. WiCom '09. 5th International Conference on, Publication Year: 2009 , IEEE CONFERENCE PUBLICATIONS, pp. 1 – 4, (2009).
- [47] J.J. Garcia-Luna-Aceves, C. L. Fullmer, "Floor Acquisition Multiple Access," *Mobile Networks and Applications* (1999) 157-174.
- [48] J. M. Morris, "Optimal block lengths for ARQ error control schemes," *IEEE trans. on commun.*, vol. COM-27, pp. 488–493, (1979).
- [49] Zhang, S., Qian, L., Liu, M. et al., A Slotted-FAMA based MAC Protocol for Underwater Wireless Sensor Networks with Data Train, *Journal of Signal Processing Systems*, pp 1–10, April 2016.
- [50] Liang-fang QIAN, Sen-lin ZHANG, Mei-qin LIU, (2015). "A slotted floor acquisition multiple access based MAC protocol for underwater acoustic networks with RTS competition," *Frontiers of Information Technology & Electronic Engineering*, Jan. 28, 2015, 16(3): pp. 217-226.
- [51] L. Pu et al., "Comparing underwater MAC protocols in real sea experiments," *Comput. Commun.*, vol. 56, pp. 47–59, Feb. 2014.
- [52] Nils Morozs, Paul Mitchell, Yuriy Zakharov, "TDA-MAC: TDMA Without Clock Synchronization in Underwater Acoustic Networks", *IEEE Access*, Volume: PP, Issue: 99, 27 November 2017.
- [53] Yongsop Jong, Wei Zhang, "A study on the MAC protocol for dynamic underwater acoustic sensor networks", *IEEE 9th International Conference on Communication Software and Networks (ICCSN)*, Date of Conference: 6-8 May 2017, Date Added to IEEE Xplore: 21 December 2017, PP 142-148.
- [54] B. Peleato, and M. Stojanovic, "Distance aware collision avoidance protocol for ad-hoc underwater acoustic sensor networks," *IEEE Communications Letters*, Vol. 11, no. 12, pp(s): pp(s):1025-7, Dec. 2007.
- [55] Min Kyoung Park, and Volkan Rodoplu, "UWAN-MAC: An Energy-Efficient MAC Protocol for Underwater Acoustic Wireless Sensor Networks", *IEEE JOURNAL OF OCEANIC ENGINEERING*, VOL. 32, NO. 3, JULY 2007, pp(s): 710-720.
- [56] L. T. Tracy, and S. Roy, "A Reservation MAC Protocol for ad-hoc Underwater Sensor Networks," in *The Third ACM International Workshop on Underwater Networks (WUWNet 2008)*, San Francisco, California, USA, pp(s): 95-8, Sep. 2008.
- [57] L. G. Roberts. "Aloha packet system with and without slots and capture," *Computer Communication Review*, 5(2), pp(s): 28–42, Apr. 1975.
- [58] A. Joon, S. Affan, K. Bhaskar, H. John. "Design and analysis of a propagation delay tolerant ALOHA protocol for underwater networks," *Ad Hoc Networks*, vol. 9, pp(s): 752-766, 2011.
- [59] Nitthita Chirdchoo, Wee-Seng Soh, Kee Chaing Chua, "Aloha-based MAC Protocols with Collision Avoidance for Underwater Acoustic Networks," *IEEE INFOCOM 2007 proceedings*. pp(s): 2271-2275.
- [60] Yen-Da Chen, Chan-Ying Lien, Yan-Siang Fang, Kuei-Ping Shih, "TLPC: A two-level power control MAC protocol for collision avoidance in underwater acoustic networks", *OCEANS - Bergen, 2013 MTS/IEEE, IEEE Xplore*: 26 September 2013.
- [61] Chaima Zidi, Fatma Bouabdallah, Raouf Boutaba, Ahmed Mehaoua, "MC-UWMAC: A multi-channel MAC protocol for underwater sensor networks", *Wireless Networks and Mobile Communications (WINCOM)*, 2017 International Conference on, *IEEE Xplore*: 25 December 2017.
- [62] Wang Ping, Fu Donghao, Xing Jianchun, Yang Qiliang, Wang Ronghao, Wu Wenhao, "An Improved MAC Protocol for Underwater Acoustic Networks," 2013 25th Chinese Control and Decision Conference (CCDC)-2013 *IEEE*, pp(s):2897-2903.
- [63] Y. Noh et al., "DOTS: A propagation delay-aware opportunistic MAC protocol for mobile underwater networks," *IEEE Trans. Mobile Comput.*, vol. 13, no. 4, pp. 766–782, Apr. 2014.
- [64] G. Acar, and A. E. Adams, "ACMENet: An underwater acoustic sensor network for real-time environmental monitoring in coastal areas," *IEEE proceedings. Radar, sonar and navigation*, Vol. 153, no. 4, pp(s): 365-80, Aug. 2006.
- [65] Prasad Anjani and Mandar Chitre "Experimental Demonstration of Super-TDMA: A MAC Protocol Exploiting Large Propagation Delays in Underwater Acoustic Networks", 2016 *IEEE*.

- [66] J. I. Namgung, N. Y. Yun, S. H. Park, C. H. Kim, J. H. Jeon, and S. J. Park, "Adaptive MAC Protocol and Acoustic Modem for Underwater Sensor Networks" in The Fourth ACM International Workshop on Underwater Networks (WUWNet 2009), Berkeley, California, USA, Nov. 2009.
- [67] Xiaoxing Guo, Michael R. Frater, Michael J. Ryan, "Design of a Propagation-Delay-Tolerant MAC Protocol for Underwater Acoustic Sensor Networks", IEEE Journal of Oceanic Engineering, Vol. 34, No.2, pp- 170-180, April 2009.
- [68] S. Y. Shin, J. I. Namgung, and S. H. Park, "SBMAC: Smart blocking MAC mechanism for variable UW-ASN (underwater acoustic sensor network) environment," Sensors, Vol. 10, no. 1, pp(s): 501-25, Jan. 2010.
- [69] Miguel-Angel Luque-Nieto, José-Miguel Moreno-Roldán, Javier Poncela, and Pablo Otero, "Optimal Fair Scheduling in S-TDMA Sensor Networks for Monitoring River Plumes", Journal of Sensors, Volume 2016 (2016), Article ID 8671516, 7 February 2016.
- [70] Xiaoning Feng, Zhuo Wang, Guangjie Han, Wenjie Qu, Akang Chen, "Distributed Receiver-oriented Adaptive Multichannel MAC for Underwater Sensor Networks", 2169-3536 (c) 2018 IEEE, DOI 10.1109/ACCESS.2018.2800703, IEEE Access, 2018.
- [71] Chao Li, Yongju Xu, Member, IEEE, Chaonong Xu, Zhulin An, Boyu Diao, and Xiaowei Li, DTMAC: A Delay Tolerant MAC Protocol for Underwater Wireless Sensor Networks, IEEE SENSORS JOURNAL, VOL. 16, No. 11, JUNE 1, 2016 pp-4137-4146.
- [72] Ming Xu, Guangzhong Liu, Jihong Guan, "Towards a Secure Medium Access Control Protocol for Cluster-Based Underwater Wireless Sensor Networks", Hindawi Publishing Corporation International Journal of Distributed Sensor Networks Volume 2015, Article ID 325474, 11 pages <http://dx.doi.org/10.1155/2015/325474>.
- [73] Jin-Young Lee, Nam-Yeol Yun, Sardorbek Muminov, Soo-Young Shin, Young-Sun Ryuh, Soo-Hyun Park, "A Focus on Practical Assessment of MAC Protocols for Underwater Acoustic Communication with Regard to Network Architecture," IETE Technical Review, Year : 2013, Volume : 30, Issue : 5, pp(s) : 375-381.
- [74] G. Bianchi, (2000). "Performance analysis of the IEEE 802.11 distributed coordination function," IEEE J. Sel. Areas Commun., vol. 18, no. 3, pp. 535–547.
- [75] S. Shahabudeen, M. Motani, and M. Chitre, "Analysis of a High-Performance MAC Protocol for Underwater Acoustic Networks" IEEE JOURNAL OF OCEANIC ENGINEERING, vol. 39, no. 1, pp. 74-89, Jan. 2014.
- [76] Matsuno, H. ; Ishinaka, H. ; Hamanaga, A. (2000). "A Simple Modification for the Drastic Improvement of MACA in Large Propagation Delay Situation," Wireless Communications and Networking Conference, 2000. WCNC. 2000 IEEE Volume: 2, pp 865-869.
- [77] Danfeng Zhao, Guiyang Lun, Mingshen Liang, "Handshake Triggered Chained-Concurrent MAC Protocol for Underwater Sensor Networks", WUWNET '16, October 24-26, 2016, Shanghai, China, ACM., 2016.
- [78] Liang-fang QIAN, Sen-lin ZHANG, Mei-qin LIU, (2015). "A slotted floor acquisition multiple access based MAC protocol for underwater acoustic networks with RTS competition," Frontiers of Information Technology & Electronic Engineering, Jan. 28, 2015, 16(3): pp. 217-226.
- [79] Lyad Tumar, "Energy Analysis of Routing Protocols for UWSNs". [Online]. Available: <http://cnds.eecs.jacobs-university.de/courses/nds-2010/tumar-energy-routing.pdf> (Accessed May. 17, 2017).
- [80] G. A. Shah, "A Survey on Medium Access Control in Underwater Acoustic Sensor Networks," Proceeding of WAINA '09, May 2009, pp.1178-1183.
- [81] Anuj Sehgal, Catalin David, Jürgen Schönwälder, Energy Consumption Analysis of Underwater Acoustic Sensor Networks, Conference: OCEANS '11 MTS/IEEE Kona, DOI: 10.23919/OCEANS.2011.6107287, September 2011.
- [82] M. C. Domingo and R. Prior, "Energy analysis of routing protocols for underwater wireless sensor networks," Computer Communications, (Elsevier), vol. 31, pp. 1227–1238, 2008.
- [83] "ns-3" is a discrete-event network simulator for Internet systems, licensed under the GNU GPLv2 license, and is publicly available for research, development, and use. (Online). Available: <https://www.nsnam.org/> (Accessed: May 24, 2014).
- [84] MathWorks, "MATLAB", a Proprietary commercial software. (Online). Available: <https://www.mathworks.com/products/matlab.html> (Accessed: June 15, 2015).

PUBLICATIONS

Journals

- [1] (submitted, Nov. 2017) Seema Ansari, Javier Poncela, Pablo Otero & Adeel Ansari, "Performance Analysis of MultiACK-SFAMA for Underwater Acoustic networks," Nov. 2017, submitted in Wireless Personal Communications, Springer Journal, IF: 1.200.
- [2] July, 2017 Seema Ansari, Javier Poncela, Pablo Otero & Adeel Ansari, "Comparative Analysis of MAC Protocols and Strategies for Underwater Applications," Sept. 5-7, 2016, published in Wireless Personal Communications, Springer Journal, IF: 1.200.
- [3] May, 2015 Seema Ansari, Javier Poncela Gonzalez, Pablo Otero & Adeel Ansari, "Analysis of MAC Strategies for Underwater Applications," Wireless Personal Communications, An International Journal, ISSN 0929-6212, DOI 10.1007/s11277-015-2743-1, Volume 82, number 3, June (I), 2015, IF: 1.200.
- [4] June 2015 Seema Ansari, Javier Poncela, Adeel Ansari and Osama Mahfooz (June 2015):" Research in Pakistan: Structure, Funding and Results", PJETS Vol 5, No 1 (HEC Z-Category Journal), IoBM.
- [5] Sept. 2014 Adeel Ansari, Afza Bt Shafie, Seema Ansari, Abas B. Md Said, Elisha Tadiwa Nyamasvisva, "Filtration of Airwave in Seabed Logging Using Principal Component Analysis", Communication Technologies, Information Security and Sustainable Development Communications in Computer and Information Science Volume 414, 2014, Chapter No: 6, pp 56-64, 11 Sep 2014. http://link.springer.com/chapter/10.1007%2F978-3-319-10987-9_6#page-2
- [6] April 2014 Seema Ansari, Adeel Ansari, "Comparative Analysis of Routing and Wavelength Assignment Algorithms used in WDM Optical Networks", Research Journal of Applied Sciences, Engineering and Technology 04/2014; 7(13):2646-2654. Indexed in: ISI-Thomson, Scopus. H-Index: 5.0.
<http://www.maxwellsci.com/jp/abstract.php?jid=RJASET&no=419&abs=09>
- [7] April 2014 Adeel Ansari, Afza Shafi, Abas B Md Said, Seema Ansari, Muhammad Rauf, Elisha Tadiwa Nyamasvisva, , "Infomax Algorithm for Filtering Airwaves in the Field of Seabed Logging," Research Journal of Applied Sciences, Engineering and Technology 04/2014; 7(14):2914-2920. Indexed in: ISI-Thomson, Scopus. H-Index: 5.0.
<http://www.maxwellsci.com/jp/abstract.php?jid=RJASET&no=420&abs=19>
- [8] May 2013 Adeel Ansari, Afza Bt Shafie, Abas B Md Said, Seema Ansari, "Transverse product effect on CSEM with double Hydrocarbon reservoir in seabed logging " International Journal of Scientific and Engineering Research, (IJSER), http://www.ijser.org/ResearchPaperPublishing_May2013.aspx, <http://www.ijser.org/>, Index: SCRIBD; DOAJ, GOOGLE SCHOLAR; SCIRUS; SENSEI, SciRATE.COM, Impact Factor: 1.4, Volume 4, Issue 5, May 2013, PP: 69-74.
- [9] Feb. 2013 Adeel Ansari, Afza Bt Shafie, Abas B Md Said, Seema Ansari, "Independent Component Analysis for Filtering Airwaves in Seabed Logging Application" International Journal of Advanced Studies in Computers, Science & Engineering (IJASCSE), <http://www.ijascse.org/>, Cornell University Library: <http://arxiv.org/abs/1303.2593>, Impact Factor: 0.0892, Volume2, Issue1, February 2013, PP: 48-54.

Conferences

- [10] 2017 Adeel Ansari, Seema Ansari, "Performance Evaluation of FASTICA for Signal Data Processing", International Conference on Experiential Learning-2017 at Institute of Business Management, October 21-22, 2017.
- [11] 2014 Adeel Ansari, Afza Shafie, Abas Md Said, Seema Ansari, Elisha Tadiwa Nyamasvisva, Muhammad Abdulkarim, Muhammad Rauf, "Infomax and FASTICA Using PCA as Preprocessor for Airwave Removal in Seabed Logging", *International Conference on Computer & Information Sciences 2014, June 3-5, 2014*, Kuala Lumpur, Malaysia. 978-1-4799-0059-6/13 ©2014 IEEE.
- [12] 2014 Adeel Ansari, Afza Shafie, Abas Md Said, Seema Ansari, Elisha Tadiwa Nyamasvisva, Muhammad Abdulkarim, Muhammad Rauf, "Subsurface Exploration of Seabed Using Electromagnetic Waves for the Detection of Hydrocarbon Layers", *International Conference on Computer & Information Sciences 2014, June 3-5, 2014*, Kuala Lumpur, Malaysia. 978-1-4799-0059-6/13©2014 IEEE.
- [13] 2013 Adeel Ansari, Afza Bt. Shafie, Abas B M Said, Seema Ansari, Muhammad Rauf, "Transverse product effect on CSEM with double Hydrocarbon reservoir in seabed logging", 3rd Global Conference for Academic Research on Scientific and Emerging Technologies (GCARSET). Scopus indexing <http://www.gcar2012.com/> Kuala Lumpur, Malaysia, March 9 to 11, 2013.

Conferences Attended in Spain

- [14] 2015 13th International Conference on Wired & Wireless Internet Communications, at University of Malaga, Spain: May 25-27, 2015.
- [15] 2015 "Addressing Spectrum Scarcity through Optical Wireless Communications" by Prof. Mohamed-Slim Alouini, IEEE fellow, Computer, Electrical and Mathematical Science & Engineering (CEMSE) Division, King Abdullah University of Science and Technology (KAUST), at University of Malaga, Spain. June 02, 2015, At 10:30 Hrs.
- [16] 2015 "Emerging Mathematical Tools and Transmission Technologies for 5G Wireless Networks: The Stochastic Geometry and Spatial Modulation Saga" by Prof. Marco Di Renzo, IEEE Fellow. Laboratory of Signals & Systems (L2S), French National Center for Scientific Research (CNRS), at University of Malaga, Spain. June 02, 2015, At 17:00 Hrs.
- [17] 2015 "A new low-complexity and energy-efficient multiple-antenna transmission technology known as Spatial Modulation" by Prof. Marco Di Renzo, IEEE Fellow. Laboratory of Signals & Systems (L2S), French National Center for Scientific Research (CNRS), at University of Malaga, Spain. June 03, 2015, at 11:00 Hrs
- [18] 2015 Conference on June 08, 2015: At 12:00 noon, "Virtual Acoustic Reality-Auralization" by Prof. Dr. Michael Vorlander, Director, Institute for Technische Akustik, RWTH Aachen University, Germany.

APPENDIX A

Curriculum Vitae

Positions

- **Head of Electrical Engineering & Management Sciences Department.** Institute of Business Management (IoBM) (August 2012-todate)
- **Associate Professor, & Head of Curriculum Review,** College of Engineering, Dept. of Electronics & Telecommunication, Pakistan Air Force Karachi Institute of Economics & Technology (PAFKIET), April 2006-Dec. 31, 2011
- **Head of Department, CCSIS & MS Telecom Engg,** City Campus, PAF-KIET. Sep. 2005--Apr. 2009
- **Director,** Asia Pacific Institute of Information Technology-Karachi (APIIT-Karachi), a joint venture with APIIT-MALAYSIA & affiliated with the Staffordshire University, United Kingdom Feb. 2002- Aug. 2005
- **Director** BSc(Hons) Program & Head of Student Affairs, (APIIT-Karachi), affiliated with the Staffordshire University, United Kingdom. Dec. 1998--- Feb. 2002
- Assistant Professor, Department of Electronics, Dawood College of Engineering & Technology, Karachi, Oct. 1982-Dec. 1998

Education

- Ph.D(Telecomm. Engg), University of Malaga, Spain (in progress); Final thesis submitted.
- Ph.D.(Telecomm. Engg), Hamdard University; Completed Course work with CGPA 4.0. Cleared Comprehensive part-I & II. Qualified for PhD Research Scholar, 2005-2010
- MS/CS Telecommunications, University of Missouri KC, USA, 1991-1993
- B.E., Electronics, NED University of Engineering & Technology Karachi-1979.

Journal papers

- Seema Ansari, Javier Poncela, Pablo Otero & Adeel Ansari, “ Performance Analysis of MultiACK-SFAMA for Underwater Acoustic networks,” Nov. 2017, submitted in Wireless Personal Communications, Springer Journal, IF: 0.751.
 - Seema Ansari, Javier Poncela, Pablo Otero & Adeel Ansari, “Comparative Analysis of MAC Protocols and Strategies for Underwater Applications,” July 2017, published in Wireless Personal Communications, Springer Journal, IF: 0.751.
 - Seema Ansari, Javier Poncela Gonzalez, Pablo Otero & Adeel Ansari, “Analysis of MAC Strategies for Underwater Applications,” Wireless Personal Communications, An International Journal, ISSN 0929-6212, DOI 10.1007/s11277-015-2743-1, Volume 82, number 3, June (I), 2015, IF: 0.979
 - Seema Ansari, Javier Poncela, Adeel Ansari and Osama Mahfooz (June 2015):” Research in Pakistan: Structure, Funding and Results”, PJETS Vol 5, No 1 (HEC Z-Category Journal), IoBM.
-

- Adeel Ansari, Afza Bt Shafie, Seema Ansari, Abas B. Md Said, Elisha Tadiwa Nyamasvisva, "Filtration of Airwave in Seabed Logging Using Principal Component Analysis", Communication Technologies, Information Security and Sustainable Development Communications in Computer and Information Science Volume 414, 2014, Chapter No: 6, pp 56-64, 11 Sep 2014.
- Seema Ansari, Adeel Ansari, "Comparative Analysis of Routing and Wavelength Assignment Algorithms used in WDM Optical Networks", Research Journal of Applied Sciences, Engineering and Technology 04/2014; 7(13):2646-2654. Indexed in: ISI-Thomson, Scopus. H-Index: 5.0.
- Adeel Ansari, Afza Shafi, Abas B Md Said, Seema Ansari, Muhammad Rauf, Elisha Tadiwa Nyamasvisva, , "Infomax Algorithm for Filtering Airwaves in the Field of Seabed Logging," Research Journal of Applied Sciences, Engineering and Technology 04/2014; 7(14):2914-2920. Indexed in: ISI-Thomson, Scopus. H-Index: 5.0.
- Adeel Ansari, Afza Bt Shafie, Abas B Md Said, Seema Ansari, "Transverse product effect on CSEM with double Hydrocarbon reservoir in seabed logging " International Journal of Scientific and Engineering Research, (IJSER), Impact Factor: 1.4, Volume 4, Issue 5, May 2013, PP: 69-74.
- Adeel Ansari, Afza Bt Shafie, Abas B Md Said, Seema Ansari, "Independent Component Analysis for Filtering Airwaves in Seabed Logging Application" International Journal of Advanced Studies in Computers, Science & Engineering (IJASCSE), Impact Factor: 0.0892, Volume2, Issue1, February 2013, PP: 48-54.

Conference papers

- Adeel Ansari, Seema Ansari, "Performance Evaluation of FASTICA for Signal Data Processing", International Conference on Experiential Learning-2017 at Institute of Business Management, October 21-22, 2017.
 - "Wi-Fi Controlled Power Generation by Combined Cycle", International Conference on Experiential Learning-2017 at Institute of Business Management, October 21-22, 2017, Muhammad Rizwan, Seema Ansari.
 - Adeel Ansari, Afza Shafie, Abas Md Said, Seema Ansari, Elisha Tadiwa Nyamasvisva, Muhammad Abdulkarim, Muhammad Rauf, "Infomax and FASTICA Using PCA as Preprocessor for Airwave Removal in Seabed Logging", International Conference on Computer & Information Sciences 2014, June 3-5, 2014, Kuala Lumpur, Malaysia. 978-1-4799-0059-6/13 ©2014 IEEE.
 - Adeel Ansari, Afza Shafie, Abas Md Said, Seema Ansari, Elisha Tadiwa Nyamasvisva, Muhammad Abdulkarim, Muhammad Rauf, "Subsurface Exploration of Seabed Using Electromagnetic Waves for the Detection of Hydrocarbon Layers", International Conference on Computer & Information Sciences 2014, June 3-5, 2014, Kuala Lumpur, Malaysia. 978-1-4799-0059-6/13©2014 IEEE.
 - Adeel Ansari, Afza Bt. Shafie, Abas B M Said, Seema Ansari, Muhammad Rauf, "Transverse product effect on CSEM with double Hydrocarbon reservoir in seabed logging", 3rd Global Conference for Academic Research on Scientific and Emerging Technologies (GCARSET). Scopus indexing, Kuala Lumpur, Malaysia, March 9 to 11, 2013.
-

Management and Organization Experience

Head of Electrical Engineering & Management Sciences: Looks after the entire B.E. program from Curriculum design to Accreditation from Pakistan Engineering Council (PEC);

Successfully launched and takes care of MS-Engineering Management Program at IoBM from Fall 2014. (HEC approved)

Launched and starting MS-Electrical Engineering Program at IoBM from Fall 2018.(HEC approved)

Launching of PhD-Electrical Engineering Program at IoBM is in process. (HEC approval awaited)

Launching of Mechatronics Engineering program is also in process (documents submitted to PEC)

Workshops & Conferences Organized at IoBM in 2017-2018:

Arduino Workshop: April 8, 2018

Organized a Two-Day Mega event “WHY-PHY-2.0” Inter University Gaming Competition at the College of Engineering & Sciences, at the Institute of Business Management: April 4-5, 2018

Sixth Student Project Exhibition: April 24, 2018

Seminar on “Mind Sparks”, Dec. 02, 2017: where entrepreneurs related with the field of technology were invited to share their ideas and insights pertaining to their respective fields.

Fifth Student Project Exhibition & Competition, December 12, 2017: It was largely attended by students, faculty and management.

ICEL-17, DIRECTOR of TRACK-3, The Engineering Track, October 21-22, 2017

Organized Workshop on “**Outcome Based Education**” (OBE) System, “Improving Education Deliverance and Attainment Standards”, May 13, 2017, College of Engineering & Sciences, Institute of Business Management.

Organized “**International Conference on Multidisciplinary Engineering Research & Technology: Harnessing the Power of R&D**”. March 6, 2017, College of Engineering & Sciences, Institute of Business Management.

Guest Speaker Session On “University: Catalyst for Change”, January, 2017

Industrial Projects Experience

- Project Supervisor: “Wi-Fi Controlled Power Generation by Combined Cycle”, International Conference on Experiential Learning-2017 at Institute of Business Management, October 21-22, 2017.
 - **Course projects made by students (Spring-2018):**
 - Automated Electromagnetic Crane,
 - The home automation system,
 - Robotic Arm,
 - Radar System,
 - Automated water filling system.
 - Industrial visit of Electrical Engineering students to K. Electric Power Plant: March 06, 2017
 - Industrial Linkages for students in MS-Engineering Management: Thesis/Projects
-

Other related experience

- Reviewer Research papers, for the Elsevier Editorial System
 - Global Communication for Wireless and Optical Communication (GCWOC):
 - Papers reviewed for GCWOC-16, GCWOC-17, GCWOC-18, Univ. of Malaga, Spain
- Member Technical Program Committee, GCWOC-16, GCWOC-17, GCWOC-18, Univ. of Malaga, Spain
- Supervised 12 MS-Telecomm. Engineering (MS-TE) students from 2007-2011 at PAFKIET. The MS program involved developing a thesis with original research results. Details can be seen on PAFKIET Website.
- Member of Curriculum Review Committee, Pakistan Engineering Council. Appointed as Expert for finalizing curriculum of Telecomm. Engineering for Engineering Practice Examination (EPE)-2009.
- Restructured Research and Independent Study work for MS students. Added new courses to the curriculum 2006-2009 at PAFKIET
- Chairperson Women Advisory Committee, PAF-Karachi Institute of Economics and Technology, 2007- To 2011
- Thesis & Research supervisor of MS-TE students at PAFKIET.
- Final Year Engineering Project supervisor of BE students, College of Engineering, PAF-Karachi Institute Of Economics and Technology
- Mentor for undergraduate students, College Of Engineering, PAF-Karachi Institute of Economics and Technology, 2006-To 2011